AFOSR-TR- 83-0434

RAI-FTR-04-83-01

FINAL REPORT

1 OCTOBER 1979 TO 31 DECEMBER 1982

VOLUME II

THE USE OF REGIONAL SEISMIC WAVES FOR DISCRIMINATION AND YIELD DETERMINATION

1 JANUARY 1983

Approved for public release; distribution unlimited.

RONDOUT ASSOCIATES INCORPORATED
P.O. Box 224
STONE RIDGE, NEW YORK 12484

Sponsored By
Advanced Research Projects Agency (DOD)
ARPA Order No. 3291-31
Monitored By AFOSR Under Contract #F49620-80-C-0021

AD A128376

DTIC FILE COPY

DTIC ELECTE MAY 23 1983 A

83 05 23 017

UNCLASSIFIED

SECURITY CLASSIFICATION OF THIS PAGE (When Data Entered)

REPORT DOCUMENTATION PAGE		READ INSTRUCTIONS BEFORE COMPLETING FORM
1. REPORT NUMBER AFOSR-TR- 83-0434	2. GOVT ACCESSION NO.	3. RECIPIENT'S CATALOG NUMBER
4. TITLE (and Subtitle) The Use of Regional Seismic Waves for Discrimination and Yield Determination		5. TYPE OF REPORT & PERIOD COVERED Final Technical 1 Oct. 1979 - 31 Dec. 1982 6. PERFORMING ORG. REPORT NUMBER
7. AUTHOR(s) Paul W. Pomeroy, George H. Sutton, and Jerry A. Carter		8. CONTRACT OR GRANT NUMBER(s) F49620-80-C-0021
9. PERFORMING ORGANIZATION NAME AND ADDRESS Rondout Associates, Incorporated		10. PROGRAM ELEMENT, PROJECT, TASK AREA & WORK UNIT NUMBERS Element 61101 E Code 0D60 ARPA Order 3291-32
11. CONTROLLING OFFICE NAME AND ADDRESS Air Force Office of Scientific Research (NP) Building 410 Bolling Air Force Base, D.C. 20332		12. REPORT DATE 1 January 1983 13. NUMBER OF PAGES 211
14. MONITORING AGENCY NAME & ADDRESS(if different from Controlling Office) DCASMA, Bridgeport 550 South Main Street Stratford, CT 06497		15. SECURITY CLASS. (of this report) Unclassified 15a. DECLASSIFICATION/DOWNGRADING SCHEDULE

16. DISTRIBUTION STATEMENT (of this Report)

Approved for public release; distribution unlimited.

17. DISTRIBUTION STATEMENT (of the abstract entered in Block 20, if different from Report)

NA

18. SUPPLEMENTARY NOTES

NA

19. KEY WORDS (Continue on reverse side if necessary and identify by block number)

Regional Seismic Phases
Lg Waves
Catskill Seismic Array
Wake Island Hydrophone Array
Oceanic Pn and Sn
HARZER
Seismic Discrimination
Yield Determination
Remote Seismic Terminal

20. ABSTRACT (Continue on reverse side if necessary and identify by block number)

This report, which is presented in two volumes as follows:

Volume I entitled "Enhance and Test the Remote Seismic Terminal" describes the terminal system and, in greater detail, the Seismic Recording System add-on to the terminal.

Volume II entitled "The Use of Regional Seismic Waves for Discrimination and Yield Determination" deals with the following topics:

DD FORM 1 JAN 73 1473

83 05 25 012

UNCLASSIFIED

SECURITY CLASSIFICATION OF THIS PAGE (When Data Entered)

a. Discrimination Techniques at Regional Distances,
b. Yield Determination Using Regional Seismic Waves,
c. The Catskill Seismic Array (CSA),
d. The Nevada Test Site explosion HARZER Recorded at CSA,
e. Explosion P Waves Recorded at CSA and the Wake Island Hydrophone Array (WHA),
f. Q of the Northwest Pacific Lithosphere,
g. The Instrumental Upgrade of WHA to Digital Recording.

Table of Contents

AIR FORCE OFFICE OF SCIENTIFIC RESEARCH (AFSC)
NOTICE OF TRANSMITTAL TO DTIC
This technical report has been reviewed and is approved for public release IAW AFR 190-12.
Distribution is unlimited.
MATTHEW J. KERPER
Chief, Technical Information Division

List of Figures

Page

Accession For
NTIS GRA&I
DTIC TAB
Unannounced
Justification
By
Distribution/
Availability
Dist | Avail and/or Special
A

DTIC COPY INSPECTED

List of Tables

EXECUTIVE SUMMARY

This volume of the contract Final Report is divided into seven (7) sections. The principal conclusions of each section are listed below in numerical order corresponding to their order in the text.

1. Discrimination

a. Regional ($\Delta \leq 30^{o}$) phases such as P, Pg, S, and Lg are recorded with significant amplitudes in many parts of the world and, where observed, can provide significant information for monitoring test ban treaties and, in particular, can improve discrimination capability.

b. Numerous techniques for discrimination using regional data have been suggested and, in some cases, developed. However, most of these potential tools have been tested on limited data sets, usually from one geographic region and often utilizing only one or two recording stations.

c. Regional discriminants which appear to be most promising include:

1. the regional variant of the M_s: m_b criterion.
2. the excitation of short period SH waves.
3. generation of higher mode surface waves.
4. long period surface wave energy density.
5. spectral ratios in Pg and Lg.
6. arguably, Lg/P amplitude ratios.

d. Most importantly, a regional discrimination experiment is required to systematically evaluate these proposed discriminants using a common data base covering all of the test sites. The discriminants should be evaluated systematically for their success/failure ratio both individually and in combinations using multivariate statistical tools.

2. Yield determinations

a. Lg(Z), Lg(T), Pg (Z) and Pg(T), where observed, all appear to have significant potential as indicators of yield.

b. For Nevada Test Site events, Lg amplitudes either (Z) or (T) do not appear to be contaminated by non-isotropic source components indicated by the generation of long period Love waves.

c. Lg(T) amplitudes are consistently larger than Lg(Z) amplitudes at the same station for all of the epicentral distances studied.

d. Amplitude-yield curves have been determined from 12 NTS events for each of three components of P, Pg and Lg as recorded at WWSSN stations in the conterminous United States.

e. Some WWSSN stations show significantly smaller scatter in Lg amplitude-yield data than other stations. Another group of stations shows smaller scatter in Pg amplitude-yield data. The scatter in Lg and Pg data is generally smaller than that of P data in the same distance range.

3. Catskill Seismic Array (CSA)

CSA was a tripartite array (about 3 km sides) of three component, broad-band (from long period to 12.5 Hz) seismometers ($T_o \approx 15$ sec) with digital recording that operated from September 1980 to November 1981 near RAI headquarters at Stone Ridge, New York, on the high Q lithosphere of eastern North America. This array, and, therefore, its data are unique for the central and eastern United States. A significant quantity of high quality data from CSA are available for studies of regional North American earthquakes and explosions, and earthquakes and explosions from other regions.

4. HARZER recorded at CSA

Excellent recordings were obtained at CSA from the NTS explosion HARZER. P has high S/N and coherence across the array. Energy in P drops rapidly above .7 Hz.

Lg has its highest amplitude on the transverse component; lowest on the longitudinal horizontal. Spectra of all three components are similar except most of the additional energy on the transverse lies below 0.3 Hz. Transverse and vertical components of Lg are well correlated across the array.

Well dispersed sedimentary Rayleigh waves (12 to 3 secs) are the largest signals (ground velocities) on the vertical and longitudinal horizontal components. Because of radical changes in the upper 5 km of the wave guide between NTS and CSA,these strong arrivals were unexpected.

5. Explosion P Waves at CSA and Wake Hydrophone Array (WHA)

Array processing of explosion P waves at both CSA and WHA improve the signal to noise ratio significantly. The P arrival is highly coherent across both arrays. In the case of WHA, the first ocean-surface reflected arrival can be added to direct P on each bottom hydrophone to make an equivalent two element vertical array. Delay sum stacking produces near theoretical improvement in signal to noise. Pre-filtering before spectral-analysis seems to

improve spectral S/N, perhaps because of smaller windowing effects, (i.e., pre-filtered, stacked spectra produced the best S/N).

Apparent Q and t*, as functions of frequency, for explosion P waves from three USSR sites and NTS to WHA and to CSA were determined for 7 propagation paths. The method assumes a simple source function with arbitrary corner frequency, f_o, and a reasonable frequency dependence for Q, $Q = Q_o + Kf$. Q_o, K, and f_o are determined by matching the P wave spectrum with a theoretical curve. For all paths, Q increases strongly above 1 Hz. Near 1 Hz, Q for NTS paths is much lower than for USSR paths. However, at higher frequencies ($\sim$10 Hz), the difference is not so great; the regional (33^o) path NTS-CSA has the lowest Q values. Q for the upper mantle under CSA is somewhat higher than under WHA. In order of decreasing Q, the USSR sites rank: Novaya Zemlya; Eastern Kazakh, and Western Siberia.

6. The Northwest Pacific Lithosphere

The lithosphere of the northwest Pacific is an extremely efficient seismic wave guide, passing frequencies as high as 15 and 20 Hz to 3300 km for telesesimic Pn and Sn respectively. Using WHA recordings of high-frequency, teleseismic Pn and Sn signals, which are believed to travel within the lithosphere, apparent Q as a function of frequency from about 1 to 10-15 Hz, was obtained by two methods, and the apparent source spectra (i.e., with the effects of finite Q removed) for Pn and Sn were determined. The results indicate that Q is higher for Sn than for Pn, above 10,000 and above 5,000 for Sn and Pn, respectively, near 10 Hz.

7. Upgrade of WHA for Digital Recording

In September 1982 the recording system at WHA was upgraded from analog recording (on tape cassettes) of three hydrophones to digital recording of all eleven (possibly 12) operational hydrophones in the array. The operation of WHA (and this upgrading) are primarily the responsiblity of the Hawaii Institute of Geophysics; RAI provides advice and technical support in this program. The new system is microprocessor controlled and, therefore, quite flexible. The nominal configuration is 11 channels, 80Hz sampling rate, 16 bit resolution, 4 tape reels per day. The data returned to date appear to be excellent; this is demonstrated by a seismogram and spectra of P, Pn, Sn and T from a large earthquake south of Honshu, Japan.

1. DISCRIMINATION TECHNIQUES AT REGIONAL DISTANCES

EXECUTIVE SUMMARY

The following material is extracted from a paper by Pomeroy, Best, and McEvilly entitled "Test Ban Treaty Verification with Regional Data-A Review". This paper was prepared for a State of the Art Symposium at the Seismological Society of America (SSA) meeting in Anaheim, California in 1982. The entire paper will be published in the Bulletin of the SSA in 1982. Work on regional discriminants carried out under this (and preceding) contract is summarized together with the work of other investigators in this field to indicate the current state of knowledge in this area.

This portion of the report summarizes the use of regional ($\Delta \leq 30$ seismic data in a test ban context for identifying underground nuclear explosions. In many areas of the world (Eastern North America, Africa, Eastern USSR) Lg is the largest amplitude wave recorded on standard seismograph systems at regional distances and thus is the most appropriate phase for monitoring small magnitude events. Lg and other regional phases may contain information on source depth, but such information has not been exploited to date. Fifteen classes of regional discriminants other than depth have been identified including:

1. First Motion
2. $M_S:m_b$
3. P^2/P^1 Ratio
4. Excitation of Short Period SH Waves
5. Lg/Rg Amplitude Ratios
6. Pn/Lg, Pg/Lg, and P_{max}/Lg Amplitude Ratios
7. Lg Group Velocity and Energy Ratios in Lg
8. Excitation of Sn
9. Third Moment of Frequency
10. Generation of Higher Mode Surface Waves
11. Peak Amplitudes of Love and Rayleigh Waves and Long Period Surface Wave Energy Density
12. Prevailing Period of Long Period Love Waves
13. Spectral Ratio-Long Period S Waves to Rayleigh Waves
14. Spectral Ratio-Long Period Love Waves to Rayleigh Waves
15. Frequency of the Peak Spectral Amplitudes and Spectral Ratios in Pn, Pg, S, and Lg.

Each of these proposed discriminants has, with differing degrees of success, separated some explosions from some earthquakes. However, most have been tested only on limited data, usually from one geographic region and only one or two recording stations. No systematic analyses have been done to determine the best individual discriminant or combination of them.

The major conclusion of the present study is that a systematic and comparative evaluation of all the proposed regional discriminants is now required, utilizing a common data base derived from all present day test sites. This evaluation would suggest the optimal discrimination procedure using regional waves, and would also define areas of needed research. Without such an integrated evaluation, it is still possible to speculate, using existing results, on the most promising regional discriminants.

DISCRIMINATION TECHNIQUES AT REGIONAL DISTANCES

Introduction

Since the first public discussion of underground nuclear test monitoring at the Geneva meeting of a Committee of Experts in July and August, 1958, the problem of discrimination using regional seismic phases has proven to be remarkably difficult to solve. During this time, however, a large number of ideas for empirical discriminants have been put forth and tested. Most of these techniques suffer from one or more of the following problems:

1. Insufficient evaluation of azimuth and distance variation effects.
2. Insufficient evaluation of regional variation.
3. An insufficient size of the explosion and earthquake populations tested.
4. A lack of comparable explosions and earthquakes in the same geographical area recorded at the same station(s).

In this section of the report, we will describe each of the regional discrimination techniques and point out the limitations in their applicability.

Regional discriminants include:

1. First Motion
2. $M_S:m_b$
3. P^2/P^1 Ratio
4. Excitation of Short Period SH Waves
5. Lg/Rg Amplitude Ratios
6. Pn/Lg, Pg/Lg, and P_{max}/Lg Amplitude Ratios
7. Lg Group Velocity and Energy Ratios in Lg
8. Excitation of Sn
9. Third Moment of Frequency
10. Generation of Higher Mode Surface Waves
11. Peak amplitudes of Love and Rayleigh Waves and Long Period Surface Wave Energy Density
12. Prevailing Period of Long Period Love Waves
13. Spectral Ratio-Long Period S Waves to Rayleigh Waves
14. Spectral Ratio-Long Period Love Waves to Rayleigh Waves
15. Frequency of the Peak Spectral Amplitudes and Spectral Ratios in Pn, Pg, S, and Lg.

These discrimination techniques can be classified into three major groups involving:

1. radiation patterns
2. relative excitation of various phases and modes
3. frequency content.

Some of these techniques overlap one another in that they rely partially on the same parameters but they are separated here for ease of discussion.

1. First Motion

Historically, this method was one of the first proposed for distinguishing earthquakes. At Geneva in 1958, the monitoring system proposed by the Committee of Experts was designed around this criterion which involves the observation of the direction (up or down) of the ground motion in the initial P wave. These observations require reasonable signal to noise ratios and, given the knowledge of amplitude attenuation at the time, required observing stations within 500 to 1000 km of the source. In this criterion, the explosion source is assumed to be symetric and to radiate compressive motion in all directions while the source models for earthquakes exhibit two quadrants of compressional first motion and two quadrents of dilatational first motion. As Douglas (1980) notes, this criterion essentially allows the identification of earthquakes; that is, if one or more clear dilatational phases are observed, the source is presumed to be an earthquake. If compressional phases are observed at all stations, the source cannot be discriminated--it could be an explosion or an earthquake with an orientation such that observing stations lie only in the compressional quadrants of the P wave radiation pattern. Although this methodology works in principle, the signal to noise requirements for the initial P arrival coupled with complexity of P wave arrivals in the distance range 0 to 1000 km presented formidable obstacles to its utilization in this distance range. In fact, in testimony to Congress in 1971, Lukasik (1971) classified this technique as "not as useful as expected" although his remarks do not indicate whether he was referring to teleseismic distance ranges, regional distance ranges or both. In any case, the idea of using polarity of first motions and the resulting requirement for reasonable signal to noise ratios led to the numerous developments in array design and deployment that ultimately contributed greatly to our knowledge in seismology.

2. M_S:m_b

In the early 1960's, partially because of the formidable complexities in observations at regional distance ranges and partially because of enhanced knowledge of propagation characteristics, the emphasis in the seismological research programs associated with monitoring explosions shifted from regional to teleseismic

distance ranges. Major improvements in observational and theoretical capabilities led, in the mid-60's, to the discovery, extensive use, and acceptance of the M_S:m_b discrimination criterion at teleseismic distances. For descriptions of the evolution, use, and acceptance of this teleseismic criterion, the reader is referred to Douglas (1980), Dahlman and Israelson (1977), and Bolt (1976). Here, we are concerned with the extension of this technique to regional distances. The detection of surface waves, of course, becomes easier as the distance decreases and thus some type of M_S data from monitoring stations at regional distances will be particularly valuable. Given a measure of M_S, the major problem then is to obtain a measure of m_b at these distances. What is being sought is a measure of the high frequency body wave energy and the low frequency surface wave energy. Key evidence to evaluate the parameters is provided by McEvilly and Peppin (1972) and Peppin and McEvilly (1974). In their 1972 paper, these authors examine 51 NTS explosions in the magnitude range M_L = 4.0 to 6.3, as recorded at the Berkeley seismic station, and 34 other events including earthquakes, explosion collapses, and aftershocks in the Nevada region in the magnitude range M_L = 3.8 to 6.5. The distance range is about 500 km. The authors plot relative Pn amplitudes versus Rayleigh wave amplitudes and show (Figure 1-1) good separation between the two sets of events. In 1974, the same authors extended this study, examining 16 events at the four University of California Lawrence Livermore Laboratory (UC-LLL) stations. These data show good separation between the different types of events (Figure 1-2). Marshall (personal communication) uses the Marshall and Basham (1972) M_S formulation and an unspecified m_b conversion to convert the UC-LLL amplitude data M_S and m_b values. He shows good separation on m_b:M_S plots down to m_b = 4 and M_S = 2 for the Berkeley data and good separation down to M_S = 1 and $m_b \simeq 3.0$ for the Mina station of the UC-LLL network. He states that these values correspond to a yield of approximately 0.1 kt in hard rock. Whether we agree with these conversions or not, the important conclusion is that, as the original data demonstrate, the discrimination technique works down to low magnitude levels and might be particularly useful in these distance ranges. This conclusion, like most of the others discussed here, is valid only at the particular stations studied for NTS events. Peppin (personal communication), more recently reported Pn and LR amplitude data for the Jamestown station and did not achieve the same satisfactory separation of the two populations. Since the Jamestown station lies, in an approximate way, along the same azimuth from NTS as Mina and Berkeley and lies between the

latter two stations, the reason for this failure is not understood. Peppin did report that the use of a ratio of the Pg to Sg amplitude envelope did separate these data. Basham (1969) studies the data from stations of the Canadian network as recorded from 26 explosions (25 NTS events) in the magnitude range m_b 4.5 to 6.3 (M_S 3.5 to 6.3) and 28 earthquakes from the southwestern portion of North America in the magnitude range m_b 3.8 to 5.7 (M_S 4.0 to 6.3). M_S:m_b plots of this data show good separation between the two populations. The Canadian network stations cover a distance range that technically falls both in the regional and teleseismic ranges although they are, of course, on the same continental land mass as the event populations studied. The derived magnitudes are calculated in the same manner for all events. Network averages for M_S and m_b were the values plotted.

Pomeroy (1977) uses a somewhat different approach for the eastern United States. He determines m_bLg (Nuttli, 1973) and M_{SR} for four eastern United States earthquakes using all available NEUSSN and WWSSN data. M_{SR} is evaluated using measured Rayleigh amplitudes which, using appropriate theoretical factors, are extrapolated to the larger distances where M_S are considered applicable (i.e. the methodology in Lieberman and Pomeroy, 1969). The resultant M_S:m_b values are plotted together with those of four eastern United States earthquakes as determined by Nuttli (1973). Similar values are derived for the SALMON nuclear explosion. The results are presented in Figure 1-3. The explosion with m_bLg $\cong$ 4 and M_S $\cong$ 3 does not appear to be significantly different from the admittedly sparce earthquake population.

In any case, the promising results in the western United States make this variant of the M_S:m_b technique an extremely promising discrimination technique.

3. P^2/P^1 Ratio

Press et al. (1963) follow an earlier suggestion that the ratio of the amplitude of the second half cycle of the P motion (P^2) to the first half cycle amplitude (P^1) might be larger for explosions than for earthquakes. To test this hypothesis, Press et al. test three populations:

1. a random sampling of 47 Kern County shocks recorded in the 100 to 200 km distance range with magnitudes (M_L) of 3.8 to 5.9 and focal depths 0 to 18 km
2. 40 southern California earthquakes recorded at distances of 30 to 300 km with magnitudes of 1.6 to 4.7 and focal depths of 0 to 41 km

3. 44 Nevada Test Site explosions plus GNOME recorded at distances of 100 to 500 km.

For this sample, 20% of the earthquakes fall outside the range occupied by 95% of the explosions. Although the explosion and earthquake populations overlap severely in this test of the technique, a statistical test showed a highly significant difference in the means of the explosion and earthquake populations. With the shift of emphasis in the research program away from regional distance observations, this potential discriminant faded from view. In 1971, Lukasik, Director of DARPA in a Congressional Testimony, classified this technique in the "poor and have been abandoned" category. Given the current understanding of regional wave propagation and recording, this is not a valid discrimination technique.

4. Excitation of Short Period SH Waves

A 'pure' explosion would not be expected to generate horizontally polarized shear waves. This discrimination technique, as well as several others to be discussed below, is based on the premise that earthquakes are more efficient generators of SH motion than explosions of equivalent size. Press et al. (1963), to evaluate this technique, use a procedure involving the integration of SH energy in an eight second window centered on the arrival time of the SH waves. The authors identify this wave as Sg but the associated group velocity (3.49 km/sec for the explosions or 3.54 km/sec for the earthquakes) identifies the wave as Lg in our terminology. The variation of energy with time in this eight second window is taken as the indicator of SH excitation. The rapidity of build up of the energy and the ratio of energy in the four second window before and after the SH arrival time are the factors used to describe the SH excitation. Thirty-two NTS underground explosions and 13 earthquakes in the California-Nevada region are used in the analysis. The mean energy ratio for the explosions is 8.4 ± 4.3 and for the earthquakes 41.2 ± 32.8. Although the SH excitation by the earthquakes is highly variable, the differences are highly significant statistically. Thirty percent of the earthquakes have higher energy ratios than any of the explosions and 90% of the earthquakes have higher ratios than 67% of the explosions. As the authors point out, the SH generation by earthquakes is azimuth dependent and the station used (Tinemaha) might be located on a node of SH excitation for some of the earthquakes. Although this particular measurement has not been used further, other discriminants based on relative excitation of short period SH motion have been suggested. Field experiments (McEvilly, personal communication) indicate that SH, is observed at close-in distances from explosions.

Although this technique has not been tested extensively, its theoretical basis is reasonable and the initial results are encouraging. The extension of the method to utilize recordings at a number of stations at different azimuths to minimize radiation pattern effects in the earthquake population should provide a meaningful evaluation of its usefulness as a discrimination technique.

5. Lg/Rg Amplitude Ratios

Lg and Rg are defined in Press et al. (1963) as short period Love and Rayleigh waves corresponding to relatively flat portions of higher mode dispersion curves. In their study, Lg amplitude is derived from the vector sum of the peak horizontal motion in the phase Lg arriving in the group velocity window 3.4 to 3.6 km/sec. Rg is the peak amplitude of vertical motion occurring on the window of 2.9 to 3.1 km/sec and thus, may be higher mode or fundamental mode energy. Larger values of the Lg/Rg ratio should be associated with earthquakes and smaller values with explosions. In an earlier presentation, Press (1959) reported that 50% of the earthquakes he studied had values higher than any explosion. Press et al. extend the data base of the earlier study to include 50 earthquakes and 50 explosions. Forty-six percent of the earthquakes fall entirely outside of the range of the explosion data. Sixty percent of the earthquakes fall outside of the range of data for 96% of the explosions. Again, the difference in the mean values for the earthquakes (2.13 ± 1.8) and the explosions (0.77 ± 0.05) is statistically highly significant.

The Lg/Rg ratio may be a discriminant but it requires further evaluation and refinement. The amplitude distributions of these waves are not well understood theoretically and require further work.

6. Pn/Lg, Pg/Lg, and P_{max}/Lg Amplitude Ratios

In the past few years, discriminants based on the amplitude of Lg relative to the amplitude in P have received a major reevaluation. The first presentation of this idea and supporting data is given by Willis et al. (1963) and Willis (1963). Willis (1963) reports on recordings made of one NTS explosion and one earthquake that occurred on NTS and computes 12 amplitude ratios for different portions of these relatively wide band magnetic tape recordings. The distance is approximately 450 km. Among the 12 ratios are Pg/Sn, Sn (essentially)/Pn and Lg/Pn. The largest difference between the two events is shown by the Lg/Pn ratio--2.0 for the explosion and 10.6 for the earthquake.

In a companion paper, Willis et al. (1963) reports on particle velocity ratios of the maximum shear surface waves to the maximum compressional waves (essentially Lg_{max}/P_{max}) for 70 underground NTS explosions and more than 200 earthquakes that cover a world-wide geographic range. The majority of the earthquakes fall in the magnitude range from 1 to 4. To quote the authors, "...it was apparent that earthquakes in general generated larger shear surface waves than the underground nuclear shots". The authors also point out that it is comparatively easy to separate the predominant compressional waves from the predominantly shear surface waves. The results show 78% of the earthquakes have larger ratios than the nuclear shots. Comparing the Lg_{max}/P_{max} ratio as a function of frequency, the authors find that 58% to 83% of the earthquakes can be distinguished. Although the data are not entirely unambiguous (because most of the earthquakes were recorded at distances less than 190 km and most of the explosions were recorded at distances of 190 to 460 km) these papers provide the basis for much of the later work.

Using multivariate statistical analyses, Booker and Mitronovas (1964) study the combined discriminating capability of seven energy ratios computed from 20 earthquakes, 27 nuclear explosions and three explosion collapses. Nine integrals involving the vertical, Z, radial, R, and transverse, T, amplitudes individually squared, and integrals of $T^2 + R^2 + Z^2$ for different group velocity windows are computed. The authors estimate about an 85% probability of correctly classifying a given event as an explosion or an earthquake. Perhaps the most powerful discriminators in this analysis are ratios of energy following S to energy preceding S. This study is important in another sense in that it indicates the major value of using multivariate statistical analyses in discriminating the two populations. The use of the Lg/P ratio was apparently not pursued through the late 1960's. In 1970, Ryall reported on the use of Pg/Sg amplitude ratio in the distance range of 0 to 300 km, which is essentially the same measurement. The earthquake ratio tends to be ≤ 1 while most of the explosion data fall above that line. As the author correctly notes, some of the low Sg generation by earthquakes (resulting in high values of the ratio) may be the result of azimuthal variations in the radiation pattern.

Lukasik (1971) in Congressional Testimony identifies S to P wave amplitude ratios as a discriminant, but does not indicate its degree of usefulness. Following these papers, there is again a hiatus in studies involving this discriminant until the renewal of interest in regional propagation in late 1977. At that time Pomeroy (1977) reported on Lg and P amplitudes in the eastern United

States from 12 earthquakes and the SALMON nuclear explosion detonated in Mississippi. The author shows that, for the earthquakes, Lg amplitudes are approximately ten times the P amplitudes (Lg/P = 10) whereas for SALMON, the ratios are of the order of two to three. Blandford and Hartenberger (1978) report that the ratio of the maximum amplitude before Sn to the maximum amplitude after Sn, as measured on short period vertical instruments, is a "good discriminant". They also report that better separation between explosions and earthquakes is observed in the eastern United States relative to the western United States. At this point, although there was general agreement that the Lg/P discriminant was useful, certain data began to indicate that the application of the discriminant might be difficult, particularly for the USSR where there are essentially no earthquakes in the geographic areas of many of the explosions, so that direct comparison of amplitude ratios along essentially identical paths is not possible. All of the studies reported below suffer this defect. Pomeroy and Nowak (1979) report that for 20 explosions and seven earthquakes, primarily in the western USSR, Lg amplitudes are roughly equal to P wave amplitudes. This is in sharp contrast to the data in eastern North America. The authors note that all of their observations are from WWSSN stations located outside the USSR and that propagation paths crossed significant tectonic boundaries. Plots of $\log \frac{(A/T)\ Lg}{A/T\ (P)}$ indicate that, for the western USSR, the admittedly small earthquake population brackets the explosion population. The authors note that this result requires further refinement and evaluation of the method prior to its use as a discriminant. Although the data sample for the above study contains three East Kazakh events, Pomeroy (1979) extends the study with 25 additional East Kazakh events, four other central USSR explosions, and the Gazli earthquakes as recorded at KBL and MHI, and reported essentially identical results. Pomeroy (1979) also points out that Nersesov and Rautian (1968) had reported on the efficiency of propagation of Lg across Central Asia using seismograms from up to 54 stations along a 3500 km profile labeled Pamir-Lena River from epicentral regions in Cisbaikal, Sinkiang Province, the Gobi Desert, southwest China, and the Himalayas. They report their results in the form of amplitude ratios of Lg to P. For many areas and paths, the ratios are high, indicating that discrimination might be possible, but for the other paths, including all in southwest China and the Himalayas, the observed ratios are low. Pomeroy (1980) analyzes records published by Ruzaiken et al. (1977) and shows that, for those events, Lg amplitudes are significantly higher than P

amplitudes, except for events with propagation paths crossing the Himalayas. Thus the Lg/P amplitude ratio discriminant might be highly useful in those portions of the USSR east of the East Kazakh test site. However, Chen and Pomeroy (1980) point out the necessity for careful regionalization of this discriminant.

Gupta et al.(1980) investigate the propagation of the phases Pn, Pg, Sn, and Lg at regional distances from explosions and earthquakes in western USSR. Their data set includes 19 shallow earthquakes, four intermediate depth earthquakes and ten explosions in the western USSR,as recorded at the WWSSN stations MSH and KBL. They define zones of efficient consistent Lg propagation bounded by azimuths N 30°W to N 60°E of KBL and paths northeast to east of MSH. For transmission paths lying within the regions of efficient Lg propagation, they find that the maximum Lg amplitude is generally larger than maximum P wave amplitude for earthquakes,but generally smaller than that for explosions. This result is not in agreement with the earlier results of Pomeroy and Nowak for the western USSR. In a further study reported in Gupta and Burnetti (1981),recordings at KBL for 13 earthquakes whose propagation paths lay in the zone of efficient, consistent Lg propagation and eight explosions in East and Central Kazakh are investigated in detail. Each vertical component record is divided into ten group velocity windows with boundaries representing the beginning of the first arrival Pn or P and group velocities of 6.0, 5.0, 4.5, 4.0, 3.8, 3.6, 3.4, 3.2, and 2.8 km/sec. The authors point out that the first three windows include Pn, Pg and Sn,respectively. Two earthquakes and three explosions do not provide data from each of the ten windows because of signal clipping in small sections of the records. For each event, the largest amplitude in each group velocity window is first divided by the average of the maximum values in all ten windows. The normalized amplitudes are then averaged over all explosions and all earthquakes. Plotting the individual values of the maximum amplitude in the 8.1 to 5.0 km/sec window (the maximum value before Sn) against the values in the 5.0 to 2.8 km/sec window (the maximum amplitude after Sn or maximum amplitude in Lg) shows the earthquake data and explosion data to overlap. The least square linear regression fit to the explosion data is a factor of approximately 3.5 higher than the earthquake data. This result is similar to the results of Blandford and Hartenberger (1978) and Blandford and Klouda (1980) for western United States which will be discussed below. Gupta and Burnetti also show that comparison of Pn and Lg amplitudes and Pn versus Pg amplitudes also show about the same separation as P_{max} and Lg. They point out that Shurbet (1969) found the amplitude ratio $\overline{P}/P$ (where $\overline{P}$ corresponds to Pg) to be several times larger for NTS explosions than for western United States earthquakes. The Gupta and Burnetti results for these events in the USSR as recorded at MSH are opposite to those of Shurbet. Fitch et al.(1978)

examine four explosions in western USSR and ten eastern US earthquakes and find the ratio of Sn to Lg amplitudes to be substantially larger for explosions than for earthquakes. Gupta and Burnetti's results show negligible discrimination between the two populations based on this discriminant.

Mykkeltveit and Husebye (1980) study 32 explosions and nine earthquakes in the western and central portions of the USSR as recorded at 16 WWSSN stations in Fennoscandia and in areas south of the USSR. They note that Lg is a rather stable phenomenon for propagation in Western Russia/Baltic Shield. These authors find that the most striking feature in the P/Lg type amplitude ratios is the large scatter in the observational data. They conclude that they could find no discriminant of the P/Lg ratio type that could be applied to their data with any degree of success.

Nuttli (1981) investigates Lg propagation in western and central Asia using 16 explosions and six eastern Caucasus earthquakes as recorded at 13 WWSSN stations around the USSR. He obtains values for the coefficient of anelastic attenuation from the Russian uplands region of $0.15\,\mathrm{deg}^{-1}$ and for the region from the Caspian Sea to the southern USSR border of $0.35\,\mathrm{deg}^{-1}$. Using these values and the Vieth and Clawson (1972) P wave attenuation, he determines the theoretical variation of the Lg/P amplitude ratio as a function of the anelastic attenuation. He then plots the deviation of the observed Lg/P ratios from the predicted values as a function of distance. He states "...it can be seen that there is no simple separation between the earthquake and explosion populations such as would be desirable for a discriminant. There is a tendency for the explosion data to lie below the zero value of the ordinate and for the earthquake data to lie above that ordinate value but there are a number of exceptions to such an observation. For the 46 explosion values, the average deviation is -0.280 ± 0.671 and for the 20 earthquake values, it is 0.261 ± 0.494. On the basis of the average deviations, one might conclude that a separation between earthquakes and explosions exists but the large values of the standard deviations indicate that there is an appreciable overlap between the deviations of the explosions and earthquakes. Thus, the ratio of Lg to P amplitudes by itself does not appear to be a reliable discriminant between earthquakes and explosions. Nuttli's study shows that the Lg/P amplitude ratio is strongly dependent on both the epicentral distance and the anelastic attenuation from the source to the receiver. Nuttli also notes that some explosions have Lg to P amplitude ratios that make them more earthquake-like in appearance then most of the earthquakes. Blandford (1980), somewhat in rebuttal, suggests that, in Nuttli's study, the P_{max} was picked only in the first five to ten seconds and, on some crucial seismograms in Nuttli's paper, the maximum occurs much later. Blandford also points out that the Vieth-Clawson P wave amplitude attentuation

curves used for normalization are correct for the P measurements Nuttli used but they are not in agreement with the amplitude-distance results of Nersesov and Rautian (1964). Blandford also argues that the Lg amplitudes were corrected for distance using a formula which varied according to an absorption coefficient determined from the waveform coda instead of a more standard value. Finally, Blandford shows some revised data for the Gupta and Burnetti (1981) data set plotted as a function of azimuth which shows that part of the overlap can be resolved by looking at individual azimuths.

Blandford (1980) provides an excellent summary of the character of regional phases in the US and in Eurasia and provides an excellent overall examination of the use and limitations of the P_{max}/ Lg amplitude ratio technique. His paper summarizes work in his own organization done in the United States which we will describe in greater detail below. Blandford and Klouda (1980) measure amplitudes in the group velocity windows (for Pg between 6.0 and 5.0 km/sec) and Lg (defined as Rg_1 3.6 to 3.4 km/sec; Rg_2 3.4 to 3.0 km/sec, and Rg_3 3.0 to 2.8 km/sec) as recorded at the Tonto Forest Observatory (TFO) from 260 NTS events. Their plot of P_{max} against the log Rg_2 shows remarkably small scatter for explosions in vastly different geologic regimes. The authors point out that the ratio should be plotted for these same events as recorded at different stations to determine if small ratios at one station imply small ratios at all stations. They suggest that the same ratio be measured at TFO for a large number of earthquakes all over the southwestern United States to determine how stable the ratio is in small source regions. Bennett and Murphy (1980) study a sample of 21 earthquakes with an m_b range of 3.3 to 4.6 which occurred within 1^o of the Nevada Test Site as recorded at TFO to compare with the Blandford and Klouda (1980) explosion data Bennett and Murphy exclude all but two events located on the Nevada Test Site and these two events were definitely earthquakes. They measure peak amplitudes in time windows corresponding to the expected regional phases. Plotting, as Blandford and Klouda (1980) did, the log Pg_{max} against the log Lg_{max}, they note that most of their earthquake data fall below the mean explosion line. However, the scatter of the earthquake data is so large that the error bounds envelope the explosion data. Plotting Pn against Lg amplitudes shows the earthquake data to be intermingled with the explosions and thus is not a promising discriminant. Bennett et al. (1981) report measurements on a group of 16 California earthquakes with focal depths of 1 to 16 km as recorded at three different locations on the Nevada Test Site. Although the different recording site geologic conditions result in different amplifications for Lg in agreement with Barker et al. (1980a), the two populations overlap. They plot the

Pg/Lg amplitude ratios as a function of depth and show a tendency for the ratio to increase with increasing focal depth in qualitative agreement with theoretical calculations.

Pomeroy (1980) analyzes data from 45 earthquakes and explosions which occurred in western North America as recorded on the Yellowknife, Canada (YKA) array. P and Lg amplitudes are read. The first significant amplitude in the P train is utilized. The data for NTS explosions tends to separate from the earthquake data but the overlap is considerable.

Finally, Noponen and Burnetti (1980) measure amplitudes at five Alaskan stations from a number of regional earthquakes. Lg is selected as the largest amplitude in the 3.9 to 3.1 km/sec window. Amplitude ratios Lg/P and Pg/P show approximately a 20db change (a factor of 10) with increase in depth from 0 to 70 km. The authors point out that Lg waves are unexpectedly weak at some stations from some shocks e.g. paths crossing a region around a portion of the Denali Fault have the weakest Lg waves. They note that large variations in the Lg/P ratios are observed in the different regions of Alaska and that these variations appear to be related to the region of propagation.

The extensive discussion above indicates that amplitude ratio discriminants of the P/Lg type must be carefully regionalized and compared, where possible, for earthquakes and explosions in the same geographic region. Most researchers agree that the Lg/P amplitude ratio discriminants show a tendency to separate the explosion and earthquake populations but most also agree that the two populations overlap significantly. Disagreement remains as to whether the overlap can be removed by regionalization and by careful comparison of the two populations drawn from the same geographic region.

7. Lg Group Velocity and Energy Ratios in Lg

Pomeroy and Nowak (1978) study 19 eastern North American earthquakes and the SALMON nuclear event as recorded at WWSSN, NEUSSN, the University of Minnesota array, WMSO and CPSO. They show that the Lg group velocity for most of the earthquake data falls at 3.35 km/sec or greater but that values for SALMON fall into the group velocity range of 3.0 to 3.35 km/sec providing some immediate discrimination. To quantify their approach, Pomeroy and Nowak (1978) devise an energy ratio approach. Two group velocity windows 4.0 to 3.4 km/sec and 3.4 to 2.8 km/sec are defined. The faster group velocity window encompasses the range of group velocities which might be encountered in higher

mode Rayleigh waves while the lower window includes group velocity values normally associated with the fundamental mode. The area enclosed by the envelope of the wavetrain in each window is measured and the area is proportional to the energy in the window. Plotting E high versus E low achieves good separation for the eastern North America events. Transferring this technique to the USSR was not a satisfying experience. Pomeroy and Nowak (1979) and Pomeroy (1979) measure group velocities and energy ratios for earthquakes and explosions in the western, central and eastern USSR. Pomeroy (1980) summarizes all of the observations and an examination of the summary figures indicates major overlap and no discrimination using either group velocity or energy ratios. Gupta and Burnetti (1981),using their data set, reach the same conclusion.

Mykkeltveit and Husebye (1980) present Lg group velocity data for the western Russian/Baltic Shield areas and the Eurasian area as measured on WWSSN recordings. All of the group velocity data show an extremely wide scatter from 2.8 to 4.6 km/sec at any distance range. When the authors only plot the group velocity of the strongest phase in the window 4.8 to 2.7 km/sec, a rather clear set of Lg arrivals around 3.5 km/sec is observed.

Noponen and Burnetti (1980) show that Lg group velocity is influenced by source depth at least for Alaskan events recorded in Alaska with the shallowest shocks having the slowest Lg.

The observed anomalies in Lg group velocity appear to be related primarily to differences in crust and upper mantle structure along the propagation paths and thus, neither the Lg group velocity nor the energy ratio appear to be a useful discriminant.

8. Excitation of Sn

Ryall (1970) points out that at 110 km distance from the Nevada Test Site, the Tonapah station recorded only Pg and Sg phases from the explosions, but that recordings of NTS aftershocks had an additional large phase before Sg. Ryall notes that, for this station, the extra S phase, identified as Sn, is characteristic of earthquakes, and the lack of such arrivals is characteristic of explosions. A similar observation was made at the Battle Mountain station for earthquake events along the Fairview Fault contrasted with open pit quarry blasts in the same area. Beyond 140 km, the 'extra' S phase has an apparent velocity of 4.1 km/sec, which is low but not unreasonable for Sn in the Basin and Range region. At smaller distances, the identification is less clear. This suggested discriminant requires further evaluation since the use of this observation as a discriminant has not been pursued.

9. Third Moment of Frequency

Weichert (1971) described a spectral discriminant which expressed the relative high frequency content. The third moment of frequency (TMF) is defined:

$$TMF = \frac{\int_0^5 f^3 A(f)\, df}{\int_0^5 A(f)\, df}$$

where A(f) is the Fourier spectral amplitude and f is frequency in Hertz. This formula effectively weights the high frequency components more than the low frequency components and therefore explosions usually yield high values of this ratio. Investigators in Europe (Dahlman and Israelson, 1977) have found this to be a quite useful discriminant at teleseismic distances. The latter authors show a plot of TMF versus m_b for explosions in East Kazakh and earthquakes in the Kirghiz-Sinkiang region as recorded at Hagfors, Sweden. The two populations show strong separation. While these data are at teleseismic distances, the principle should be tested at regional distances.

10. Generation of Higher Mode Surface Waves

This is really a variant of discriminant 4 above, but the distinction here is that we are considering waves in the 2 to 12 second period range as commonly recorded on broad band or long period instruments. It is striking, in reviewing the history of the discrimination programs in both the United States and the USSR, how the results of the respective programs have been shaped by the differences in instrumentation available to the scientists in each country. In the United States, the short period (1-.75) instruments and the long period (15-100) instruments of the WWSSN focused attention on the short period ($\sim$ 1 Hz) body waves and the long period (12 to 50 sec) fundamental mode surface waves. In the USSR, the Kirnos system with response in the 1 to 12 second period range focused attention on higher mode surface waves. To our knowledge, no systematic study has been carried out for higher mode surface waves in this period range for explosions recorded at regional distances. There are very few discussions in the literature of the excitation of higher mode surface waves by explosions. Shurbet (1969) examines seismograms for a number of NTS events recorded at Lubbock, Texas as well as those from two small earthquakes which occurred near the Nevada Test Site and had propagation paths similar to the explosions. The explosion records show an absence of higher mode waves while the

higher mode Rayleigh energy is clearly recorded for the earthquakes. Examination of other WWSSN records (JCT, DAL, TUC, and GOL) confirm the absence of the higher mode data for the explosions. Forsyth (1976) describes a magnitude scale using higher mode surface wave amplitudes and,using that scale, he is able to classify some 'anomalous' USSR earthquakes correctly. That study indicates the value of the intermediate period range waves for discrimination. While some aspects of higher mode propagation by explosions and earthquakes are currently under investigation, much additional work is required. (The important point here and for the long period discriminants discussed below is that the nearer the recording station is to the source, the stronger are the short, intermediate, and long period surface waves. At regional distances, long period waves (both body and surface) can be more easily recorded and used in discrimination studies.)

11. Peak Amplitudes of Love and Rayleigh Waves and Long Period Surface Wave Energy Density

Brune et al. (1963) originated the concept of measuring the difference in energy content of long period surface waves from explosions and earthquakes. These authors use data from explosions and earthquakes in the California-Nevada region and show a remarkable distinction between the two source types using the envelope of the surface wavetrain as a measure of the energy content. Press et al. (1963) extend this work by examining records at shorter distances. These authors first measure peak amplitudes from Pasadena seismograms for 54 earthquakes and 50 NTS explosions. The earthquake magnitudes range from 3.5 to 5.3 and distances range from 250 to 650 km. Maximum amplitudes were measured for both Love and Rayleigh waves. Regression lines fitted to maximum amplitudes as a function of magnitude show no statistical difference between the explosion and earthquake populations. For a sample of seven explosions and 24 earthquakes, 40% of the earthquakes have peak Love wave amplitudes that fall outside the explosion range. For a sample of 11 explosions and 21 earthquakes, 30% of the earthquakes have peak Rayleigh wave amplitudes that fall entirely outside the explosion range. The authors then compute the energy density ($\int g^2(\omega)\, d\omega$) over the period band 7 to 30 seconds for a population of 10 earthquakes and 10 explosions in the same distance and magnitude range. A separation similar to that achieved by Brune et al. (1963) is achieved; i.e., 80% of the earthquake values fall entirely outside the range observed for explosions.

Although the peak amplitude methodology does not appear useful, the energy density method holds out promise as a discriminant. It should be evaluated at a number of recording stations at different azimuths and distances from known sources particularly on broad band recordings.

12. Prevailing Period of Long Period Love Waves

Press et al.(1963) note the greater excitation of long period Love waves by many earthquakes at regional distances. All the explosion Love wave spectra they studied peak at periods of less than 8 seconds whereas the earthquakes with corresponding distances and magnitudes peak at periods greater than or equal to 13 seconds. For a sample of 4 explosions and 3 earthquakes, 100% of the earthquakes fall outside the range of values of the explosions. Of course, this sample is too small to be statistically meaningful. In 1971, Lukasik (1971), in Congressional Testimony, classed this diagnostic in the "poor and have been abandoned" category.

As noted earlier, the spectral distribution of long period energy at regional distances particularly in the 2 to 12 second period range has not been adequately studied. However, the well-documented anisotropic components of explosions might preclude this method as a useful discriminant.

13. Spectral Ratio--Long Period S Waves to Rayleigh Waves

In his discussion of other methods of discriminating earthquakes from explosions at teleseismic distances, Douglas (1980) mentions several methods that have been suggested for discrimination using S waves. Among these is the ratio of long period S to Rayleigh amplitudes (Von Seggern,1972; Blandford and Clark, 1974). No evaluation of this method has been published in the literature but since the detection of these phases at regional distances becomes easier, this could be an interesting discriminant candidate.

14. Spectral Ratio--Long Period Love Waves to Rayleigh Waves

Press et al.(1963) examine broad band long period spectra of Love and Rayleigh waves for four explosions and 11 earthquakes. They note that Love to Rayleigh ratios for the explosions never exceed 2 and average about 1. Of the 11 earthquake ratios determined, eight have values exceeding 2 i.e. 70% of the earthquakes fall outside the range of the explosion data. While today we know that non-isotropic source components can have major effects on surface wave generation, this method may still be significant in a multidiscriminant approach to the identification problem.

15. Frequency of Peak Spectral Amplitudes and Spectral Ratios in Pn, Pg, S, and Lg

Ryall (1970) presents spectra of high frequency (.5 to 5 Hz) P and S waves from three explosions and three earthquakes recorded in Nevada at distance ranges of approximately 100 to 250 km. He plots the frequency of the peak spectral amplitude for the P and S waves separately and, on the basis of this admittedly small sample, achieves some separation between the two source types. His peak amplitudes fall in the range of 1 to 3 Hz.

Bakun and Johnson (1970) examined the spectral content of the Pn and Pg phases recorded at Jamestown (JAS), California for 69 explosions and earthquakes with magnitudes ranging from 2.8 to 4.5 located within 100 km of NTS. The events studied included explosions, natural earthquakes, after events of explosions, collapses of explosion cavities, and unidentified events on NTS. The authors find that a spectral ratio of average ground displacement in the 0.6 to 1.25 Hz band to that in the 1.35 to 2.0 Hz band is a satisfactory discriminant. Plotting this spectral ratio as a function of magnitude, they define two fields based on the observation that the explosion spectra for Pg are relatively richer in the high frequency band (1.35 to 2.0 Hz) than are the natural earthquake spectra. The authors note that frequency content of Pg from the afterevents of the explosions is closer to the explosion classification then to that of true earthquakes.

Bennett et al. (1981) examine digital data for SALMON and the Alabama earthquake at different LRSM stations along a northeast profile. They observe that the SALMON Pn spectrum is greater in value and peaks at a higher frequency than the earthquake spectrum and that these differences are observed even if the spectra are averaged or smoothed. In contrast, the Pg spectral estimates from the two events are roughly similar. They suggest, based on the Pn observations, that a variable frequency magnitude (spectral ratio) type of discriminant may be effective. These authors compute the spectrum of the maximum pulse in Lg for the BRPA recording of the Alabama earthquake and compared it with the Pg pulse spectrum. The Lg spectrum peaks at a lower frequency than Pg and is richer in low frequency energy. The authors also present moving window spectral estimates of Lg from SALMON as recorded at EUAL, a distance of 242 km. This type of digital implementation of analyses for regional phases, used for many years in marine seismology, may allow significant advances in our understanding of Lg wave propagation.

Murphy and Bennett (1981) recently presented an exciting idea using a data set on the spectral characteristics of Pn, Pg, and Lg as recorded at TFO from 28 NTS explosions and 15 earthquakes within 1^{o} of NTS. The magnitude range for the explosions was 3.7 to 4.8 and for the earthquakes 3.3 to 4.3. Spectra of Pn, Pg, and Lg were obtained in the frequency range of 0.5 to 5 Hz. For Pn and Pg, the authors report comparable frequency content for the explosions and earthquake populations but, for Lg, the earthquakes are shown to be significantly richer in the high frequencies than the explosions. This observation needs to be evaluated at other stations and in other geographic environments but it may provide a powerful regional discrimination capability.

Spectral ratios of Pg (from Bakun and Johnson) and for Lg (from Murphy and Bennett) appear to provide significant discrimination capability. Again, the reported studies generally involve measurements at one station and events in one geographic region. These two discriminants should be evaluated to determine 'robustness' in different areas using a number of stations at different azimuths.

Conclusions on Review of Regional Discriminants

Intercomparison of the above discriminants is extremely difficult in that 1) they have been applied to different explosion and earthquake test populations; 2) usually the same recording stations are not involved; 3) the number of recording stations is small and has poor azimuthal distribution; and 4) the discriminants have been tested on only one geologic or geographic environment. There is a clear need to evaluate all of these (and perhaps other) regional discriminants using a common data set. With the common data set, the discriminants should be evaluated individually and in multivariate statistical analyses including discriminant function analyses, factor analyses, and cluster analyses in a manner analogous to the evaluation of teleseismic discriminants. A systematic analysis of these discriminants would allow an evaluation of our present capability to effectively use regional data in monitoring underground explosions.

Nevertheless, to summarize this discussion of discriminants, the following points should be noted.

1. The most promising discriminants appear to be
   a. the regional variant of the M_S:m_b criterion
   b. the excitation of short period SH waves
   c. generation of higher mode surface waves
   d. long period surface wave energy density
   e. spectral ratios in Pg and Lg
   f. arguably, Lg/P amplitude ratios.

2. Proposed discriminants requiring additional documentation include:
   a. Lg/Rg amplitude ratios
   b. excitation of Sn
   c. third moment of frequency
   d. long period S to Rayleigh wave amplitudes
   d. arguably, the spectral ratio of long period Love to long period Rayleigh waves.

3. Proposed discriminants which probably should be abandoned include:
   a. first motion
   b. P^2/P^1 ratio
   c. Lg group velocity and energy ratios
   d. prevailing period of long period Love waves.

SUMMARY AND RECOMMENDATIONS

The principal conclusions of this review can be summarized as follows:

1. Seismic data recorded at regional distances ($< \sim 30^{\circ}$) can provide important information for monitoring test ban treaties, independent of the availability of such data from 'internal' stations, since data are available for many test locations from 'external' stations located $\sim 20^{\circ}$ to 30° from the sources.

2. A large body of regional seismic data is available for use in evaluating the usefulness of the regional discrimination and yield determination techniques discussed in the text.

3. Numerous techniques for discrimination using regional data have been suggested and, in some cases, developed. However, most of these potential tools for discrimination have been tested on limited data sets usually from one geographic region, and often utilizing only one or two recording stations. No systematic evaluation of these techniques individually has been carried out, nor has any multi-variate analysis been done of combinations of these potential discriminants. There is a high incidence of reports indicating that a particular technique works 'sometimes', but no *concensus has* developed with regard to the best combination of these discriminants.

4. A major recommendation of this study is that a systematic evaluation of all the proposed regional discriminants be carried out using a common data base covering all the different test sites. The discriminants should be evaluated systematically for their success/failure ratio, both individually and in combinations using multi-variate statistical tools. The purpose of this evaluation would be to determine the present capability for discrimination using these techniques and to point out promising directions for future research.

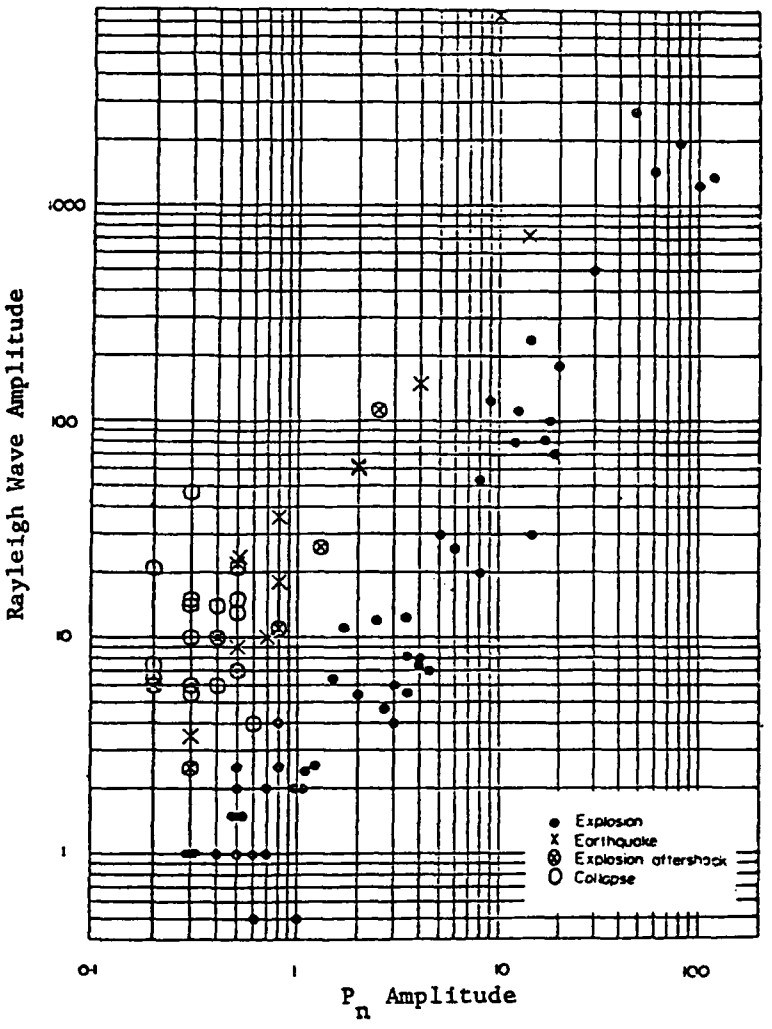

Figure 1-1. Rayleigh wave amplitude versus Pn amplitude as recorded at Berkeley, California (McEvilly and Peppin, 1972).

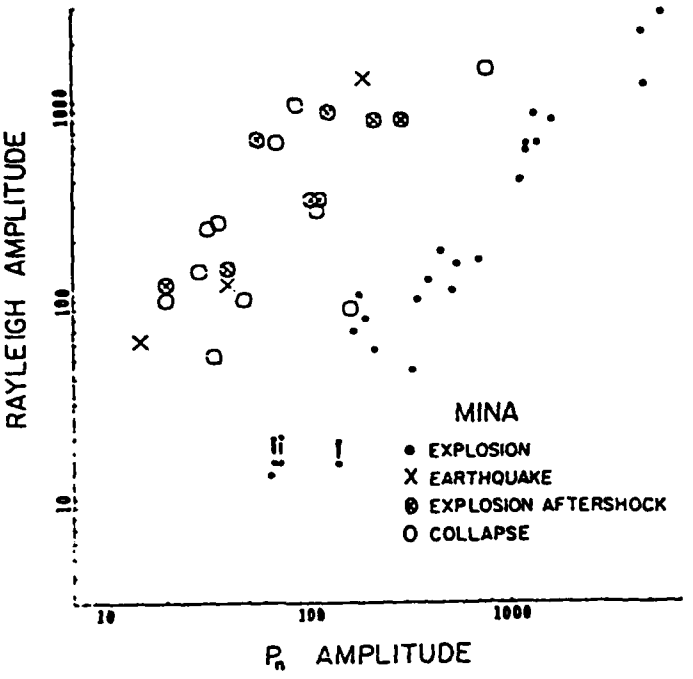

Figure 1-2. Rayleigh wave amplitude versus Pn amplitude at the Mina, Nevada station of the UC-LLL network (Peppin and McEvilly, 1974).

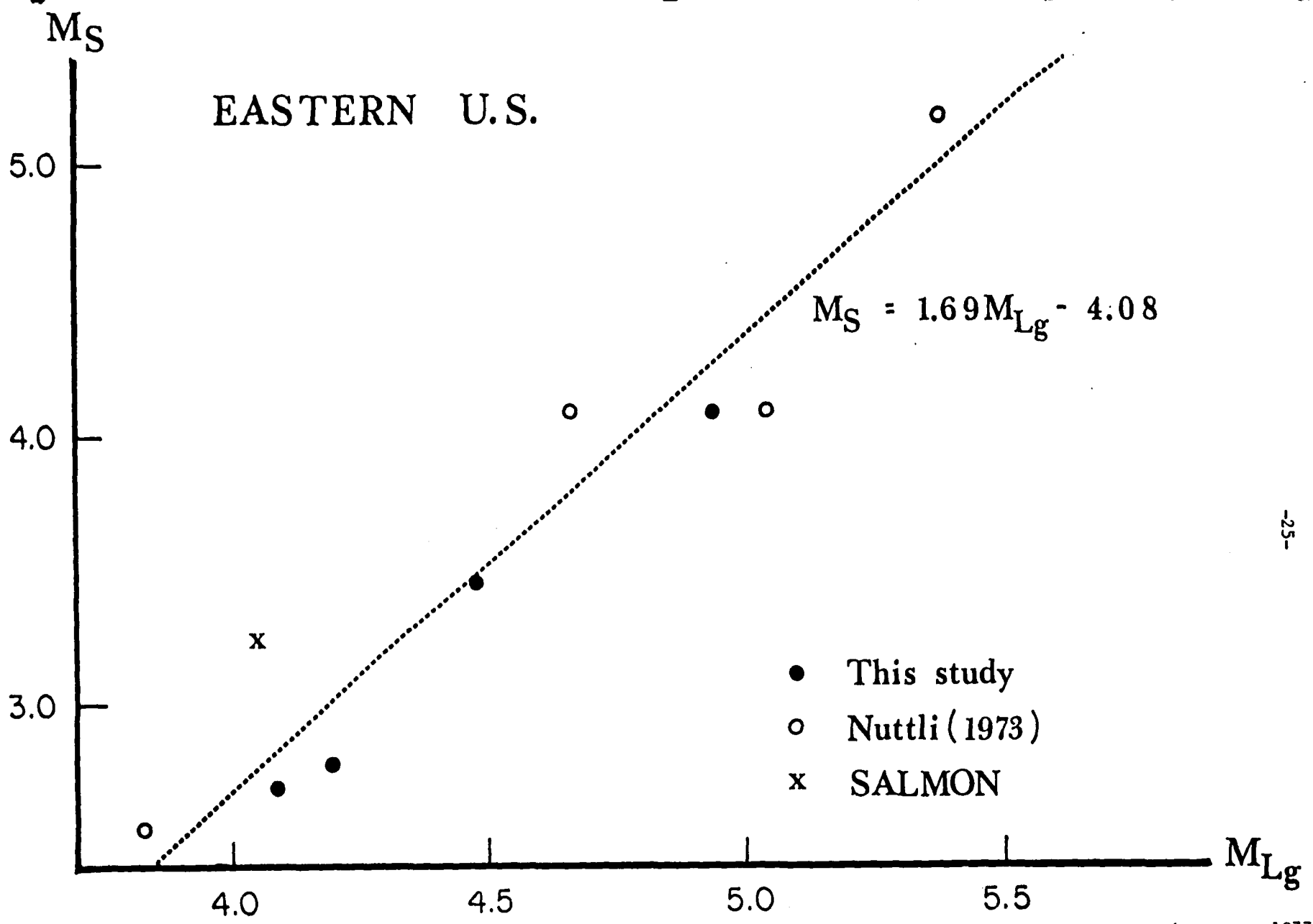

Figure 1-3. M_S:m_{bLg} relationships for eight eastern United States earthquakes and the SALMON explosion (Pomeroy, 1977).

References

Bakun, W.H. and L.R. Johnson (1970), Short period spectral discriminants for explosions, Geophys. J. Roy. Astron. Soc., 22, 139-152.

Barker, B.W., Z.A. Der and C.P. Mrazek (1980a), The effect of crustal structure on the regional phases Pg and Lg at NTS in Studies of Seismic Wave Characteristics at Regional Distances, Teledyne-Geotech Report AL-80-1, Teledyne-Geotech, Alexandria, Virginia.

Basham, P.W. (1969), Canadian magnitudes of earthquakes and nuclear explosions in South Western North America, Geophys J. Roy. Astron. Soc., 17, 1-13.

Bennett, T.J. and J.R. Murphy (1980), A study of the relative excitation of regional phases for use in event discrimination, presented at VSC Research Conference, November, 1980.

Bennett, T.J., D.G. Lambert, J.R. Murphy, J.M. Savino and C.B. Archambeau (1981), in Regional Discrimination Research VSC-TR-81-20, Systems, Science and Software, La Jolla, California.

Blandford, R.R. and D. Clark (1974), Detection of long period S from earthquakes and explosions at LASA and LRSM stations with application to positive and negative discrimination of earthquakes and underground explosions, Report SDAC-TR-74-15, Teledyne-Geotech, Alexandria, Virginia.

Blandford, R.R. and R.H. Hartenberger (1978), Regional discrimination between earthquakes and explosions (Abstract), EOS, Trans. Am. Geophys. Union, 59, 1140.

Blandford, R.R. (1980), Seismic discrimination problems at regional distances, NATO, Advanced Study Institutes, Series C, 74, D. Reidel Publishing Company, Dordrecht, Holland.

Blandford, R.R. and P. Klouda (1980), Magnitude-yield results at the Tonto Forest Observatory in Studies of Seismic Wave Characteristics at Regional Distances, Teledyne-Geotech Report AL-80-1, Teledyne-Geotech, Alexandria, Virginia.

Bolt, B.A. (1976), Nuclear explosions and earthquakes--the parted veil, W.H. Freeman and Company, San Francisco, 309 p.

Booker, A. and W. Mitronovas (1964), An application of statistical discrimination to classify seismic events, Bull. Seism. Soc. Am., 54, 961-971.

Brune, J., A. Espinosa and J. Oliver (1963), Relative excitation of surface waves by earthquakes and underground explosions in California and Nevada, J. Geophys. Res., 68, 3501-3513.

Chen, T.C. and P.W. Pomeroy (1980), Regional Seismic Wave Propagation, Semi-Annual Technical Report No. 5, Rondout Associates, Incorporated, Stone Ridge, New York.

Dahlman, O. and H. Israelson (1977), Monitoring underground nuclear explosions, Elsevier Scientific Publishing Company, Amsterdam, 440 p.

Douglas, A. (1980), Seismic Source Identification: A review of past and present research efforts, NATO, Advanced Study Institutes, Series C, 74, D. Reidel Publishing Company, Dordrecht, Holland.

Fitch, T.J., M.W. Shields and R.E. Needham (1978), Comparison of crustal-phase magnitudes for explosions and earthquakes in Seismic Discrimination, Semi-Annual Technical Summary Report: 1 October 1977 to 31 March 1978, Lincoln Laboratory, M.I.T., Lexington, Massachusetts.

Forsyth, D.W. (1976), Higher mode Rayleigh waves as an aid to seismic discrimination, Bull. Seism. Soc. Am., 66, 827-841.

Gupta, I.N., B.W. Barker, J.A. Brunetti and Z.A. Der (1980), A study of regional phases from earthquakes and explosions in western Russia, Bull. Seism. Soc. Am., 70, 851-872.

Gupta, I.N. and J.A. Burnetti (1981), An investigation of discriminants for events in western USSR based on regional phases recorded at station Kabul, Bull. Seism. Soc. Am., 71, 263-274.

Liebermann, R.C. and P.W. Pomeroy (1969), Relative excitation of surface waves by earthquakes and underground explosions, J. Geophys. Res., 74, 1575-1590.

Lukasik, S.J. (1971), Statement in Status of Current Technology to Identify Seismic Events as Natural or Man-Made, Hearings before the Sub-Committee on Research, Development, and Radiation of Joint Committee on Atomic Energy, 92nd Congress, October 27-28, 1971, pp 17-67.

Marshall, P.D. and P.W. Basham (1972), Discrimination between earthquakes and underground explosions employing an improved M_S scale, Geophys. J. Roy. Astron. Soc., 28, 431-458.

McEvilly, T.V. and W.A. Peppin (1972), Source characteristics of earthquakes, explosions, and afterevents, Geophys. J. Roy. Astron. Soc., 31, 67-82.

Murphy, J.R. and T.J. Bennett (1981), Spectral characteristics of short period regional phases recorded from NTS explosions and earthquakes (Abstract), in Program, Eastern Section, Seismological Society of America, October 26-28 at Milwaukee, Wisconsin.

Mykkeltveit, S. and E.S. Husebye (1980), Lg wave propagation in Eurasia, in Identification of Seismic Sources-Earthquake or Underground Explosions, NATO, Advanced Study Institutes, Series C, 74, D. Reidel Publishing Company, Dordrecht, Holland.

Nersesov, I.L. and T.G. Rautian (1964), Kinematics and dynamics of seismic waves to distances of 3500 km from the epicenter, Akad. Nauk SSSR, Trudy Inst. Fiziki Zemli, 32, 63-87.

Noponen, I. and J. Burnetti (1980), Alaskan regional data analyses in Studies of Seismic Wave Characteristics at Regional Distances, Teledyne-Geotech Report AL-80-1, Teledyne-Geotech, Alexandria, Virginia.

Nuttli, O.W. (1973), Seismic wave attenuation and magnitude relations for eastern North America, J. Geophys. Res., 78, 876-885.

Nuttli, O.W. (1981), On the attenuation of Lg waves in western and central Asia and their use as a discriminant between earthquakes and explosions, Bull. Seism. Soc. Am., 71, 249-262.

Peppin, W.A. and T.V. McEvilly (1974), Discrimination among small-magnitude events on Nevada Test Site, Geophys J. Roy. Astron. Soc., 37, 227-243.

Pomeroy, P.W. (1977), Aspects of Seismic Wave Propagation in eastern North America-A Preliminary Report, Rondout Associates, Incorporated, Stone Ridge, New York.

Pomeroy, P.W. and T.A. Nowak, Jr. (1978), An Investigation of Seismic Wave Propagation in eastern North America, Semi-Annual Technical Report No. 1, 15 December 1977-30 June 1978, Rondout Associates, Incorporated, Stone Ridge, New York.

Pomeroy, P.W. and T.A. Nowak, Jr. (1979), An Investigation of Seismic Wave Propagation in western USSR, Semi-Annual Technical Report No. 2, Rondout Associates, Incorporated, Stone Ridge, New York.

Pomeroy, P.W. (1979), Regional Seismic Wave Propagation, Semi-Annual Technical Report No. 3, Rondout Associates, Incorporated, Stone Ridge, New York.

Pomeroy, P.W. (1980), Regional Seismic Wave Propagation, Semi-Annual Technical Report No. 4, Rondout Associates, Incorporated, Stone Ridge, New York.

Press, F. (1959), Verbatim record of second meeting, Conference on Discontinuance of Nuclear Weapons Tests, Technical Working Group 2, United Nations.

Press, F., G. Dewart and R. Gilman (1963), A study of diagnostic techniques for identifying earthquakes, J. Geophys. Res., 68, 2909-2928.

Ruzaikin, A.I., I.L. Nersesov, V.I. Khalturin and P. Molnar (1977), Propagation of Lg and lateral variations in crustal structures in Asia, J. Geophys. Res., 82, 307-316.

Ryall, A. (1970), Seismic identification at short distances in Copies of Papers Presented at Wood's Hole Conference on Seismic Discrimination, 2, DARPA, Arlington, Virginia, unpaginated.

Shurbet, D.H. (1969), Excitation of Rayleigh waves, J. Geophys. Res., 74, 5339-5341.

Von Seggern, D.H. (1972), Seismic shear waves as a discriminant between earthquakes and underground nuclear explosions, SDL Report 295, Teledyne-Geotech, Alexandria, Virginia.

Wiechert, D.H. (1971), Short period spectral discriminant for earthquake and explosion differentiation, Z. Geophys., 37, 147-152.

Willis, D.E. (1963), Comparison of seismic waves generated by different types of sources, Bull. Seism. Soc. Am., 53, 965-978.

Willis, D.E., J. DeNoyer and J.T. Wilson (1963), Differentiation of earthquakes and underground nuclear explosions on the basis of amplitude characteristics, Bull. Seism. Soc. Am., 53, 979-987.

2. YIELD DETERMINATION USING REGIONAL SEISMIC PHASES

EXECUTIVE SUMMARY

1. Amplitude-yield curves have been determined from 12 NTS events for three components of Lg, Pg, and P as recorded at WWSSN stations in the conterminous United States.

2. The use of regional seismic phases, Lg and Pg can provide valuable semi-independent determinations of yield for NTS events recorded at the WWSSN stations in the conterminous United States. A comparison of the standard deviation of slope values of the amplitude-yield relationships for Pg(Z), Pg(L), Pg(T), Lg(Z), Lg(L), and Lg(T) with those of P(Z), P(L), and P(T) indicates a tighter cluster for the Lg and Pg values.

3. Lg amplitudes from NTS events, as recorded at WWSSN stations in the conterminous United States,do not appear to be significantly affected by non-isotropic source components.

4. Lg(T) amplitudes are consistently larger than Lg(Z) amplitudes at the same station at all the epicentral distances studied in this report.

5. Certain stations show tighter cluster of data points for Lg while other stations appear more suitable for Pg amplitude-yield determinations. A few stations appear equally reliable for Lg and Pg amplitude measurements.

6. This methodology involves the direct determination of a yield value at each recording station. For a network yield, the individual yield values should be averaged. This contrasts with other methodologies where a magnitude at each station is obtained and the magnitudes are then averaged and a single magnitude-yield curve used to obtain yield.

YIELD DETERMINATION USING REGIONAL SEISMIC PHASES

Introduction

This study deals with the usefulness of regional waves such as Lg(Z), Lg(L), Lg(T), Pg(Z), Pg(L), Pg(T), P(Z), P(L), and P(T) for determining yield from explosions detonated at the Nevada Test Site. Until recently, very little work has been done on the use of regional seismic waves, such as these to determine the yield of underground nuclear explosions. This lack is largely related to the fact that teleseismic methods of determining yield were in use throughout the late 1960's and early 1970's and,when discussions of the Comprehensive Test Ban Treaty returned to the concept of monitoring stations at regional distances, the principal use of these stations was seen as providing additional discrimination capability. During the last two years, the regional phases such as Lg and Pg, which would be recorded at these stations, have been used in studies carried out under this contract to determine yield of some United States events and the results of those studies will be outlined below.

Baker (1967, 1970) investigates the use of Lg to determine magnitude of 78 explosions (75 Nevada Test Site events) using amplitude data reported from Long Range Seismic Measurements (LRSM) stations. About 1400 measurements of Lg in the distance range of 50 to 400 km from 79 stations are utilized. Baker's study is apparently intended to determine if a methodology involving Lg could provide a better measure of size than the then current use of m_b involving Pn measurements in the regional distance range. Evernden (1967) had shown that the Pn methodology applied to NTS events gives values of m_b (or m) over-estimated by approximately 1.5 magnitude units and he developed a method of normalizing regional and near regional data bringing it into agreement with teleseismic measurements of magnitude. Springer and Hannon (1973) use Pg data in the distance range 10 to 140 km (and some Wood-Anderson data that is indicated as Pg or Sg (?) maximum at distances of 375 to 520 km) to establish amplitude-yield scaling laws for NTS events recorded at United States and Canadian stations. Baker (1970) points out that, where Lg is recorded, its trace is usually dominant and easier to measure than body wave traces and his principal conclusion is that, for the 68 events in his final data set, magnitude based on Lg shows smaller standard deviation in 60 cases than the Pn measurements.

In the mid 1970's, regional seismic networks were being established in various parts of the United States and overseas to monitor seismic hazard. Nuttli (1973) published an important paper on determining magnitudes from Lg and his methodology has become an almost standard practice in many of these regional networks. One of the principal reasons for this adoption is that, as we observed earlier, at low magnitudes, Lg is often the only clearly observable phase. Thus, to assign relative size to low magnitude events, Lg is almost the only candidate wave to measure. Similarly, if we are interested in the size of small magnitude explosions, the only records obtained for the event may be those from stations at regional distances and thus Lg (and, in some cases, Pg) may be the only waves recorded and available for magnitude (or yield) determinations. Regional studies in the eastern and central United States have shown that Nuttli m_b (Lg) is essentially equivalent to M_L in the low magnitude ranges (3 to 5) of interest here.

Alexander (1980) investigates the propagation of Lg and other crustal phases and concludes that, in North America particularly but also in Eurasia and Africa, Lg appears to provide a stable estimation of yield that is not contaminated by non-isotropic effects and is nearly independent of source medium. Blandford and Klouda (1980) measure seven phases on the vertical component records from the central element of the Tonto Forest Seismic Observatory (TFO) for 260 NTS events. The measurements made are 1) a, b, and c, the amplitudes of the first three half cycles of the initial P waves with a velocity greater than 6 km/sec, 2) P_{max} in the velocity range 5 to 6 km/sec, and 3) Rg_1, Rg_2, and Rg_3 (i.e. three portions of the Lg(Z) wavetrain with amplitudes in the velocity windows 3.6 to 3.4, 3.4 to 3.0, and 3.0 to 2.8 km/sec, respectively, as measured on vertical component short period seismograms). From their work, it can be concluded that P_{max} and Rg_2 each independently provide a measure of yield showing smaller scatter than the initial P measurements. These authors also show that the scatter of P_{max} and Rg_2 amplitudes is less than that of M_S, and the scatter or P_{max} and Rg_2 are independent of source medium. While it must be noted that these results are valid only for a single station (TFO), they point the way toward independent supplemental measurements of seismic yield when regional data are available.

After a review of the sources and receiving stations used in our study, the use of Lg to determine yield will be addressed extensively followed by shorter descriptions of the use of Pg data and P data for yield determination.

Data

Source--The pertinent source data on the 12 explosions utilized in this baseline study are listed in Table 2-1. Data on the test events is given in Table 2-2.

The nuclear explosions used in the baseline study were selected from the event set examined by Aki and Tsai (1972) in a paper entitled, "Mechanism of Love-wave excitation by explosive sources". In the paper, Aki and Tsai examined the amplitude ratios of long period ($T > 10$ sec) Love waves to Rayleigh waves from 18 underground nuclear explosions at Yucca Flat on the Nevada Test Site. Finding variations among the amplitude ratios of the explosion; they divided the explosions into three groups according to the different ratios: the strong, intermediate, and weak exciters of Love waves. They also found a correlation between the efficiency of Love wave excitation and the magnitude and/or the burial depth of the detonation. (Due to the strong correlation between source depth and source size, they were unable to separate the two effects.) Thus, by using the body wave magnitude of the event as the dependent variable, they were able to test whether the condition of different test sites affects the level of Love wave excitation. The site conditions considered were: the depth of the water table and alluvium-tuff interface and the distance between the shot point and the more competent basement rocks. The only satisfactory separation of these different groups is suggested by a plot of m_b of the event versus testing data, about which Aki and Tsai state, "a magnitude threshold (or depth threshold, since we cannot separate the two factors) may exist for strong excitation of Love waves, and the threshold apparently increased with time during the periods 1962 to 1969". Based on this observation and other arguments, they came to the conclusion that a model of tectonic strain release following a bigger explosion offered the most satisfactory interpretation.

Since the objective in this study is to investigate the various aspects of short period wave generation by underground nuclear explosions, the study by Aki and Tsai presents two desirable features. Firstly, the closely located events (the events selected for our study were confined within an area 11X6 km) providing an almost identical source-receiver geometry from the different explosions to a given station. The common propagation path (and the associated propagation effects) allows us to attribute the observed discrepancies at the

TABLE 2-1

DATA ON

U.S. NUCLEAR EVENTS

UTILIZED IN THIS STUDY

	NAME	DATE	ORIGIN TIME	DEPTH (M)	ANNOUNCED YIELD	LONG PERIOD LOVE WAVE EXCITATION
1.	CORDUROY	3 DEC. 1965	15:13:02	208	100	STRONG
2.	CUP	26 MAR. 1965	15:34:08	164	35	STRONG
3.	COMMODORE	20 MAY 1967	15:00:00	227	230	STRONG
4.	DUMONT	19 MAY 1966	13:56:28	205	190	STRONG
5.	BOURBON	20 JAN. 1967	17:40:03	171	29	INTERMEDIATE
6.	BUFF	16 DEC. 1965	19:15:00	152	36	INTERMEDIATE
7.	FORE	16 JAN. 1964	16:00:00	151	19	INTERMEDIATE
8.	TAN	3 JUNE 1966	14:00:00	171	140	INTERMEDIATE
9.	WAGTAIL	3 MAR. 1965	19:13:00	229	65	INTERMEDIATE
10.	AUK	2 OCT. 1964	20:03:00	138	12	WEAK
11.	CHARCOAL	10 SEPT. 1965	17:12:00	139	20	WEAK
12.	PIRAHNA	13 MAY 1965	13:30:00	167	100	WEAK

TABLE 2-2
TEST EVENTS

	SALMON	GASBUGGY	PILEDRIVER
DATE	22 OCT. 1964	10 DEC. 1967	2 JUNE 1966
ORIGIN TIME	16:00:00 Z	19:30:00 Z	15:30:00 Z
LOCATION	NEAR HATTIESBURG, MISS.	DULCE, NM	CLIMAX NTS
BURIAL MEDIUM	SALT	SHALE	GRANITE
ANNOUNCED YIELD	5.3	29	56
SEISMIC YIELD			
FROM L_g (NUMBER OF POINTS)	5.0 ± 4.4 (11)	22.4 ± 17.8 (27)	61.5 ± 38.0 (32)
P	7.6 ± 7.9 (10)	21.3 ± 7.4 (16) 187.5 ±113.3 (11)	156.2 ± 88.6 (27)
P_g	NO DATA	43.2 ± 46.4 (9)	107.1 ± 52.5 (14)

station to source effects. Secondly, the study of Aki and Tsai succeeded in determining tectonic strain release as the causal mechanism for the anomalous excitation of long period Love waves at Yucca Flat, NTS. Our aim is to estimate the yield of an explosion from the amplitudes of the Lg wave which results from the superposition of higher-mode Love and Rayleigh waves. Hence, we are interested in knowing whether tectonic strain release has a correspondingly large effect on Lg, and if so, what relationship between the amplitudes of long period surface waves and those of Lg exists.

Receiver

Figure 2-1 shows the geographic distribution of the underground nuclear explosions, and the WWSSN stations used in this study and one interpretation of the tectonic provinces in the United States. Even though the WWSSN short period seismograph system has a response sharply peaked around 1 sec (T pendulum $\sim$ 1.0 sec, T galvanometer $\sim$ 0.75 sec), waves with periods ranging from 0.5 to 4 to 5 seconds can usually be observed on its seismograms. Furthermore, since NTS is located in a structurally complicated region, most of the great-circle paths traverse one or more tectonic provinces.

Measuring Procedure

The amplitudes used to derive the amplitude-yield relations and the attenuation coefficients were obtained in the following fashion. For P waves, the maximum peak-to-peak amplitude is measured from the initial three cycles. For Pg and Lg waves, the measuring scheme is slightly different. When the predominant period around the appropriate group-velocity (6.0 km/sec for Pg, 3.5 km/sec for Lg) is less or equal to 1.5 sec, the peak-to-peak amplitude of the third largest wavelet is measured; otherwise ($T > 1.5$ sec), the maximum amplitude is used. The underlying motives for this approach are: 1) to reduce the chance of measuring any spuriously large amplitude resulting from constructive interference, the occurrence of which is common at short periods, and 2) to obtain a representative value for the maximum amplitude of the coda. Adverse conditions such as missing or poorly recorded seismograms, high magnification at nearby stations and vice versa, and noise (both electronic and natural) have reduced the number of usable seismograms at some stations.

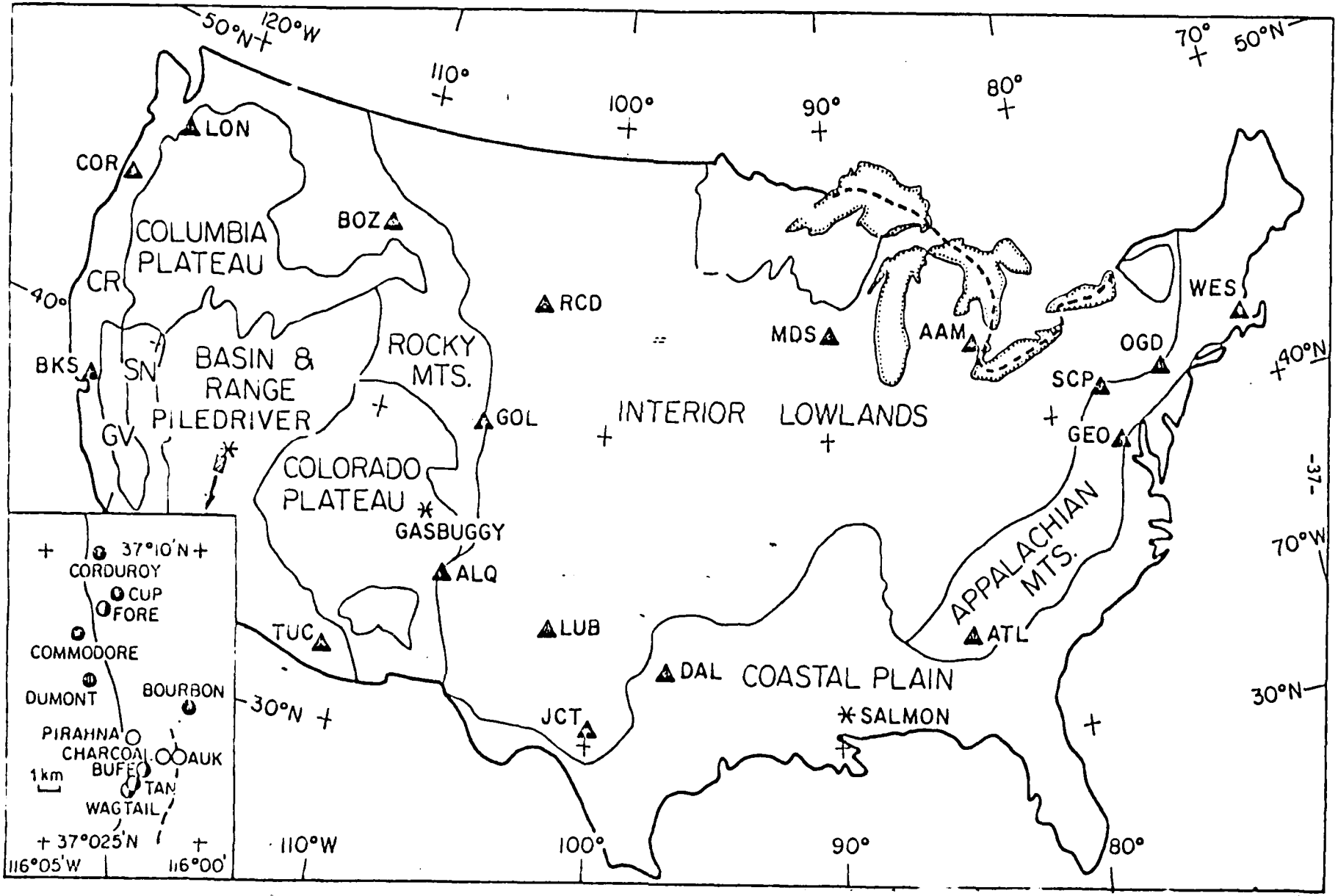

Figure 2-1. Location of the seismograph stations (solid triangles) and under[illegible]und nuclear explosions (asterisks) used in this study. The tectonic map is modified from that of King (1977). I[illegible]the insert, solid, half-filled, and open circles represent strong, intermediate, and weak exciters of Love waves (modified from Aki and Tsai, 1972). CR=Coastal Ranges, GV=Great Valley, SN=Sierra Nevada.

A. Lg versus Yield

Introduction

This study deals with the usefulness of Lg(Z, L, or T) in evaluating yield from explosions detonated at the Nevada Test Site. The issues in this study are:

1. to evaluate the effect of tectonic strain release on Lg amplitudes for NTS events as recorded at United States WWSSN stations.
2. to establish amplitude-yield relationships for Lg(Z), Lg(L), and Lg(T).
3. to evaluate usefulness of Lg(Z) and/or Lg(T) as a measure of yield.
4. to study Lg attenuation characteristics.

To carry out this baseline study, Lg(Z, L, and T) amplitudes from 12 underground nuclear explosions are examined as recorded by most of the three component short period instruments of the WWSSN within the United States. The long period surface waves of these 12 explosions seem to have been contaminated to different degrees by tectonic strain release. Thus, by examining the recorded wave amplitudes, the issues outlined above may be resolved.

The resultant amplitude-yield curves were then used to evaluate the yields of three test events: SALMON, GASBUGGY, and PILEDRIVER, all non-NTS (but continental United States) events.

Data Analysis and Discussion

In this section, we will discuss the applications of these amplitudes in estimating: A) the relationship between the excitation of long and short period surface waves by tectonic strain release, B) amplitude-yield relations, and C) the excitation of Pg and Lg waves by explosive sources.

a. Effect of Tectonic Strain Release

All of the amplitudes measured from the seismograms were first corrected for instrument magnification to obtain the amplitudes of the ground motion. To estimate the effect of tectonic strain release on the short period Lg wave, we divided the Lg amplitudes on the transverse component by those on the vertical component. (When the horizontal component, NS or EW, lies within 30° of the back azimuth to the source, it is referred to as the longitudinal component; and the other one, the transverse component. Otherwise, the horizontal components are labeled as NS or EW.) We then represented the quotient for strong,

intermediate, and weak exciters of Love waves by different symbols and plotted them versus distance (Figure 2-2). This figure shows three important features:

1. most of the data points have values greater than one, i.e. the amplitudes on the transverse component are greater than those on the vertical component.
2. at each station, no clear separation for the strong, intermediate, and weak exciters of Love waves is discernible and
3. no simple distance dependence is noted.

The second characteristic implies that there is no observable correlation between the amplitude ratios of short period higher modes of Love waves to those of Rayleigh waves and their long period, fundamental-mode counterparts. Hence, recorded amplitudes of Lg waves from these events at these stations do not suffer any discernible amplitude change from the tectonic strain release.

This finding is not surprising in view of the long period nature generally associated with the process of tectonic strain release; as a result the tectonic strain release probably has little effect on the spectral level at short periods. The effect of tectonic strain release on P waveforms has been studied theroetically (Bache, 1976; Burdick and Helmberger, 1979); the results indicate that, unless the magnitude of the accompanying tectonic event is greater than that of the explosion, maximum amplitudes of the short period P waves will not be affected.

If the small differences in source location weaken the assumption of common path effects, factors such as scattering, mode-coupling between the Love and Rayleigh type Lg waves, may become significant enough to mask the short period radiation from the tectonic event. As we shall find in a later section, attenuation rates for the vertical, transverse, and longitudinal components of Lg seem to be approximately equal. Consequently, they do not cause the lack of contamination of short period Lg by the tectonic release.

Although both mode-coupling and scattering interact with lateral heterogeneities, they do connote different physical processes. The former suggests a coherent process of energy exchange, and the latter, a random one. Their effects on wave amplitude are usually difficult to distinguish. In the following paragraph, we will discuss the effect of mode-coupling and that of scattering.

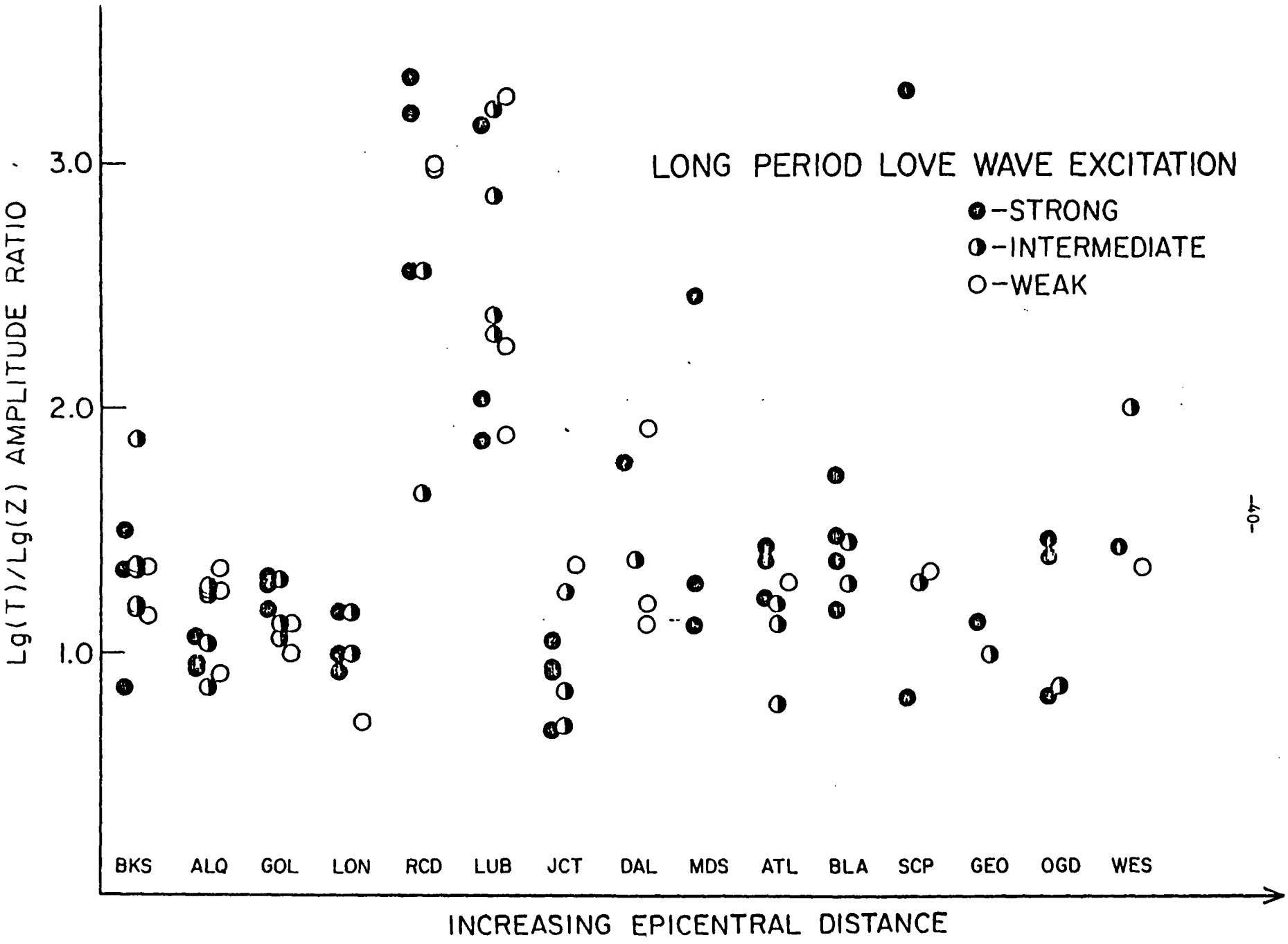

Figure2-2. Amplitude ratios of transverse component Lg wave to that of the vertical component as a function of increasing epicentral distance.

Assuming that the higher mode surface waves of the Rayleigh type do couple or exchange energy with those of the Love type at boundaries of lateral heterogeneities, then we would expect a homogenizing effect on the displacement vector as the number of boundaries increases. That is, the amplitudes of the different components would gradually become equal. The greater-than-unity amplitude ratios and the lack of any discernible distance dependence within the epicentral distance range of 5^{o} to 35^{o}, however, implies that the effect of mode-coupling is small if not negligible. Similarly, the roughly equivalent amplitude ratios at nearby and faraway stations indicate that scattering, however much it may affect the observed amplitudes, appears to have imposed equal influence on the different components of Lg amplitude. If this deduction is correct, then the observed amplitudes should reflect their source characteristics. But, as we have already noted, the amplitude ratios for strong exciters do not appear different from those for intermediate and weak exciters of Love waves; thus, there is no observable correlation between the excitation of higher-mode surface (or Rayleigh) waves at periods around 1 sec and that of fundamental-mode Love waves at periods greater than 10 sec. Consequently, the tectonic strain release which is interpreted as the causal mechanism of long period Love waves, does not seem to affect the amplitudes of short period surface waves. As a consequence, it appears valid to derive amplitude-yield relationships and to attempt to apply them to different geographic areas.

b. Amplitude-Yield Relations

The previous section has shown that the amplitudes of short period Lg waves from underground nuclear explosions at NTS do not seem to be affected by the radiation from the accompanying tectonic event. This property of short period Lg waves is potentially useful for estimating the yields of underground nuclear explosions using Lg. An example of an amplitude-yield relation is:

$$\log A = m \log Y + \gamma \Delta + S$$

where A = amplitude of the ground motion,

Y = estimated yield of the explosion, estimated from a combination of radiochemistry and other means (Springer and Kinnaman, 1975),

m = slope of the log-amplitude versus log-yield plots,

γ = attenuation rate, i.e. slope of log-amplitude versus distance plots, and

S = correction for station response.

In this section, we will confine our attention to the determination of m for Lg waves. Since the attenuation term is a constant for a given source-receiver geometry, the second and third terms in expression (1) can be considered as one, and equation (1) can be reduced to

$$\log A = m \log Y + b$$

where $b = s + \gamma\Delta$. The value, besides being the y-axis intercept on a log Y-log A plot, has the physical significance of being the ground amplitude from a 1-kt explosion at the particular recording station.

The values of m and b for each recording station and wave type (Lg(Z), Lg(L), Lg(T)) were determined separately by a least squares regression analysis. Examples are plotted in Figures 2-3 and 2-4 for Lg waves at RCD and GOL, respectively. Plots for all other United States WWSSN stations are on file at RAI. An examination of all of these plots after the initial regression reveals that the amplitudes from the 19-kt event, FORE, are consistently higher than the values predicted for the yield; consequently, the amplitudes of that event are not incorporated into the subsequent regression analysis.

Two patterns emerge from a careful inspection of all of these figures:

1. the scatter of the data points around the best fitting line,
2. the difference in the values of m and b for different wave types and stations.

The scatter of the data points in all amplitude-yield plots can be explained several ways. Firstly, lack of correlation may result because the yield used to correlate with the wave amplitudes was derived from "radiochemistry and other means" (Springer and Kinnaman, 1975), and depending on the source configuration and site conditions, the value may not correspond to the seismic yield as reflected by the amplitudes of the seismic waves. Secondly, the measuring technique may not have adequately gauged the seismic yield of the underground nuclear explosions. Thirdly, the slight variations in the source location may be anisotropic as a result of (a) interactions with near-source heterogeneities, (b) peculiar test configurations and/or nonlinear, inelastic response in the source region, and (c) random, small-scale strain release in the inelastic zone of the explosion.

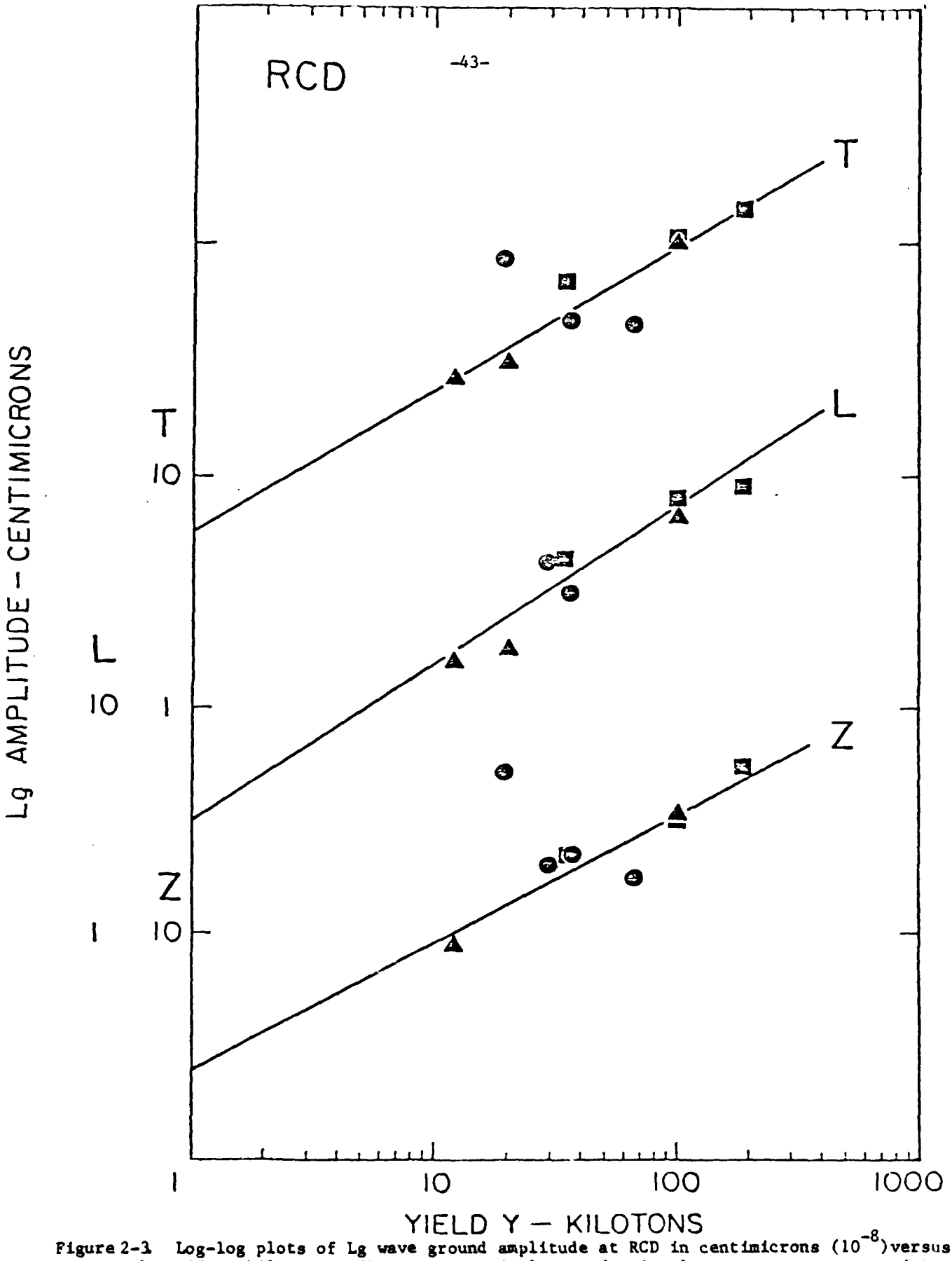

Figure 2-1 Log-log plots of Lg wave ground amplitude at RCD in centimicrons (10^{-8}) versus announced yield in kilotons. The squares, circles, and triangles represent strong, intermediate, and weak exciters of long period Love waves, respectively.

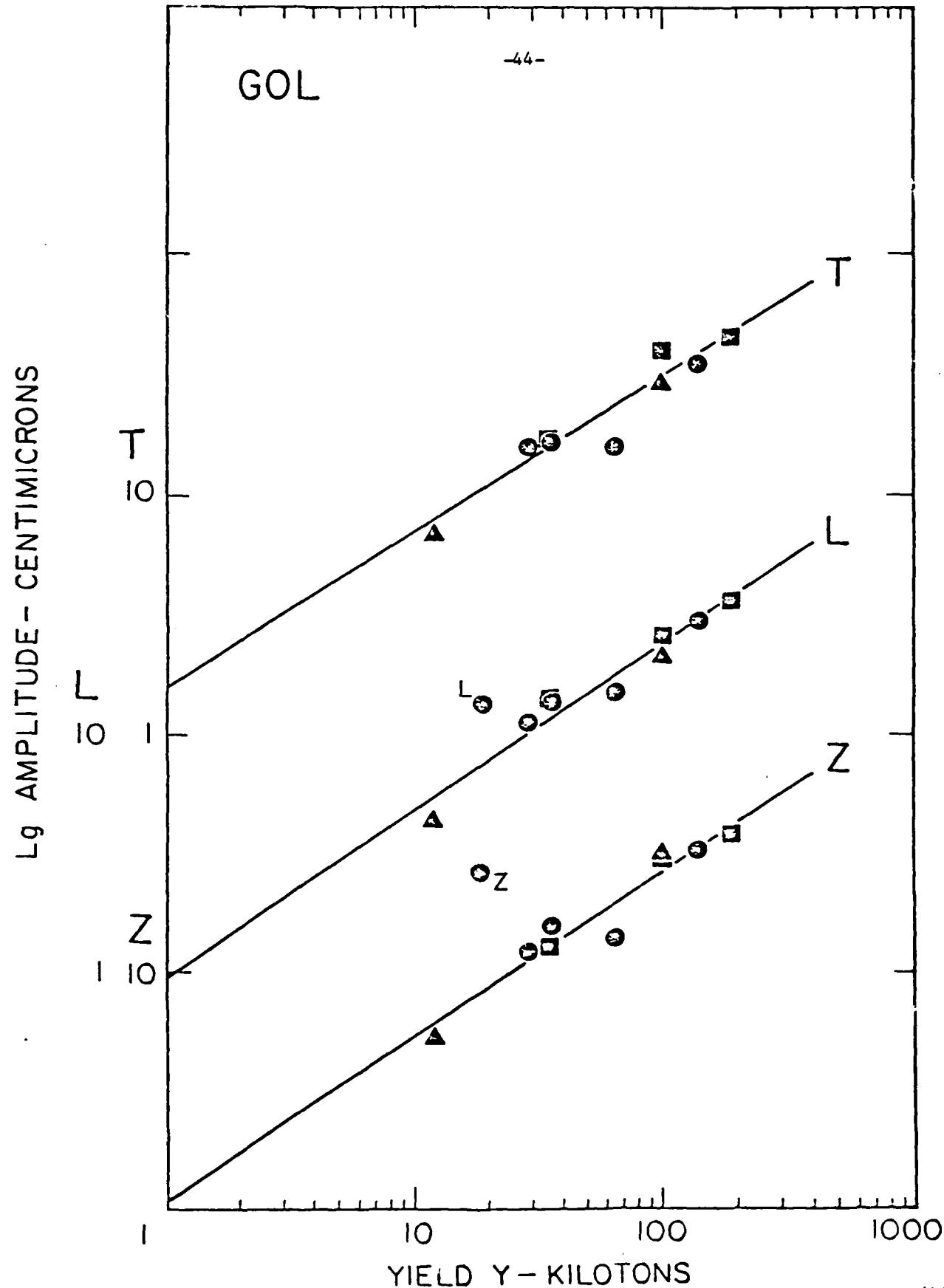

Figure2-4. Log-log plots of Lg wave ground amplitude at GOL in centimicrons (10^{-8}m)versus announced yield in kilotons. The squares, circles, and triangles represent strong, intermediate, and weak exciters of long period Love waves, respectively.

With regard to the first two possibilities, the excellent agreement between the ground amplitudes and the 'announced' yields at some of the stations seems to indicate that the yields estimated by AEC and our measuring technique can produce satisfactory results at these stations. On the other hand, the anomalously large amplitudes from FORE and the clear amplitude discrepancies between the two 100-kt events: CORDUROY and PIRAHNA highlight the differences between the announced yield and the seismic yield estimated by us.

Our experience with correlating a large number (>100) of announced yields and their corresponding m_b (ISC) indicates that a spread of up to 0.8 magnitude-unit (an amplitude difference of $\sim$6X) exists at a given value of announced yield and that, on the average, the announced yield seems to correlate well with the seismic yield as determined from the amplitudes of seismic waves (Chen and Pomeroy, 1980). (Even with our nearly identical source-receiver geometry, an offset of $\sim$0.6X of the predicted amplitude is to be expected.) Except for the period dependent approach in measuring the amplitudes of Lg waves, our scheme is commensurate with the conventional procedure for magnitude determination (Richter, 1935; Nuttli, 1973). Therefore, we believe that the measuring technique is valid, that the announced yields are also in general valid and that we must therefore examine the other two possibilities mentioned above.

With regards to the effects of scattering and anisotropic source, we tend to be more impressed with the importance of the former. For example, when looking at the relative proximity in epicentral distance and back azimuth to the source from three WWSSN stations in Texas: DAL ($\Delta\sim16.3^\circ$, azimuth$\sim99.0^\circ$), JCT ($\Delta\sim15.0^\circ$, azimuth$\sim111.3^\circ$), and LUB ($\Delta\sim12.1^\circ$, azimuth$\sim103^\circ$), one would expect the amplitude characteristics to be approximately equal. There are two marked differences among the amplitudes observed at these stations. Firstly, the observed amplitudes correlate quite well with the estimated yields at LUB and JCT, but not as well at DAL. Secondly, the average amplitudes for the ground motion at DAL are comparable to those at LUB when effects for attenuation and geometrical spreading are taken into account. The average amplitudes at JCT, on the other hand, are usually a factor of two or more smaller than those at DAL (and LUBO, even though the epicentral distance to JCT is in between those to LUB and DAL. Although the effects of source and propagation path are difficult to separate, since the range of azimuth back from these three stations differs only by$\sim12.3^\circ$ in this case, we suspect that the source radiation pattern which at short periods tend to be oval in shape (Cheng and Mitchell, 1980), could result

in such a large change ($\gtrsim$2X) in amplitude. Sutton et al. (1967) showed anisotropic energy contours from an NTS event, HARDHAT, for Pg and Lg waves. Their results indicate a strong focusing effect to the SE direction; unfortunately, DAL, JCT, and LUB lie beyond the extent of their contour map, and hence direct comparison between their findings and our results was not possible. This example from the three Texan stations and our experience with other stations show that scattering (which, as defined in this context, includes the effects of diffraction, focusing by tectonic structures, and response due to the structure beneath the recording station) along the propagation path greatly influences the characteristics of the observed waves.

We have also explored the possibility of using the amplitudes of Lg coda to determine the slope of the amplitude-yield relation. By following the recommendations of Rautian and Khalturin (1978) and Chouet et al. (1978), we measured the amplitudes of Lg waves at a group velocity of about 1.75 km/sec, i.e. about twice the time interval between the origin time and the onset of Lg, for four of the closest stations: ALQ, BKS, DUG, and TUC. We then chose the amplitude from the event with the lowest yield as a reference point, unity in our case, and plotted the relative amplitudes versus the estimated yields. This method offers one definite advantage. Even for the largest event, the wave trace was visible rather than an unmeasurable blur at the closest station ($\Delta \sim A^{\circ}$), DUG, thus increasing the number of useful data points at ALQ, DUG, and TUC significantly.

The plots of relative amplitude versus estimated yield like that shown in Figure 2-5 indicate that the results derived from coda are compatible with those derived from measurements of amplitude maxima. Finally, the slopes of log-amplitude versus log-yield plots for the Lg waves are plotted as a function of epicentral distance in Figure 2-6 Similar to our previous findings on the amplitude ratios for Lg waves, no dependence on distance or particle-motion seems to exist.

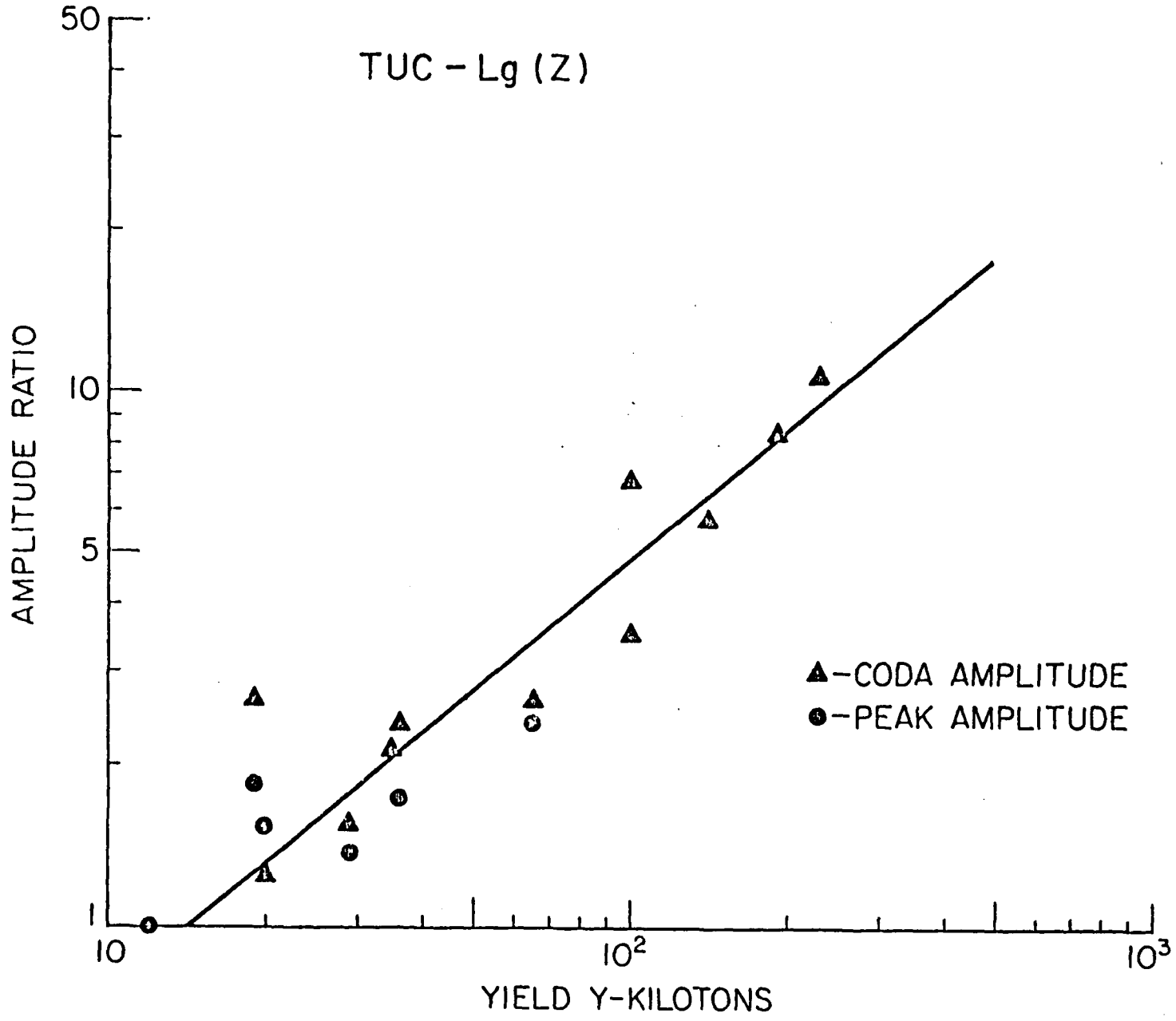

Figure 2-5. Amplitude ratios for the vertical component of Lg waves at TUC as a function of estimated yields. The ratio is taken with respect to the event with the smallest yield. Triangles and circles represent data derived from coda amplitude and amplitude maxima, respectively.

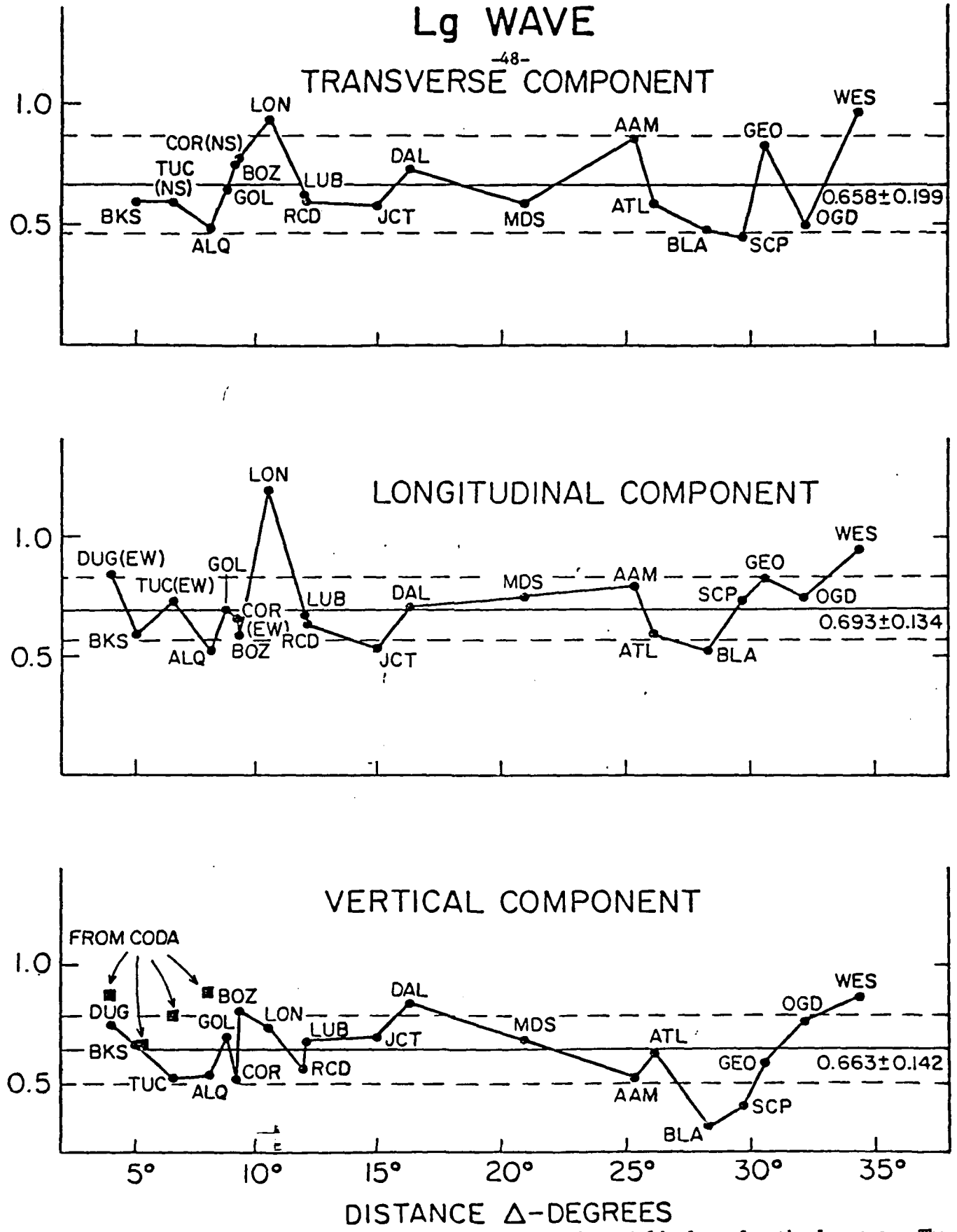

Figure2-6. The slopes of log-amplitude versus log-yield plots for the Lg wave. The solid and dashed horizontal lines denote mean and one standard deviation, respectively.

Application of Amplitude-Yield Relation to Other Tests

We have applied our amplitude-yield relations to the estimation of the yield of three underground explosions outside of Yucca Flat, NTS: PILEDRIVER at Climax Stock, NTS; GASBUGGY near Dulce, New Mexico; and SALMON near Hattiesburg, Mississippi.. The measured amplitudes for these events at each station, after correcting for instrument magnification, were equalized to a distance the same as the epicentral distance of the station to Yucca Flat, NTS. That is, the resultant amplitudes are assumed to have undergone the effects of geometrical spreading and inelastic attenuation from Yucca Flat, NTS, instead of from their respective source locations. The yields estimated by us are listed in Table 2-1.

Conclusions

The principal results of this study are:

1. Contamination of Lg(Z) and Lg(T) by the anisotropic component of the source is not significant for these events as recorded in the United States. The effects of propagation path have been qualitatively evaluated and discarded as the likely causes for the lack of correlation between the surface wave amplitudes of the long period fundamental mode and those of short period higher modes.

2. Lg(Z) and Lg(T) provide reasonable and independent supplementary estimates of the yield.

3. Amplitude-yield relationships of the type derived in this study can be used to estimate the yields of underground explosions in different geographic and geologic environments.

4. The use of Lg(Z) and/or Lg(T) to determine yield is particularly important

   a. for events from test areas like Shagan River where M_S is suspect, and

   b. for events of lower yield on the same continental land mass as the recording station.

5. Since Lg is, in many areas the largest amplitude signal observed on many regional seismograms ($\Delta = 10^{\circ}$ to 35°), it is particularly useful in providing a supplemental yield determination.

B. P versus Yield

Following the same procedure as that outlined for Lg, we have determined P wave amplitude versus yield curves for each of the WWSSN stations in the conterminous United States. Examples of these curves for GOL and RCD are presented in Figures 2-7 and 2-8. Similar plots for all other WWSSN stations in the United States are on file at RAI. From curves such as these, the slope m can be determined and that slope is plotted for each component as a function of epicentral distance in Figure 2-9.

From the data of Figure 2-9, an average slope can be determined for each component. These are

vertical	$m = 0.70 \pm 0.281$
longitudinal	$m = 0.637 \pm 0.258$
transverse	$m = 0.706 \pm 0.339$.

The relative values of the standard deviations should be noted since they are approximately 60% to 100% larger for P compared to the Lg values. Although the problems with P measurements in this distance range are well known, the smaller standard deviations in Lg indicate that Lg can provide valuable supplemental yield estimates in this distance range.

Using these curves, we have determined the yields for the three events, PILEDRIVER, GASBUGGY, and SALMON and these are listed in Table 2-2.

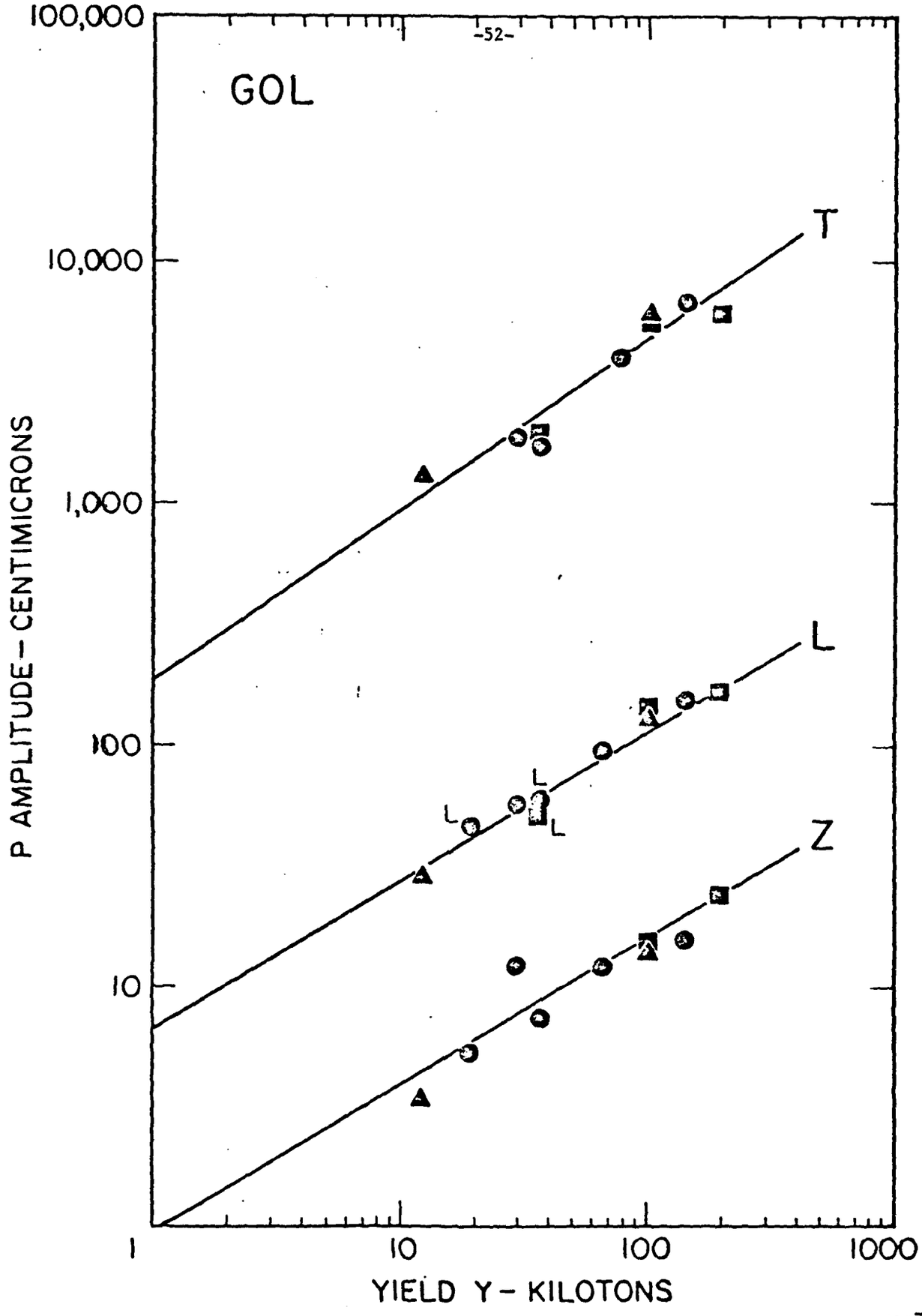

Figure 2-7. Log-log plots of P wave ground amplitude at GOL in centimicrons (10^{-8} m) versus announced yield in kilotons. Symbols are the same as those in Figure 2-4.

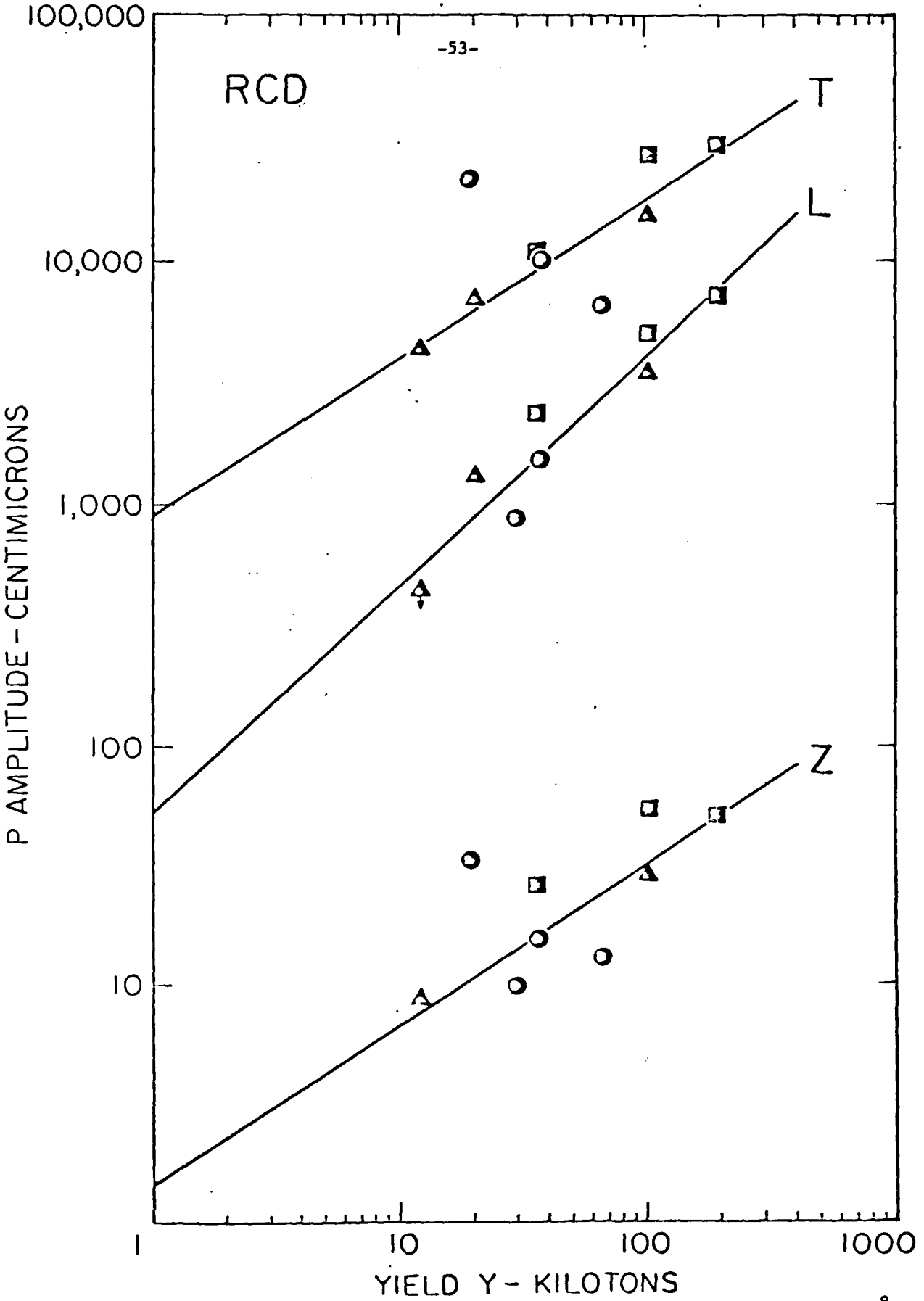

Figure 2-8. Log-log plots of P wave ground amplitude at RCD in centimicrons (10^{-8}m) versus announced yield in kilotons. Symbols are the same as those in Figure 2-4.

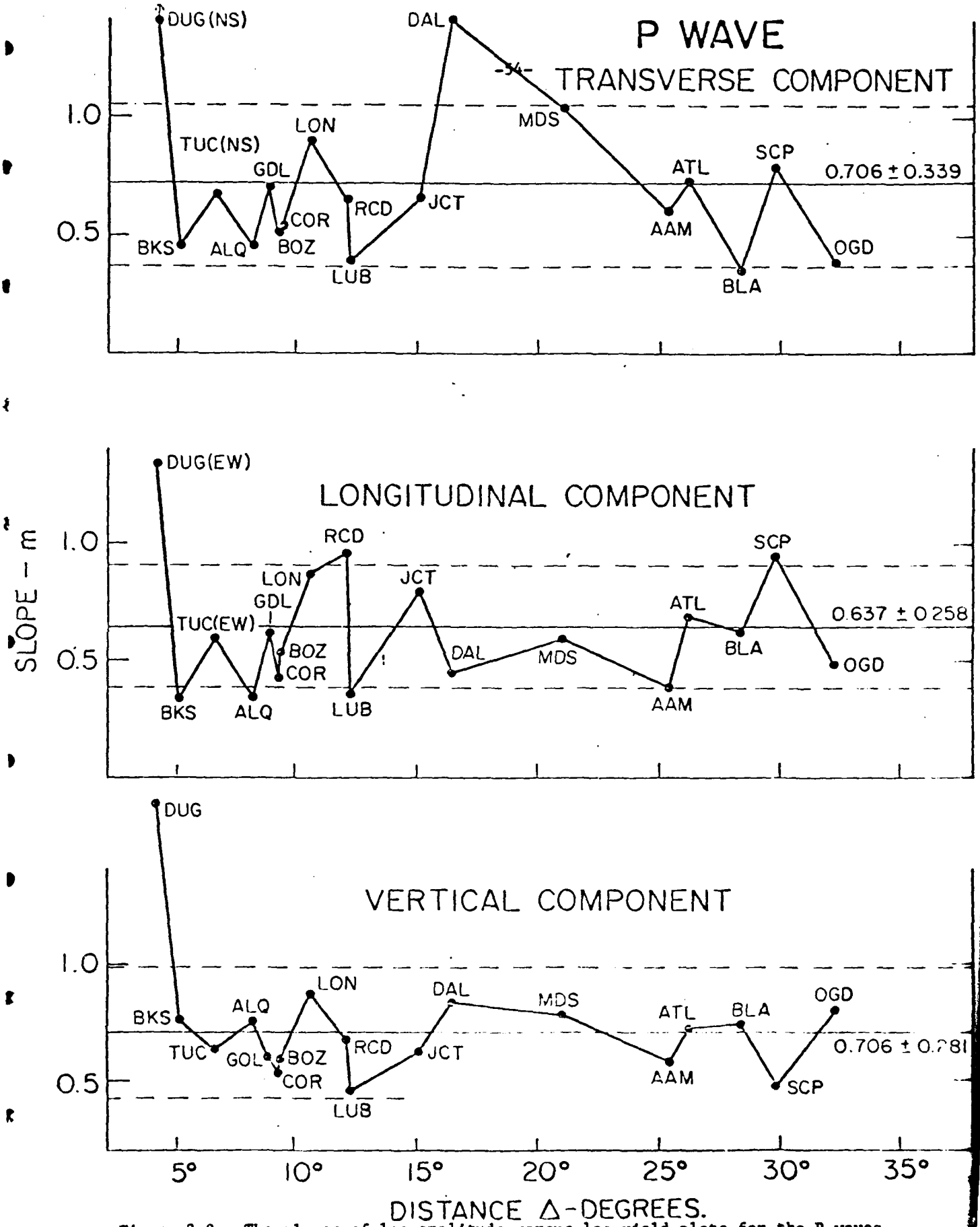

Figure 2-9. The slopes of log amplitude versus log yield plots for the P waves. The solid and dashed horizontal lines denote mean and one standard deviation.

C. Pg versus Yield

Again, following the same procedure as that outlined for Lg, we have determined Pg amplitude versus yield curves for each of the WWSSN stations in the conterminous United States where Pg is recorded from NTS events. All of these curves are on file at RAI. From these plots, the slope m can be determined and that slope is plotted for each component as a function of epicentral distance in Figure 2-10.

From the data in Figure 2-10, an average slope can be determined for each component. These are

vertical	$m = 0.580 \pm 0.177$
longitudinal	$m = 0.594 \pm 0.186$
transverse	$m = 0.647 \pm 0.259$.

Again, the relative values of the standard deviations should be noted. Although they are larger than those for Lg, they are significantly smaller than those for P. Thus, Pg, where recorded, can provide, through measurements of Pg(Z), Pg(L), and Pg(T), valuable semi-independent measurement of yield at regional distances.

Using these values, we have computed the yields for the two test events, PILEDRIVER and GASBUGGY. Values for SALMON could not be computed since, as is well known, Pg is not observed with significant amplitudes above background in the Eastern United States at distances greater than a few hundred kilometers. Yield values from Pg data for PILEDRIVER and GASBUGGY are given in Table 2-2.

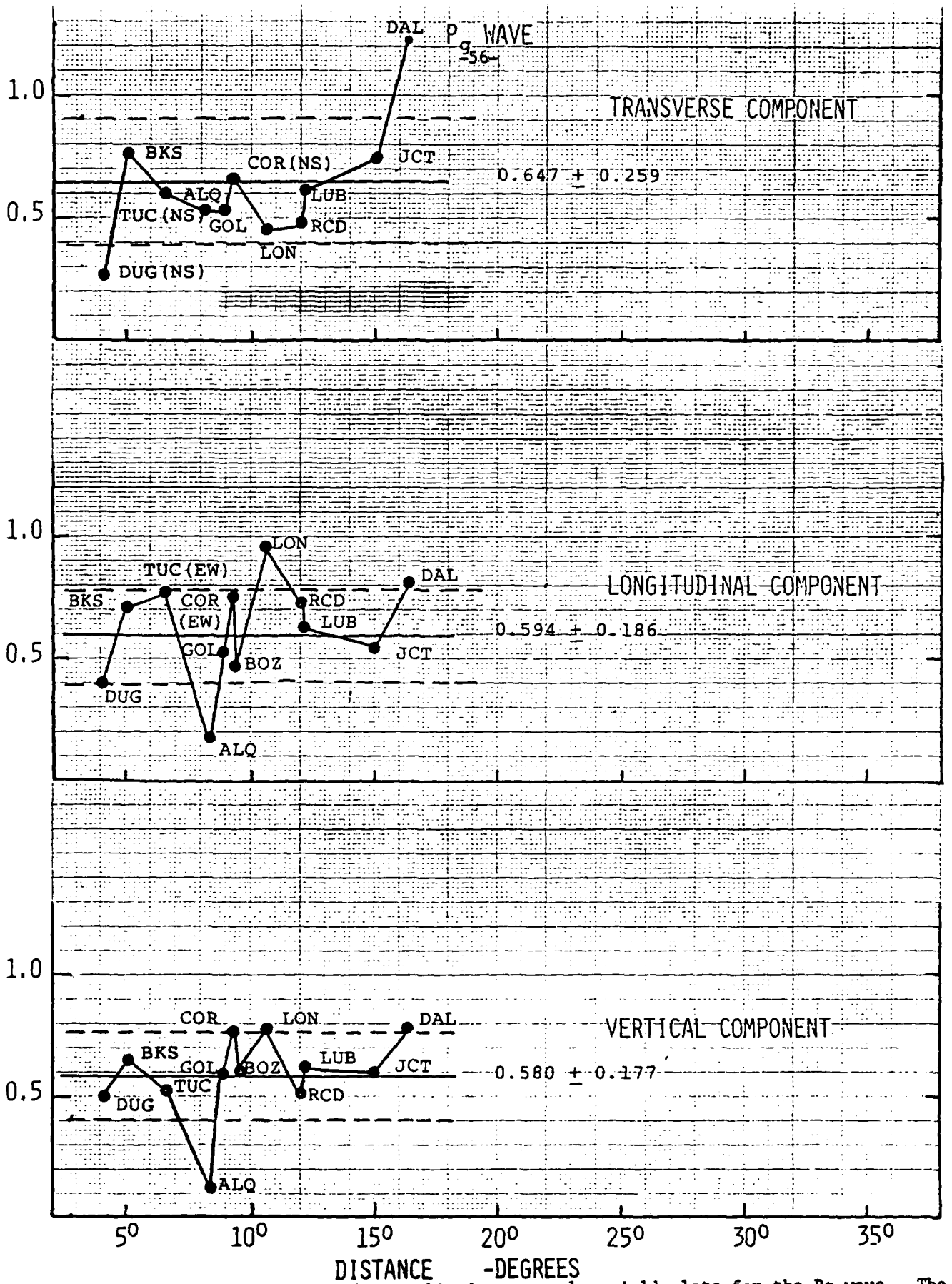

Figure 2-10. The slopes of log-amplitude versus log-yield plots for the Pg wave. The solid and dashed horizontal lines denote mean and one standard deviation, respectively.

References

Aki, K. and Y.B. Tsai, 1972, Mechanism of Love-wave excitation by explosive sources, J. Geophys. Res., 77, 1452-1475.

Alexander, S.S. (1980), Comparison of source and propagation characterisitics in Eurasia, North Africa, and the U.S. using regional seismic and remote sensing observations (Abstract), DARPA Symposium on Seismic Propagation at Regional Distance Ranges and Source Characterization, Grand Island, New York, 20-21 May 1980, Abstrac published by DARPA, Arlington, Virginia.

Bache, T.C., 1976, The effect of tectonic stress release on explosion P-wave signatures, Bull. Seism. Soc. Am., 66, 1441-1457.

Baker, R.G. (1967), Preliminary study for determining magnitude from Lg, Earthquake Notes, 38, 23-28.

Baker, R.G. (1970), Determining magnitude from Lg, Bull. Seism. Soc. Am., 60, 1907-1919.

Blandford, R.R. and P. Klouda, 1980, Magnitude-yield results at the Tonto Forest Observatory in Studies of Seismic Wave Characteristics at Regional Distances, Teledyne-Geotech Report AL-80-1, Teledyne-Geotech, Alexandria, Virginia.

Burdick, L.J. and D.V. Helmberger, 1979, Time functions appropriate for nuclear explosions, Bull. Seism. Soc. Am., 69, 957-973.

Chen, T.C. and P.W. Pomeroy, 1980, Regional seismic wave propagation, Semi-Annual Technical Report #5, Rondout Associates, Incorporated, Stone Ridge, New York.

Cheng, C.C. and B.J. Mitchell, 1980, Crustal Q structure in the United States from multi-mode surface waves, Semi-Annual Technical Report #3, Saint Louis University, St. Louis, Missouri.

Chouet, B., K. Aki, and M.Tsujiura, 1978, Regional variation of the scaling law of earthquake source spectra, Bull. Seism. Soc. Am., 68, 49-79.

Evernden, J.F., 1967, Magnitude determination at regional and near-regional distances in the United States, Bull. Seism. Soc. Am., 57, 591-639.

Nuttli, O.W., 1973, Seismic wave attenuation and magnitude relations for eastern North America, J. Geophys. Res., 78, 876.

Rautian, T.G. and V.I. Khalturin, 1978, The use of the coda for determination of the earthquake source mechanism, Bull. Seism. Soc. Am., 68, 923-948.

Richter, C.F., 1935, An instrumental earthquake scale, Bull. Seism. Soc. Am., 25, 1-32.

Springer, D.L. and W.J. Hannon, 1973, Amplitude-yield scaling for underground nuclear explosions, Bull. Seism. Soc. Am., 63, 477-500.

Springer, D.L. and R.L. Kinnaman, 1975, Seismic-source summary for U.S. underground nuclear explosions, 1971-1973, Bull. Seism. Soc. Am., 65, 343-349.

Sutton, G.H., W. Mitronovas, and P.W. Pomeroy, 1967, Short-period seismic energy radiation patterns from underground nuclear explosions and small-magnitude earthquakes, Bull. Seism. Soc. Am., 57, 249-267.

3. CATSKILL SEISMIC ARRAY (CSA)

The Catskill Seismic Array was a tripartite array of broad-band, three-component seismographs which operated near Stone Ridge, New York from 7 September 1980 to 19 November 1981. The array, shown on a map in Figure 3-1, consists of elements 213, PEK, and TON. Coordinates for these locations are given in Table 3-1 together with station elevations and interelement distances. The array impulse response is plotted in Figure 3-2. CSA was operated under a cooperative research agreement between Rondout Associates, Incorporated and the University of Nevada.

At each of the three elements, three-component (2H's-1Z) Teledyne-Geotech Model SL-210 and SL-220 seismometers operated at a natural period of 15 seconds. The velocity output from each seismometer was amplified and filtered to allow recording from long periods up to 12.5 Hertz. The analog output was then digitized at 25 samples a second and the digital data from all three instruments was multiplexed onto a 1200 Hertz carrier for telephone line transmission. Telephone lines run from the three remote sites to the central recording facility at the corporate headquarters of Rondout Associates, Incorporated at 1 Stilba Lane in Stone Ridge.

At the central recording facility, data from the three remote sites were recorded on digital magnetic tape under the control of an LSI-11 computer. Two tape drives were used and tapes were changed once a day. Accurate time was provided for the system via a Kinemetrics-True Time satellite time receiver. Data tapes from the array were nominally saved for a one week period and information on earthquakes "of interest" was obtained on a weekly basis. Unfortunately, a large number of events of current interest were lost by this procedure. Following 1 September 1981, the array data was saved entirely, up to the termination of the array operation on 19 November 1981.

The Catskill Seismic Array was unique in several respects:

1. It was the only array with <u>dimensions</u> small enough to study high frequency seismic waves in the eastern and central United States.
2. It was the only array of <u>broad-band instruments</u> in the eastern and central United States.
3. It was the only array of <u>three-component instruments</u> in the eastern and central United States.
4. It was the only <u>fully digital</u> array in the eastern and central United States.

These unique qualities have provided significant quantity of data on propagation characteristics of earthquakes within the North American continent and many other well recorded events from other regions.

The distance from the CSA to the NTS is significant in that the closest monitoring stations to the south of the USSR test site at Semipalatinsk lie in the same distance range. Moreover, the NTS-CSA propagation path starts in the western mountainous region and then traverses the high Q areas of the eastern and central United States. The propagation paths between the USSR test site and the southern stations are somewhat analogous since the waves from events at Semipalatinsk traverse broad, low lying relatively high Q areas and then, in general, cross mountainous terrain prior to being recorded at the southern stations. Thus, it is particularly important to study a well recorded event, e.g., like HARZER, at CSA to analyze the propagation characteristics in detail.

A more complete description of CSA, including a discussion of instrument calibration and an analysis of the background noise characteristics is presented in the second Annual Technical Report for this contract.(RAI, 1 November 1981)

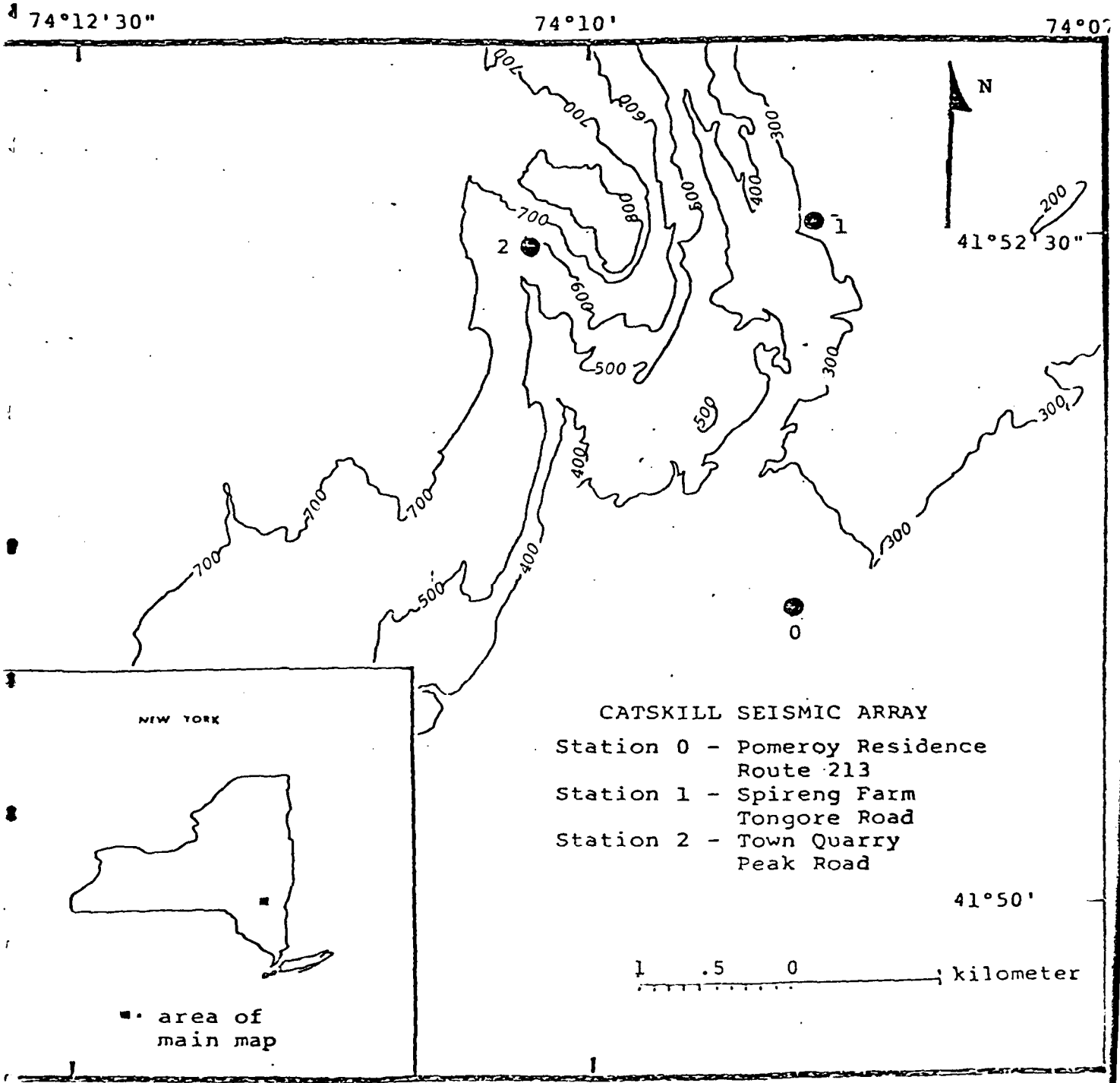

Figure 3-1. Location Map of Catskill Seismic Array.

TABLE 3-1
CATSKILL SEISMIC ARRAY

	STATION 0-213	STATION 1-ION	STATION 2-PEK
COORDINATES	41.8517°N LAT. 74.1500°W LONG.	41.8756°N LAT. 74.1492°W LONG.	41.8742°N LAT. 74.1714°W LONG.
ELEVATION	105.2 METERS	85.3 METERS	176.8 METERS
HARZER DISTANCE	32.5823°	32.5807°	32.5640°
HARZER AZIMUTH	276°	276°	276°
AZIMUTH FROM HARZER	68°	68°	68°

INTERELEMENT DISTANCES

0-1	2.64 KM
0-2	3.04 KM
1-2	1.84 KM

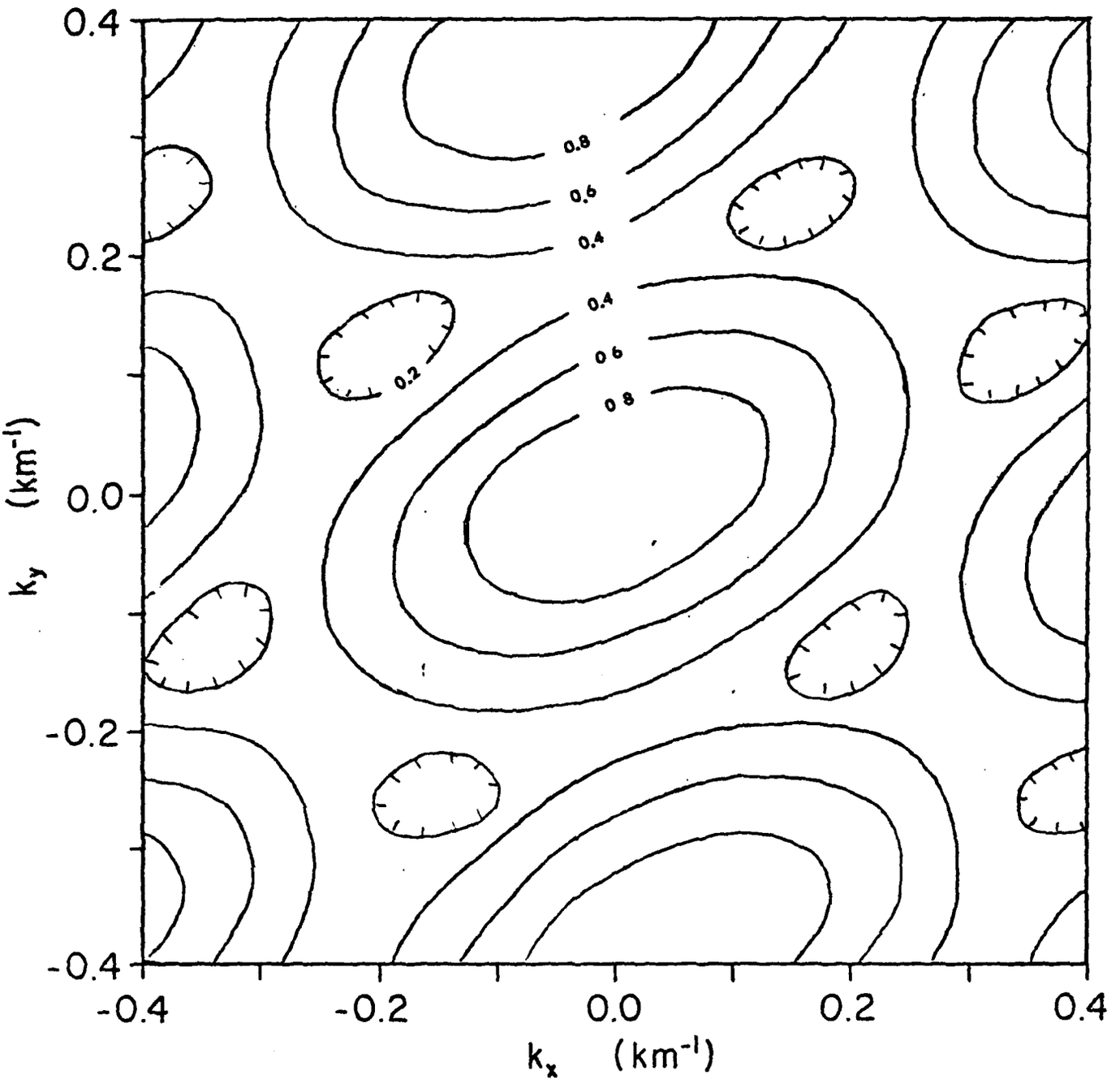

Figure3-2. CSA impulse response; $K_i = \lambda_i^{-1}(km^{-1})$; + y direction is from station 0 toward station 1, slightly east of north.

4. HARZER RECORDED AT CSA

The high quality digital recordings of the HARZER nuclear event (6/6/81, 18:00 Z, m_b=5.6, M_S=4.2) at the Catskill Seismic Array, a distance of 32.5°, provide a unique data set for the analyses of propagation characteristics. This distance range, 32.5°, is approximately the same as that between the USSR Semipalatinsk test site and the nearest recording stations to the south. The propagation path in the present case is, to a large degree, analogous to some propagation paths from USSR events. The following is a summary of a more complete discussion in the second Annual Technical Report for this contract. (RAI, 1 November 1981)

The specific results of this study include:

1. P, Lg, and sedimentary Rayleigh waves were well recorded on the array (Figures 4-1 and 4-2).
2. The impulsive P waves, as recorded on the vertical component instruments of the array, have a broad spectrum with amplitudes of 1 to 5 microns in the frequency range .1 to 1 Hertz. Spectral amplitudes in the 1 to 2 Hertz range are 2 orders of magnitude smaller. The P wave spectra are essentially identical at all three stations (Figure 4-3).
3. Cross correlation of the P waves shows very high correlation coefficients i.e.

213 Z and TON Z	.9661
213 Z and PEK Z	.9248
TON Z and PEK Z	.8747

indicating excellent signal coherence across the array (dimensions of the order of 2 kms) (Figure 4-4).
4. Coherence plots of the P waves show high values (.8 to .9) at frequencies less than 1 Hertz. At frequencies greater than 1 Hertz, the coherence drops rapidly for the station combinations TON Z-PEK Z and 213 Z-PEK Z. The station pair 213 Z- TON Z show relatively high coherence (.4 to .6) at frequencies between 1 and 2 Hertz.
5. The signal to noise ratio for the P waves on the vertical component indicates that, in the frequency range .3 to .8 Hertz signal to noise ratios are greater than 3. Band pass filtering the P wave would result in major improvements in the signal to noise ratio. Delay and sum array processing would also result in significant signal to noise improvements (Figure 4-5).

6. For Lg, the highest amplitudes are recorded on the transverse (N-S) instruments and the lowest amplitudes on the longitudinal instruments. The spectral shapes are similar on all components except that most of the additional energy on the transverse component lies below 0.3 Hz (fundamental mode LQ?). Broad band signal to noise is two or greater on the vertical and transverse components, principally between about 0.1 and 0.8 Hz over a time duration of about three minutes. Maximum signal to noise on the vertical components is 3 to 8 between 0.3 and 0.8 Hz; on the transverse components it is about 20 near 0.1 Hz (Figures 4-1, 4-6, 4-7, 4-8).

7. High values of the cross correlation functions between similar components are observed on the vertical and transverse Lg data. Some individual pulses also appear to correlate across the array. Lower correlation values are observed on the longitudinal (E-W) pairs consistent with the lower signal to noise ratios on these instruments. Maximum cross-correlation of 0.86 at a lag of 0.5 sec between PEK N and TON N, approximately along the great circle path is consistant with a propagation delay at about 3 km/sec (Figure 4-9.

8. All of the transverse and vertical component pairs show high coherence for Lg in the frequency range .1 to .3 Hertz. No coherent energy is observed at frequencies greater than 1 Hertz. With the exception of the station pair 213 Z-TON Z which exhibits a .55 coherence in the frequency band .5 to .7 Hertz, no significant coherence is observed on the vertical components at frequencies greater than .3 to .4 Hertz.

9. Significant signal to noise ratios in Lg (2 to 4) are found principally in the .3 to .8 Hertz frequency range i.e. in approximately the same frequency range as the noise maxima. Therefore, band-pass filtering may not significantly enhance signal to noise ratios in Lg.

10. The sedimentary Rayleigh waves from this event with periods from 12 to 3 seconds are highly unusual in that one would expect the shorter period waves not to exist since their propagation requires continuity in the upper 5 kms of the waveguide. Since they do exist, in spite of radical changes in the upper 5 kms of the waveguide between NTS and the Catskill Seismic Array, a detailed investigation of the propagation characteristics of these waves is in order.

The broad-band, three-component, digital data from CSA permit the study of seismic signals across the array from greater than 15 sec period, through the microseism band and up to greater than 10 Hz. The data are approximately flat to velocity, as recorded, from about .08 to 10 Hz. The most prominent portion of HARZER, as recorded at CSA, i.e., the highest ground velocity, is the 10 to 6 sec (about a one octave band) sedimentary Rayleigh wavetrain. This would have been poorly recorded on narrower band instruments with low gain and/or distortion in the microseism band. The sedimentary Rayleigh waves also happen to have a fairly high maximum signal to noise ratio (greater than 10). The 20 sec Rayleigh waves, needed for standard determination of M_S, are not evident on the unfiltered records.

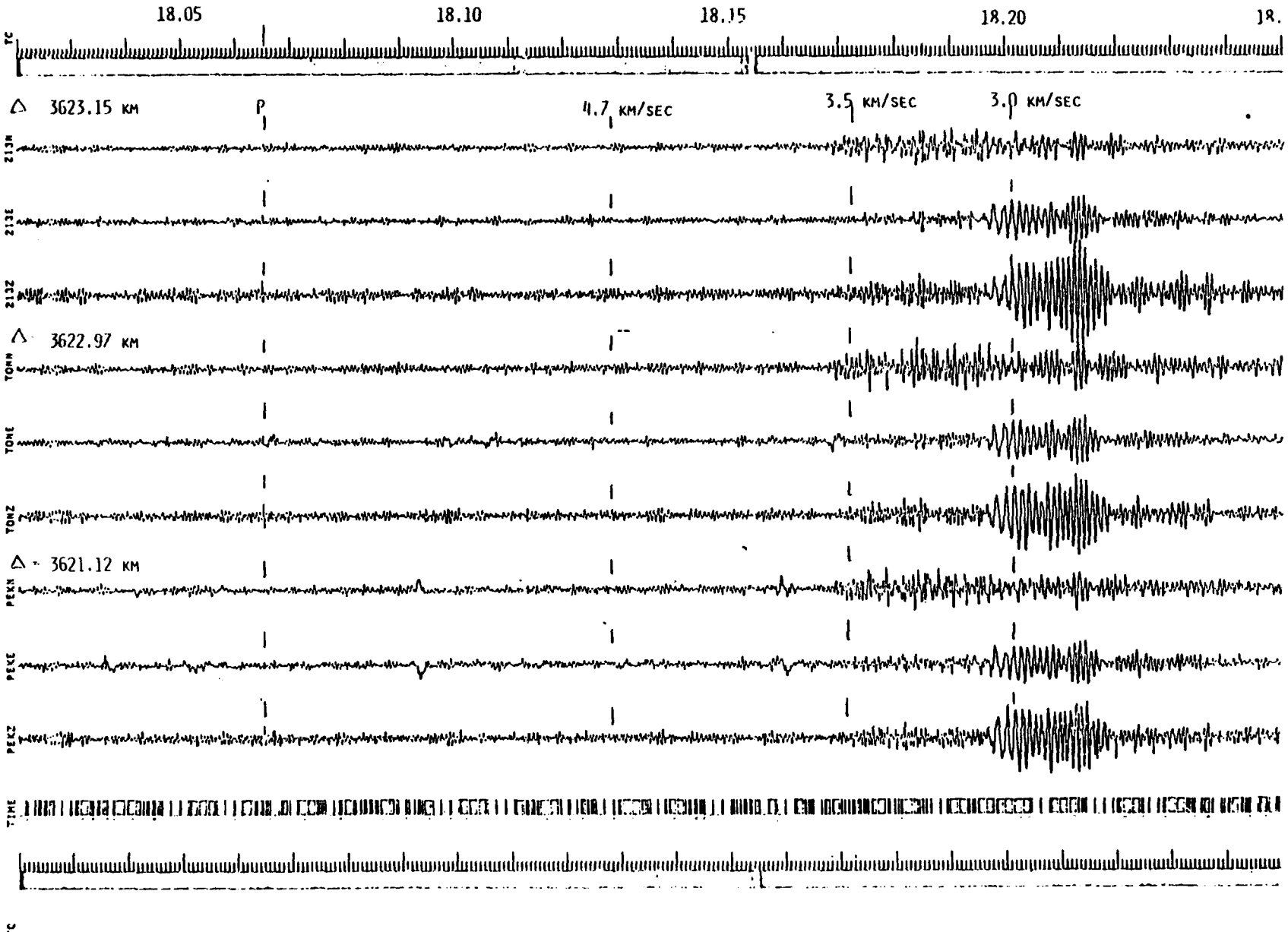

Figure 4-1. HARZER total record - all components.

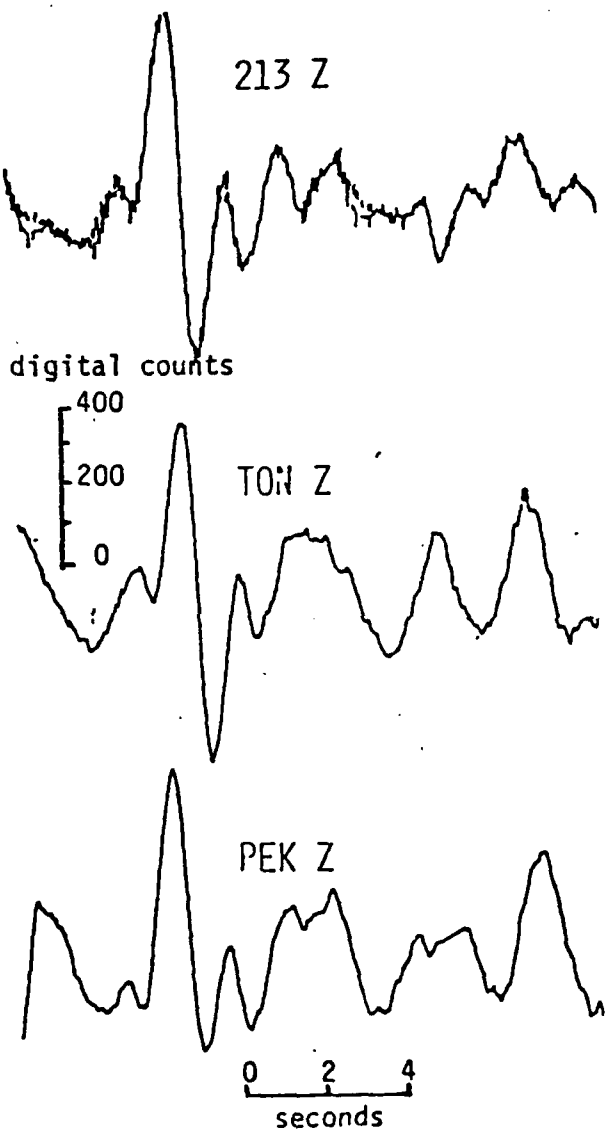

Figure 4-2 . HARZER P waves, unfiltered.

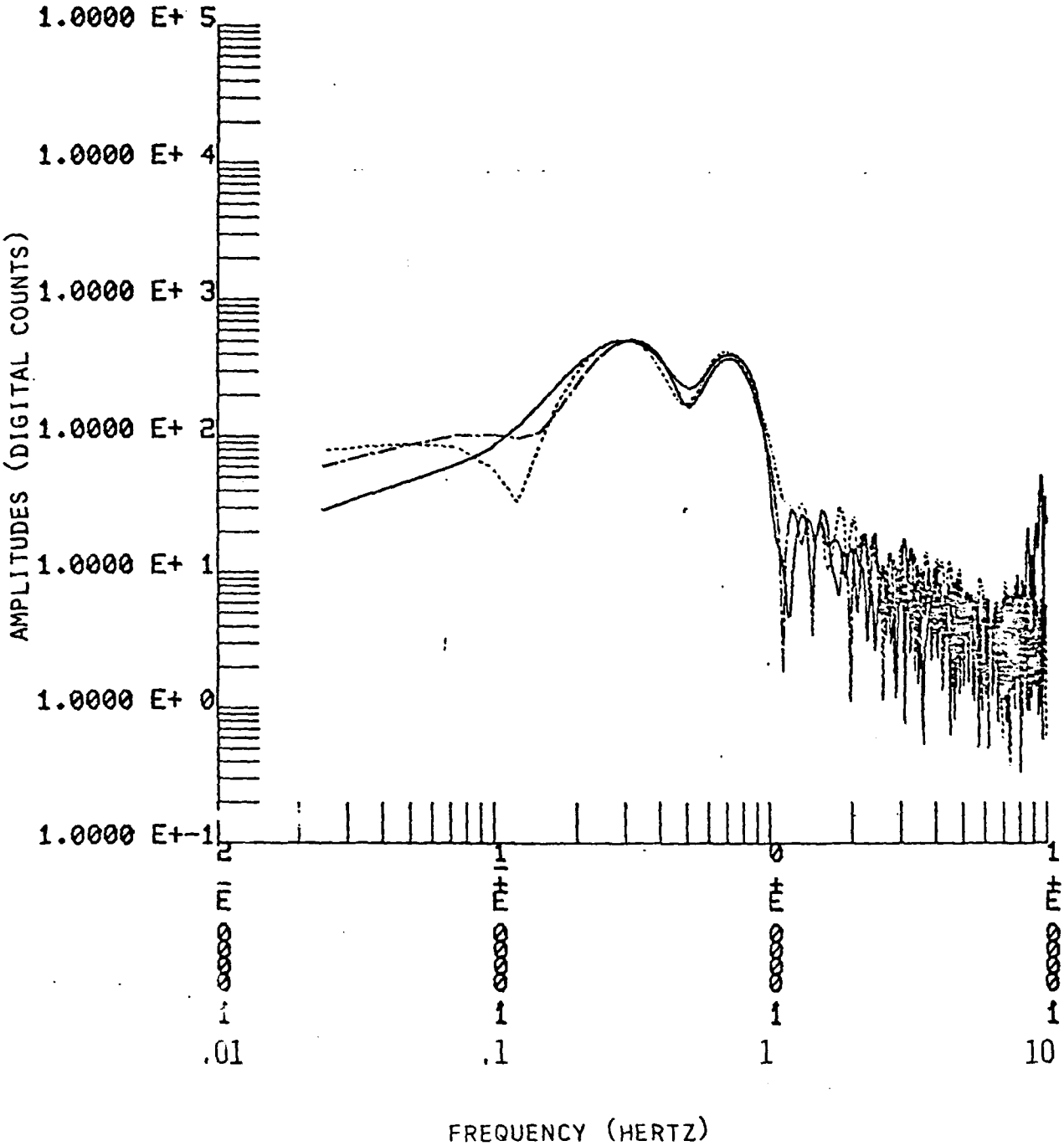

Figure4-3. HARZER P wave spectra - 213 Z, TON Z, and PEK Z, uncorrected, these spectra are approximately flat to ground velocity between about .08 and 10 Hz.

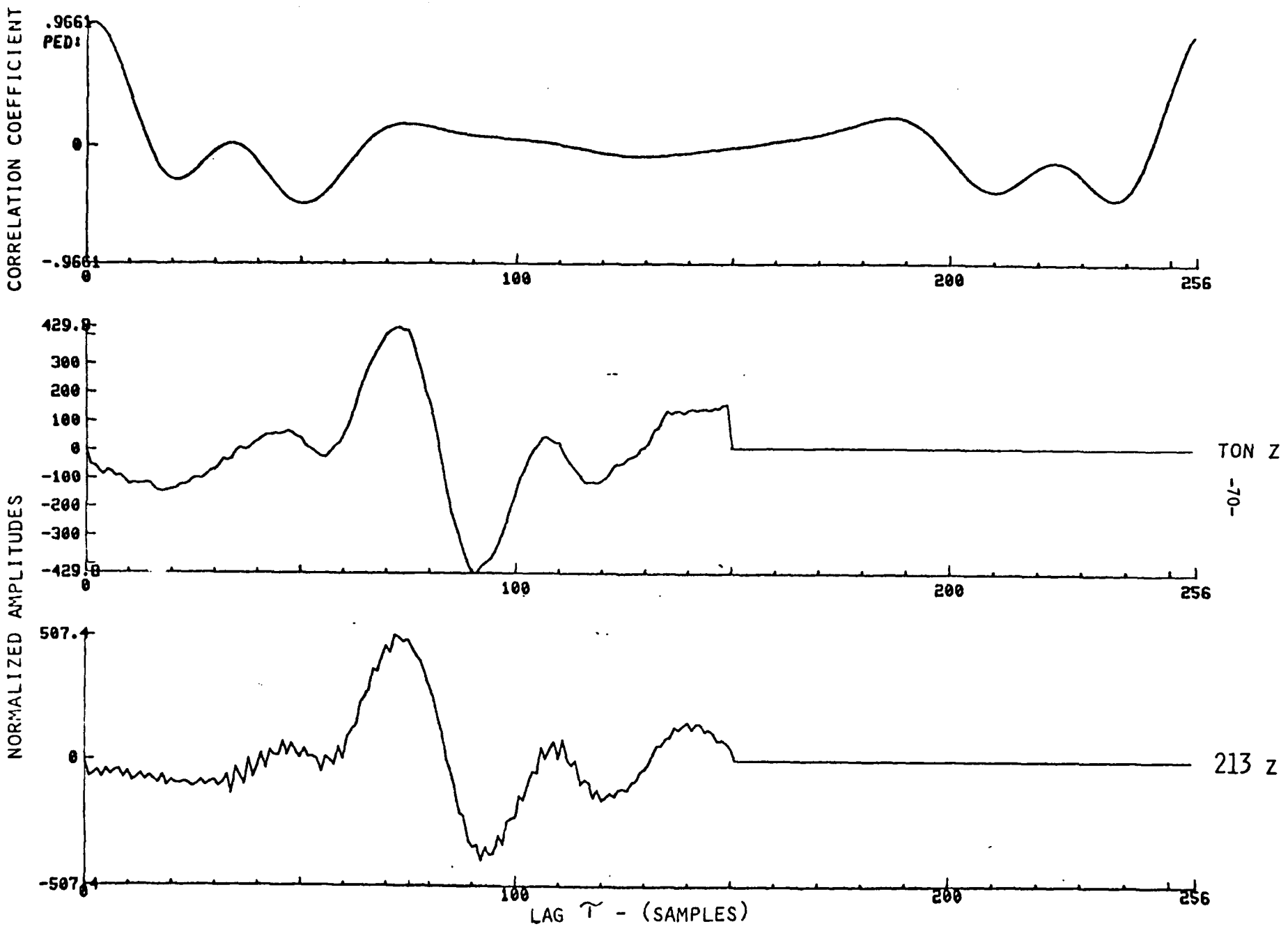

Figure 4-4 HARZER P waves, unfiltered--cross correlation.

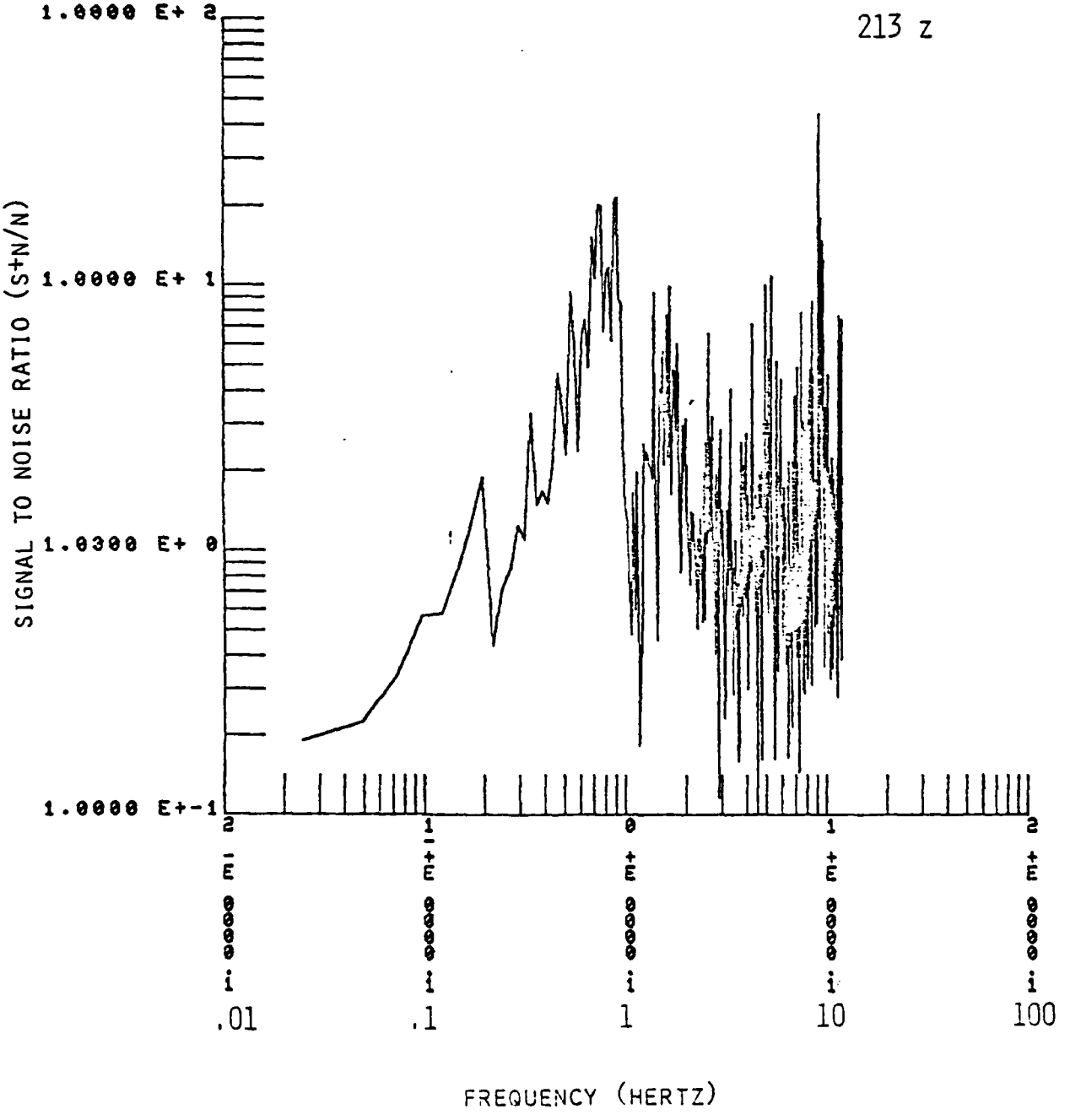

Figure 4-5 HARZER P wave signal to noise ratio. 213 Z

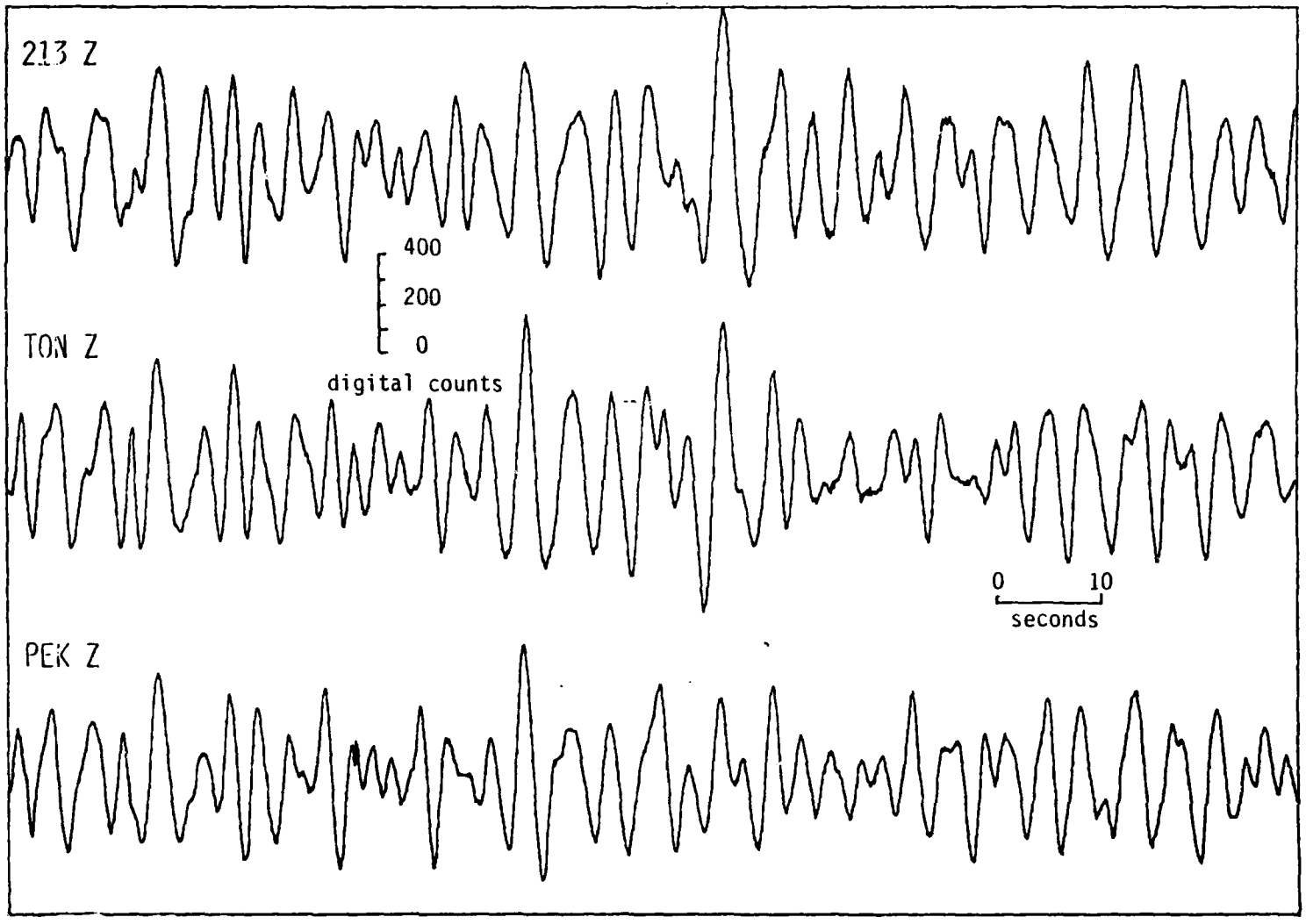

Figure 4-6 HARZER Lg waves. 120 seconds of data. 213 Z, TON Z, and PEK Z.

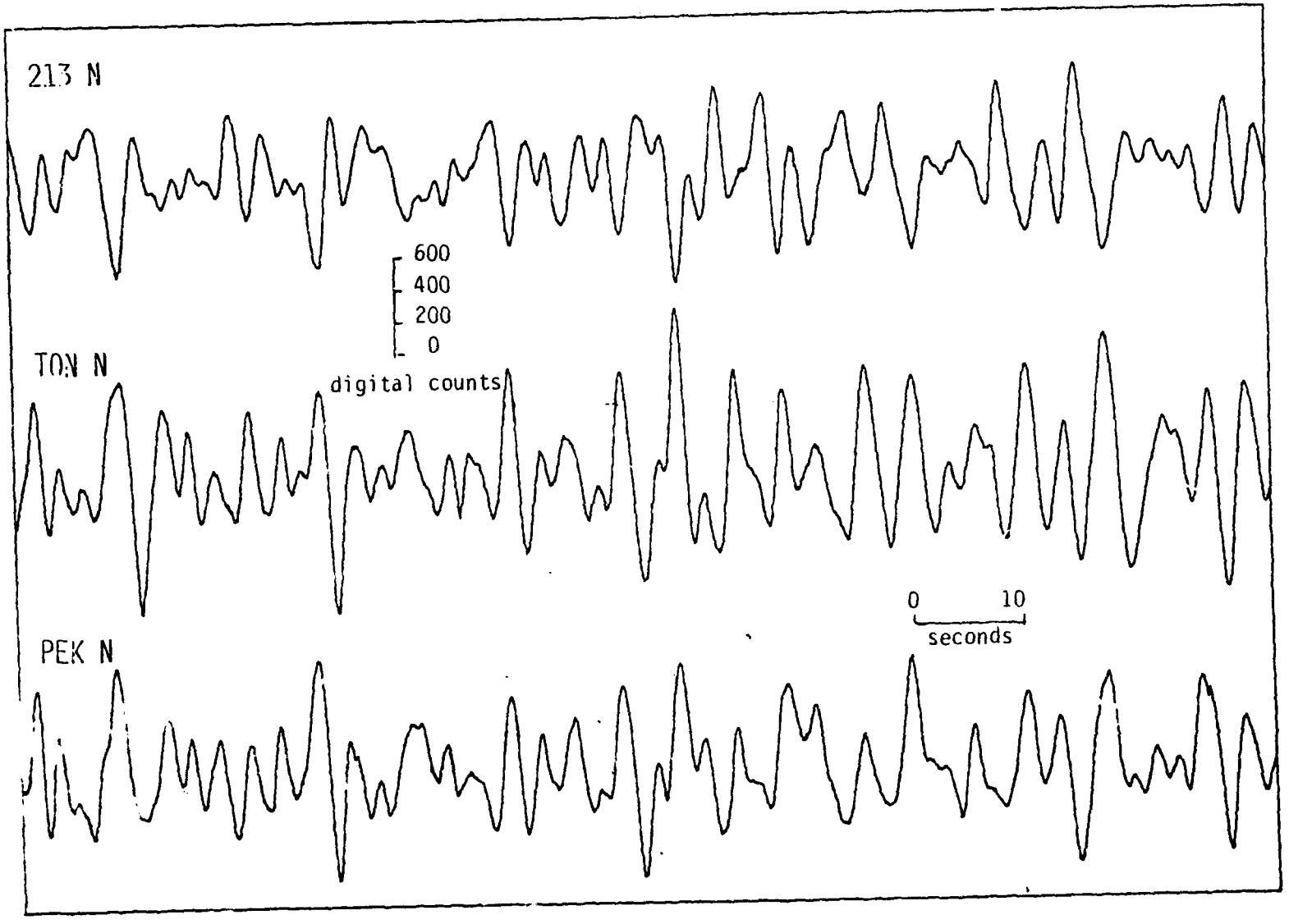

Figure 4-7. HARZER Lg waves. 120 seconds of data. 213 N, TON N, and PEK N.

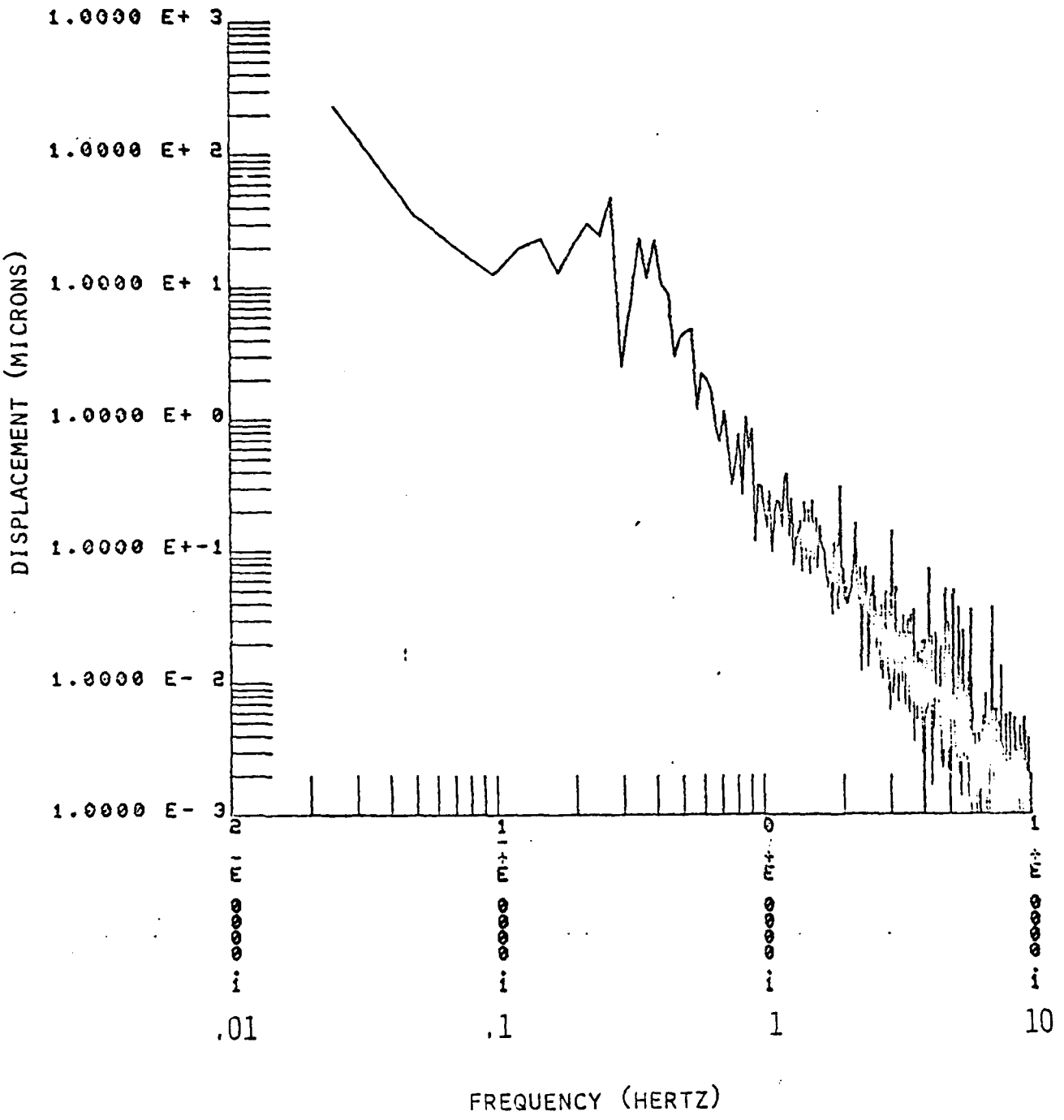

Figure 4-8. HARZER Lg wave spectrum. 213 Z

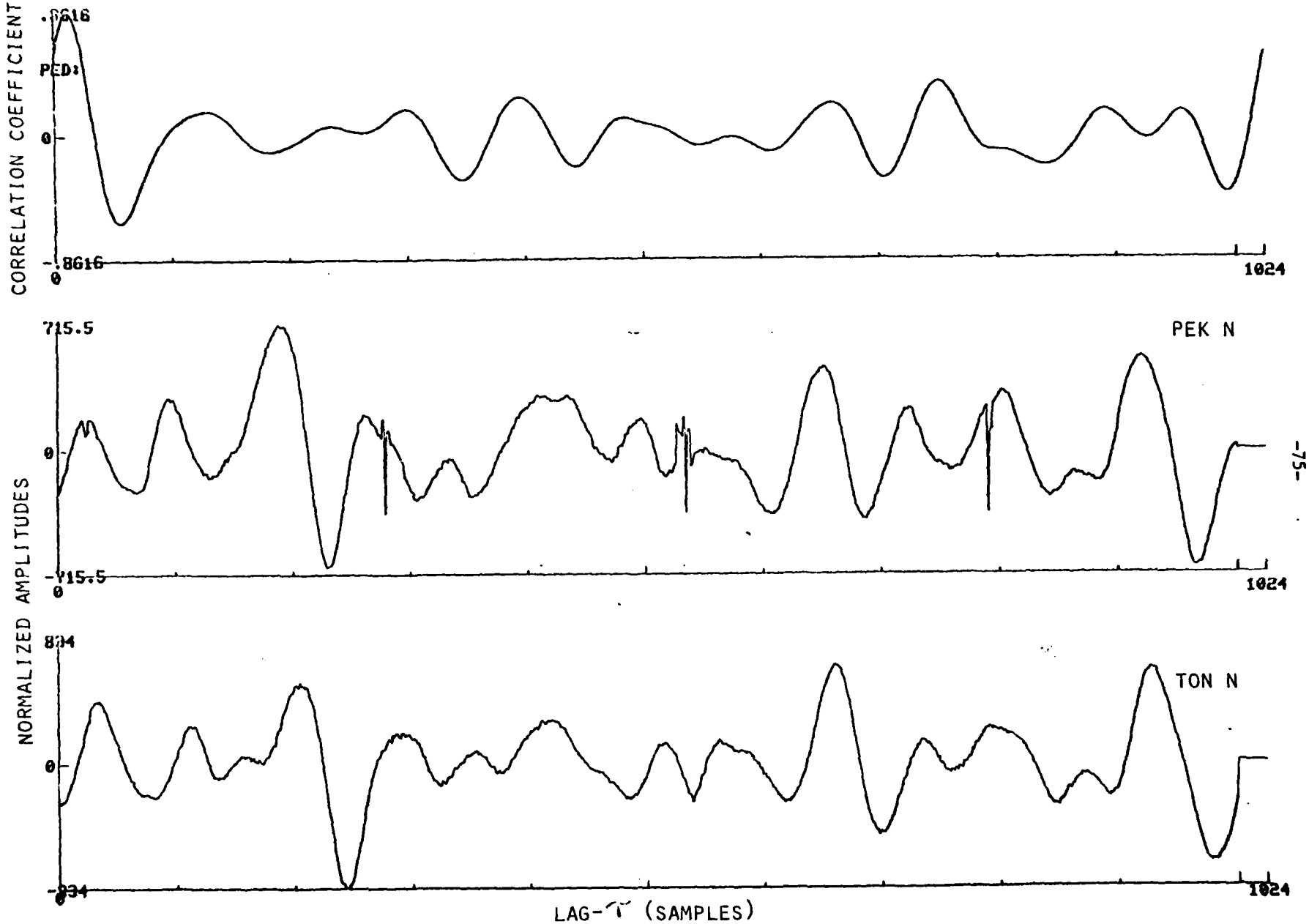

Figure 4-9 HARZER Lg waves - broad-band cross correlation.

5. EXPLOSION P WAVES AT CSA AND WAKE HYDROPHONE ARRAY (WHA)

Introduction

P waves and their associated spectra, from about 0.5 to 10 Hz, for explosions in Eastern Kazakh (EK), Novaya Zemlya (NZ), and Southwestern USSR (WS) and at the Nevada Test Site (NTS) were obtained from the Wake Hydrophone Array (WHA) and from the Catskill Seismic Array (CSA). Epicentral distances range from about 30° (NTS to CSA) to 60° to 90° (all other paths). WHA is an array of ocean bottom and suspended hydrophones near Wake Island in a water depth of 5.5 km on oceanic lithosphere greater than 100MY old (Figures 6-1 and 7-1). CSA was a tripartite array of three-component broad-band seismometers with digital recording that operated from September 1980 to November 1981 near Stone Ridge, New York, on the high Q lithosphere of eastern North America (Figure 3-1). In this section, we demonstrate the high coherence of the signals across the arrays and the array gain that can be obtained by simple processing techniques. In addition, we compare the signals and their spectra and attempt to isolate differences in the spectra related to differences in crust and upper mantle structure and to anelastic attenuation at both the source and the receiver locations. The latter is accomplished by obtaining values of average apparent Q, $\overline{Q}$ (and t*), as a function of frequency for the various source-receiver pairs.

Array Processed Data

The P arrivals from an EK event as recorded on the three vertical elements of CSA are shown in Figure 5-1. The signals shown are essentially flat to ground velocity from 0.5 to 10 Hz. The high coherence across the array is obvious. In Figure 5-2 the three verticals are shifted in time for propagation delay (on this time scale very little shift is required) and summed to produce the upper trace, STACK. The maximum theoretical processing gain for the signal (X3) is obtained for the first few seconds of the arrival. Also, there appears to be a significant improvement in signal-to-noise, although correlation of the microseism noise across the array tends to reduce the gain in wide-band signal to noise. Spectra for this P arrival are shown in Figures 5-3 through 5-5 . In Figures 5-3 and5-4effects of prefiltering (0.5 to 10 Hz band-pass) on the spectral (S+N)/N are illustrated for station 213, vertical. It is apparent that appropriate prefiltering has made a significant improvement in signal to noise ratio from about 0.4 to 4 Hz. The effects of stacking the vertical records are illustrated in Figures5-4and5-5using prefiltered signals. Between about 0.4 and 3 Hz the signal gain is about 3 and the noise about $3^{\frac{1}{2}}$ between the spectra for station 213 and the stacked spectra, as expected for correlated signal and uncorrelated noise.

Figures 5-6 through 5-9 illustrate the effects of prefiltering and stacking for an NZ event as recorded on two CSA vertical components. Some improvement in signal to noise with prefiltering and stacking is apparent in the time domain records. However, from the spectra it appears, in this case, that most of the improvement from prefiltering on the stacked records is at the lower end of the signal spectrum, from about .4 to .6 Hz.

Vertical components of the P wave at CSA from NTS event HARZER are illustrated in Figures 4-2 through 4-5 and have been discussed in Section 4.. The figures show the time domain signals, spectra, wide-band cross correlation across the array, and signal to noise ratio as a function of frequency.

A comparison of the signals from HARZER with those from EK and NZ demonstrates the deficiency of higher frequencies from NTS events, the energy from HARZER dropping rapidly above 0.7 Hz, whereas the Russian spectra start to drop near 2 to 3 Hz. It is likely that these differences in "corner frequency" are related to differences in anelastic attenuation in the vicinity of these three testing sites in addition to possible differences in source spectra as discussed in the next subsection.

Examples of two P waves from explosions in USSR as recorded at the Wake Hydrophone Array are shown in Figure 5-10. This figure is taken from a paper by McCreery, Walker, and Sutton (1983) on spectra of nuclear explosions, earthquakes, and noise at WHA.

The signals in Figure 5-10 are filtered to maximize signal/noise. The upper trace is from a single hydrophone and shows the direct arrival and its first water surface reflection. The lower trace is a composite of signals from two hydrophones with 40 km separation, obtained as follows: the filtered (1.5 to 5.0 Hz) time series from each hydrophone was inverted, shifted in time by the water surface reflection time, weighted to maximize the increase in signal/noise, and added to itself; the two resulting time series were then added with the appropriate propagation delay, and weighting to maximize the increase in signal/noise. Signal/noise was increased by 90% of the theoretical (i.e. for four equivalent hydrophones) with this method, indicating a high level of coherence between the signals added.

It should be noted that the Western Siberia event (WS), recorded at a distance of 77°, had an m_b of 4.6 which is equivalent to a yield equal to or less than 10 kt for a hard rock site. Use of all six bottom phones in WHA could

improve signal to noise by $3^{\frac{1}{2}}$ reducing m_b for the same signal to noise by 0.23 units. This in turn, is equivalent to a reduction in yield of over 50%.

Averaged spectra (and their scatter, $\pm 1\sigma$) for several EK and NZ events recorded on different phones of WHA are shown in Figures 5-11 and 5-12. Spectra are plotted only at frequencies where signal plus noise is 4 dB or greater above noise immediately preceeding the P arrival.

Determination of $\bar{Q}(f)$ and $t^*(f)$

Each individual (or averaged) P wave spectrum discussed above can be used to estimate the path averaged, frequency dependent, apparent Q, $\bar{Q}$, or its equivalent $t^* = t/\bar{Q}$, if some reasonable assumptions are made concerning the equivalent source spectrum and the form of the frequency dependence of Q. Thus, for each source region-receiving location pair individual estimates of $\bar{Q}$ (or t^*) as a function of frequency can be obtained and the results can be related to differences in the upper mantle attenuation near the sources and receivers.

Figure 5-13 is a set of master curves used to obtain the estimates of $\bar{Q}$ and t^* at 1, 5, and 10 Hz given in Table 5-1. The curves are given in terms of ground velocity, V (or, equivalently, pressure, for the hydrophone data) versus normalized frequency, F.

$$(1): V = (F/(F^2+1) \exp(-\pi t f_q F/Q)$$

where

$$Q = Q_o + K f_o F \text{ and } F = f/f_o.$$

Q_o represents the low frequency value for Q and f_o represents the corner frequency of the source. The source term, $F/(F^2+1)$, represents a simple f^{-2} fall-off in displacement for f greater than f_o with constant displacement at low frequencies and a 'critically damped' corner. Of course, actual source spectra with a more or less rapid fall-off or, e.g., a maximum near the corner frequency will produce some bias in the Q value obtained or some misfit to the curves. The frequency dependence assumed for Q, $Q = Q_o + Kf$, agrees with the observation of near constant Q at low frequencies, and with the prediction of relaxation theory (and some scattering theories) that Q should approach proportionality with f above the highest time constant involved in the dissipation mechanism.

Making the substitution $A = K/t$ and $B = Q_o/f_o t$, inspection of Equation 1 shows that the same curve will be obtained for any values of Q_o, K, f_o, and t such that the parameters A and B have the same values, since, with that substitution the exponent term reduces to $-\pi F/(B+AF)$. Thus, the curves in Figure 5-13, showing the effect of varying K from 0 to ∞ with constant Q_o and t, represent a variation of parameter A from 0 to ∞ with a constant value of B, i.e. $Q_o/f_o t$. A similar set of curves can be constructed keeping A constant and varying B.

When a match is obtained between an observed spectrum and a master curve for a given travel time, t, the source corner frequency, f_o, equals the observed frequency coincident with F = 1. The values for K and Q_o follow directly.

The match of the master curves to the EK-WHA spectrum (Figure 5-12) is shown in Figure 5-14. The spectrum is reasonably well contained between the K = 100 and K = 200 curves. A better match is obtained in Figure 5-15, which compares the spectrum with curves for constant K = 150 and Q_o = 500 and 700 (i.e. constant A and varying B). In this case, the nominal best fit is K = 150 and Q_o = 600 (for nominal t = 700 and f_o = 1). The values used to obtain $\overline{Q}$ and t* in Table 5-1 are based on the observed values of 693 sec and 1.2 Hz for t and f_o, respectively.

The values obtained for $\overline{Q}$ and t* by the procedure described above are listed in Table 5-1 at frequencies of 1, 5, and 10 Hz, in order of decreasing Q. All seven paths show a strong increase of Q with frequency, becoming almost proportional to frequency between 5 and 10 Hz for some paths. As expected, there are large differences in Q near 1 Hz with the lower values resulting from the NTS paths and the very lowest from the regional (33°) path to CSA. For common USSR sources, CSA paths have somewhat higher Q than WHA at all frequencies. In order of decreasing Q, the source regions rank: NZ; EK; WS; and NTS. NTS falls far below the others at 1 Hz but approaches the Q for other paths to WHA at 10 Hz. If correct, this would suggest that some high frequency energy might manage to survive passage through the upper mantle under NTS.

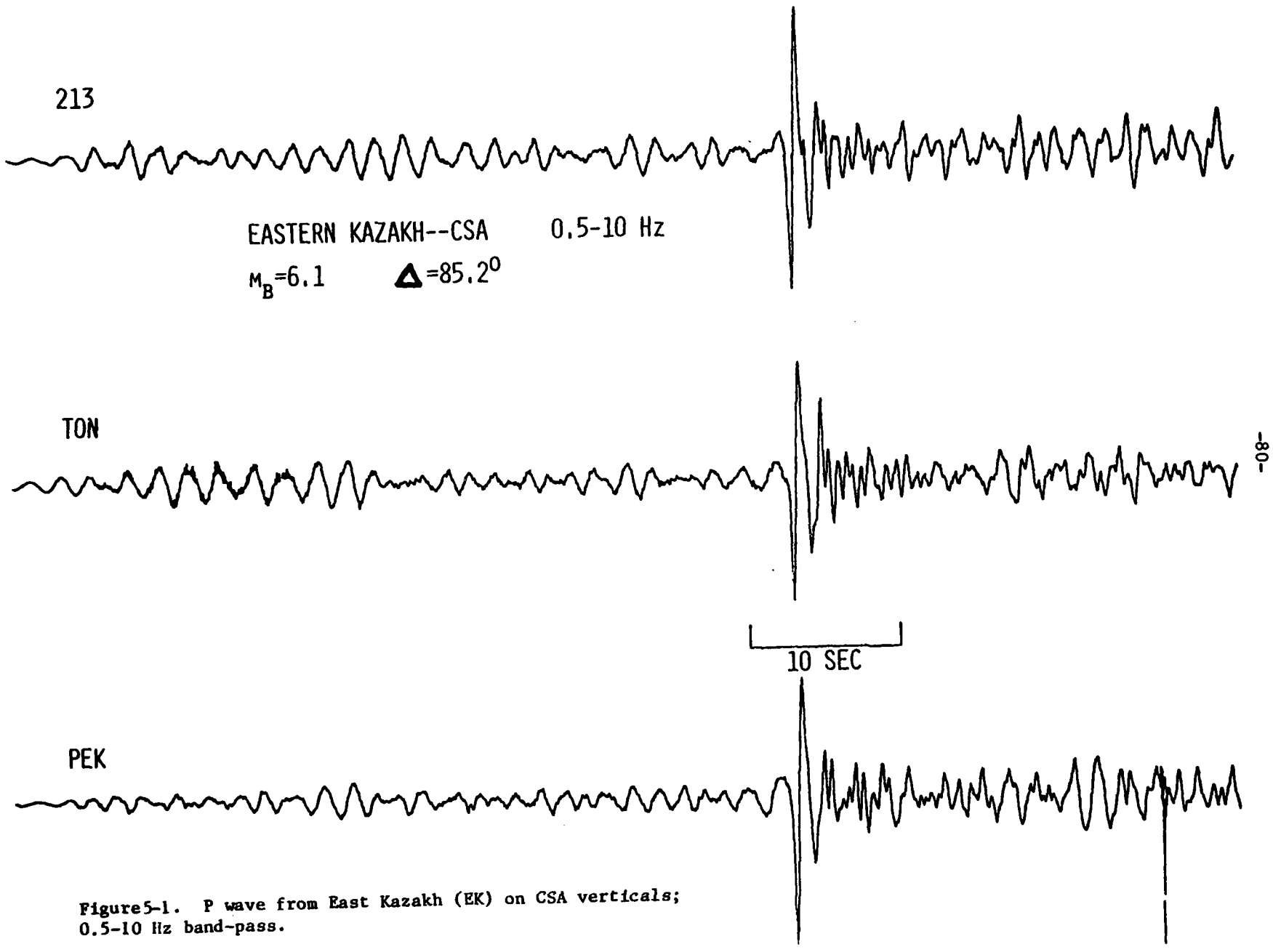

Figure5-1. P wave from East Kazakh (EK) on CSA verticals; 0.5-10 Hz band-pass.

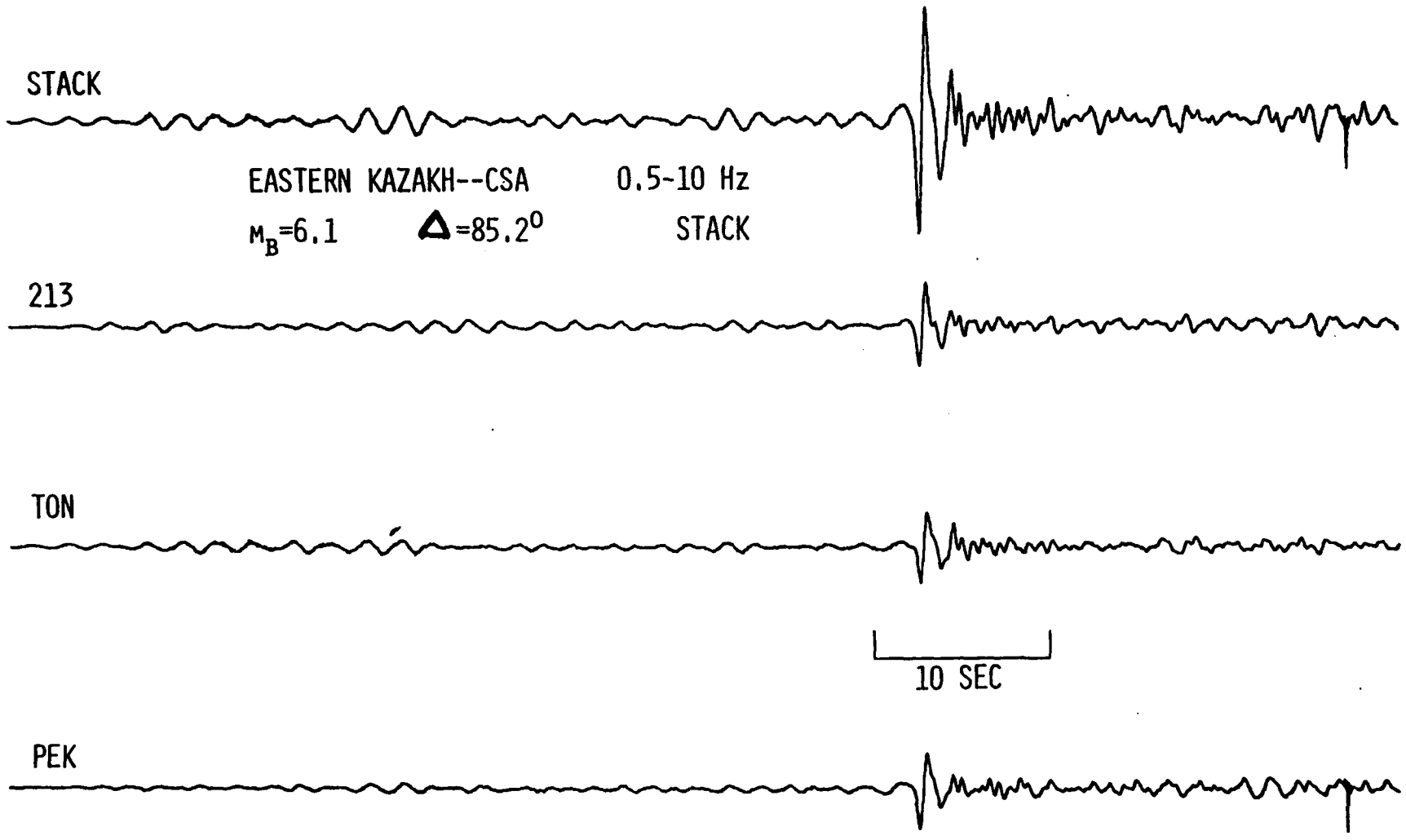

Figure 5-2 Delay-sum (stack) of P from E. Kazakh; 0.5-10 Hz band-pass.

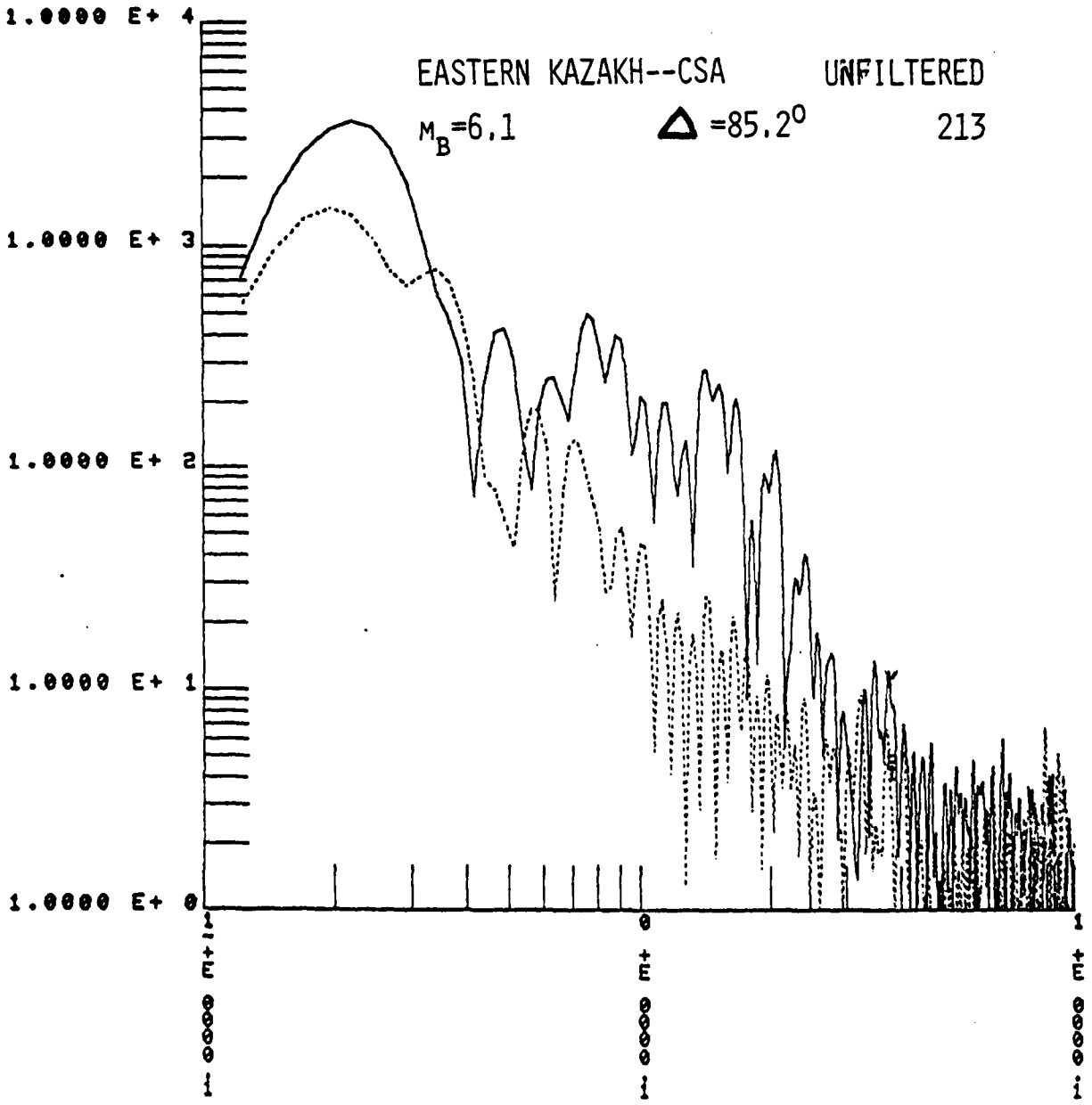

Figure 5-3. Spectrum of P from East Kazakh on station 213 vertical, unfiltered; dashed spectrum is noise immediately preceeding P.

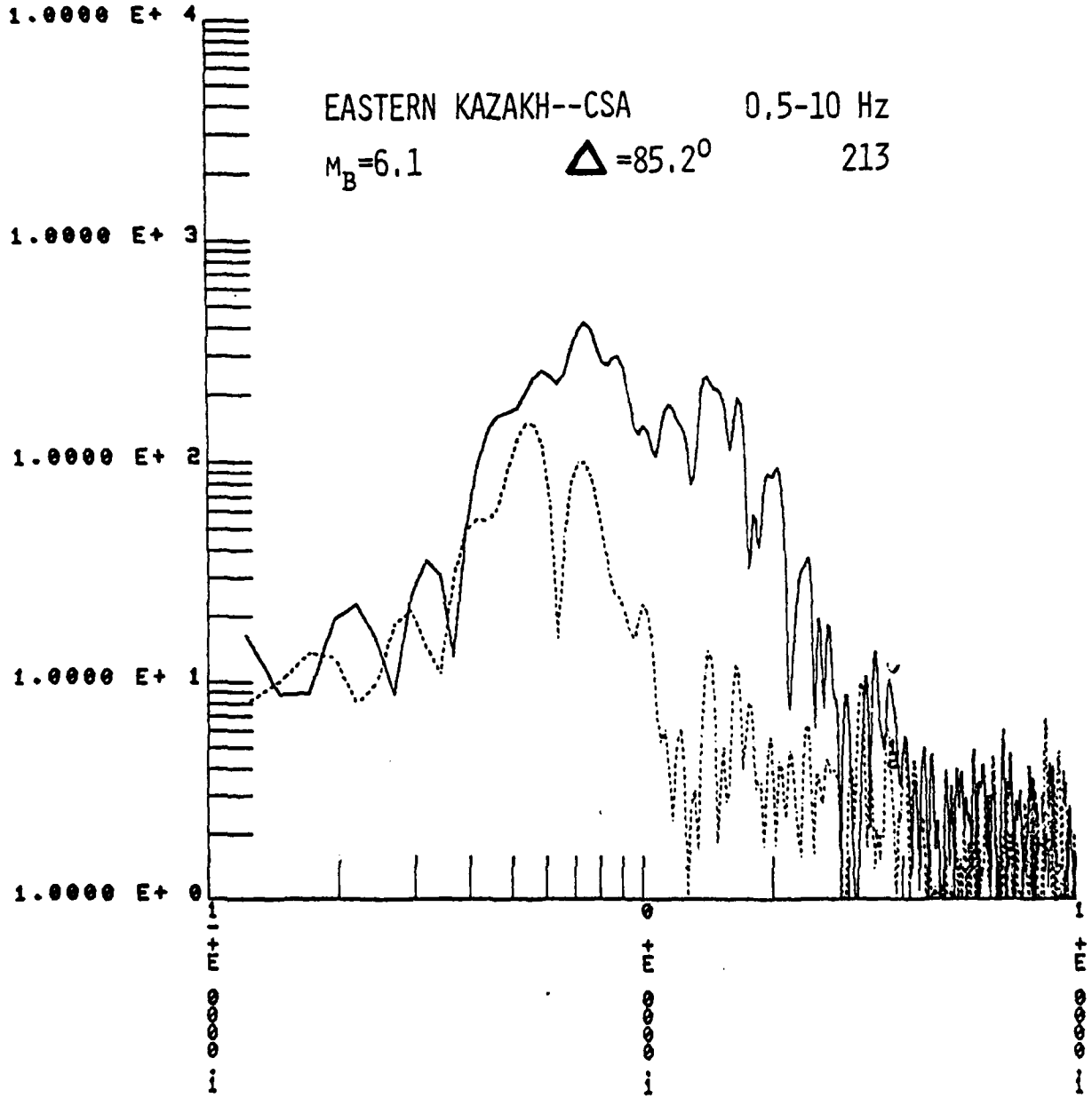

Figure 5-4. Spectrum of P from East Kazakh on station 213 vertical, 0.5-10 Hz band-pass; dashed spectrum is noise immediately preceeding P.

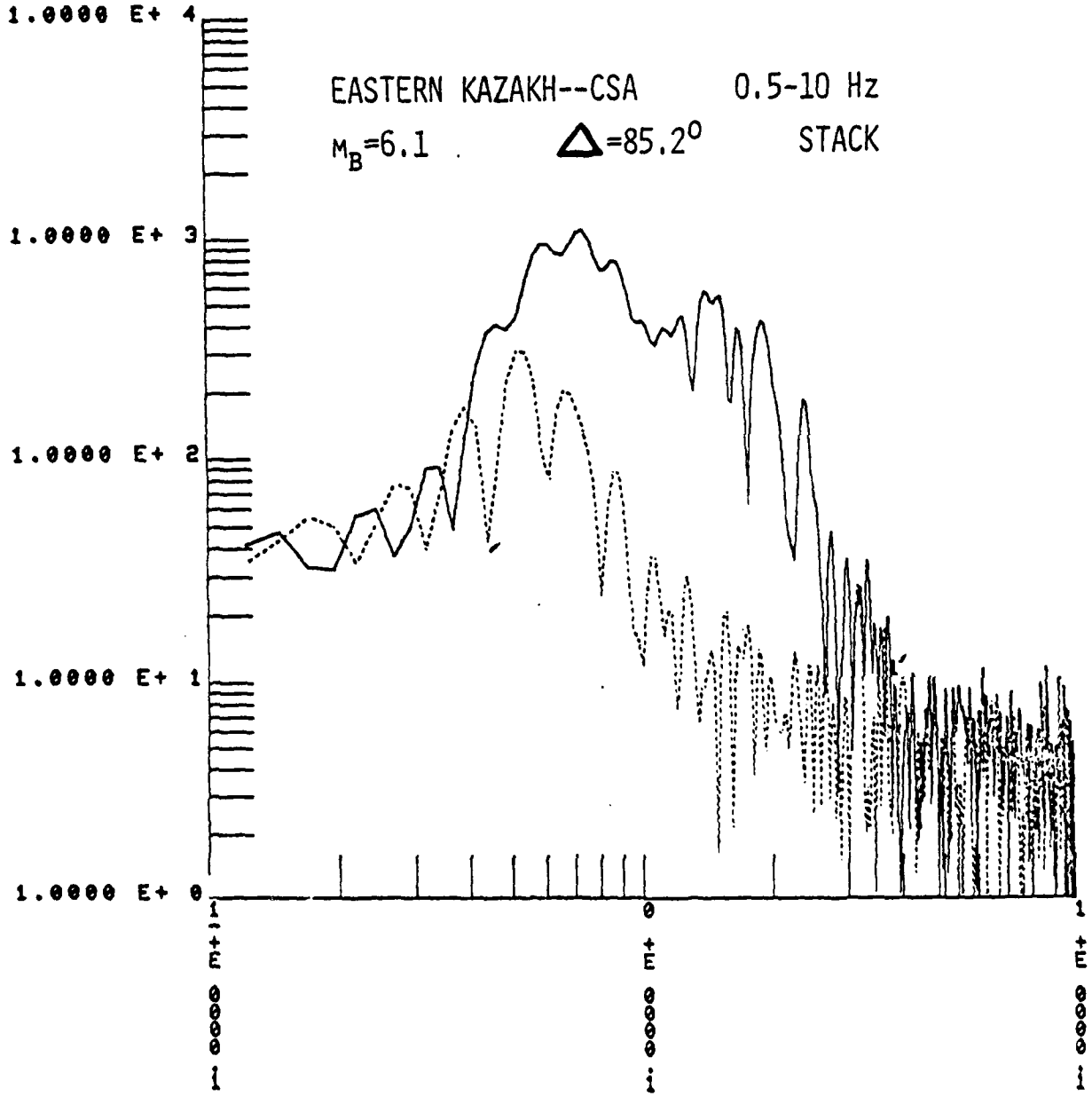

Figure 5-5. Spectrum of P from East Kazakh on stacked verticals, 0.5-10 Hz band-pass; dashed spectrum is noise level.

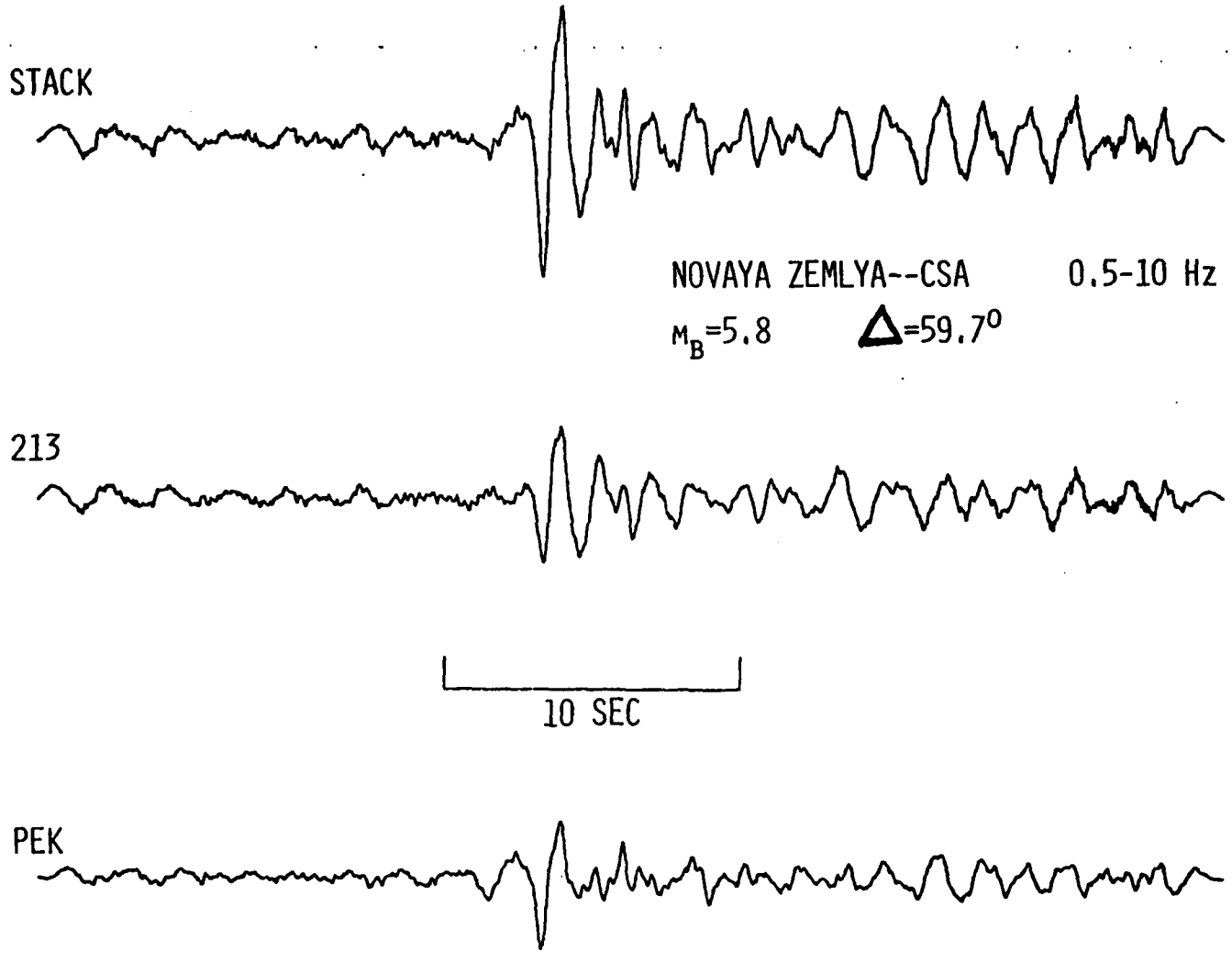

Figure 5-6 Individual and stacked CSA verticals for P wave from Novaya Zemlya (NZ); 0.5-10 Hz band-pass.

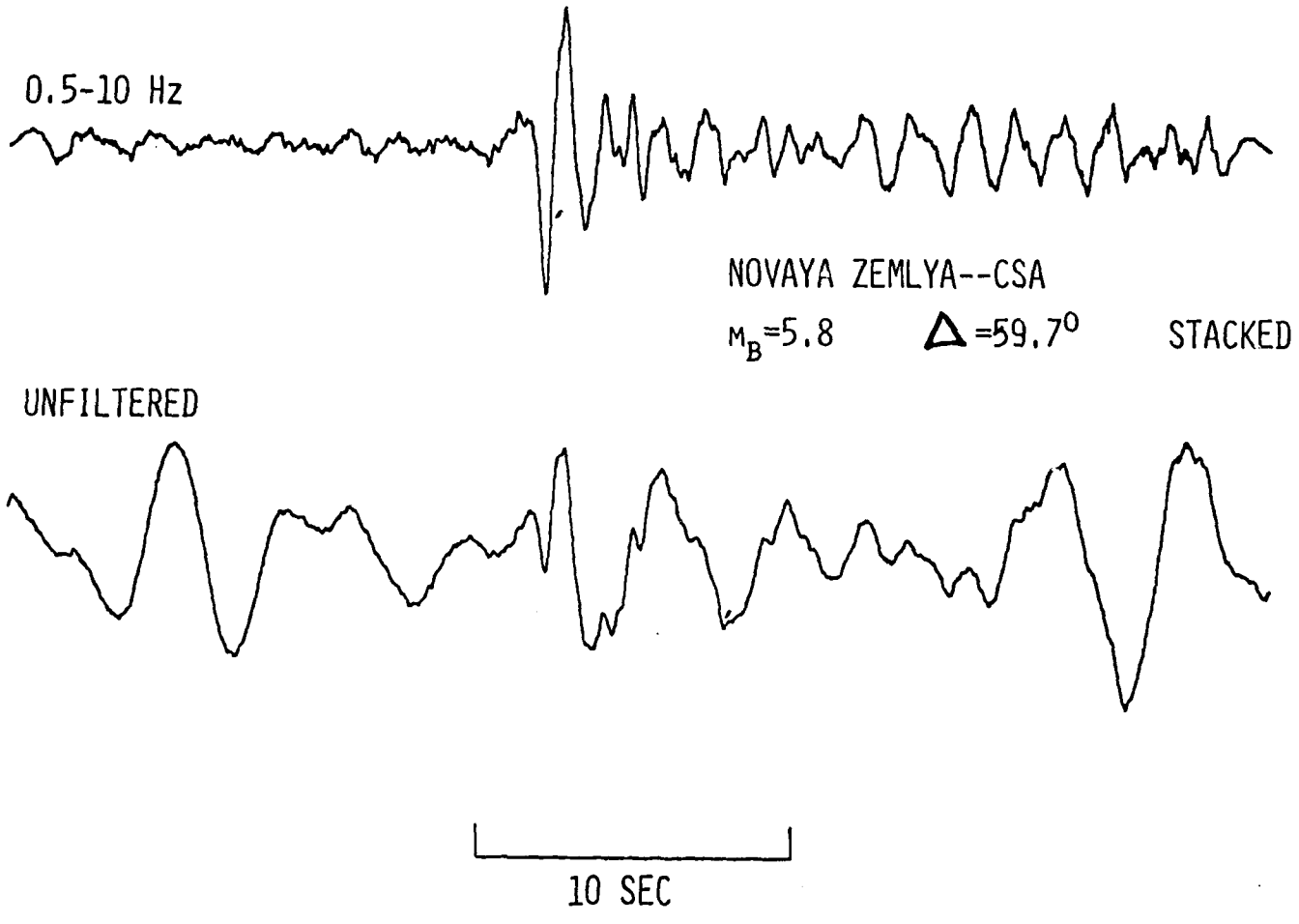

Figure 5-7. Filtered and unfiltered P from Novaya Zemlya on stacked verticals.

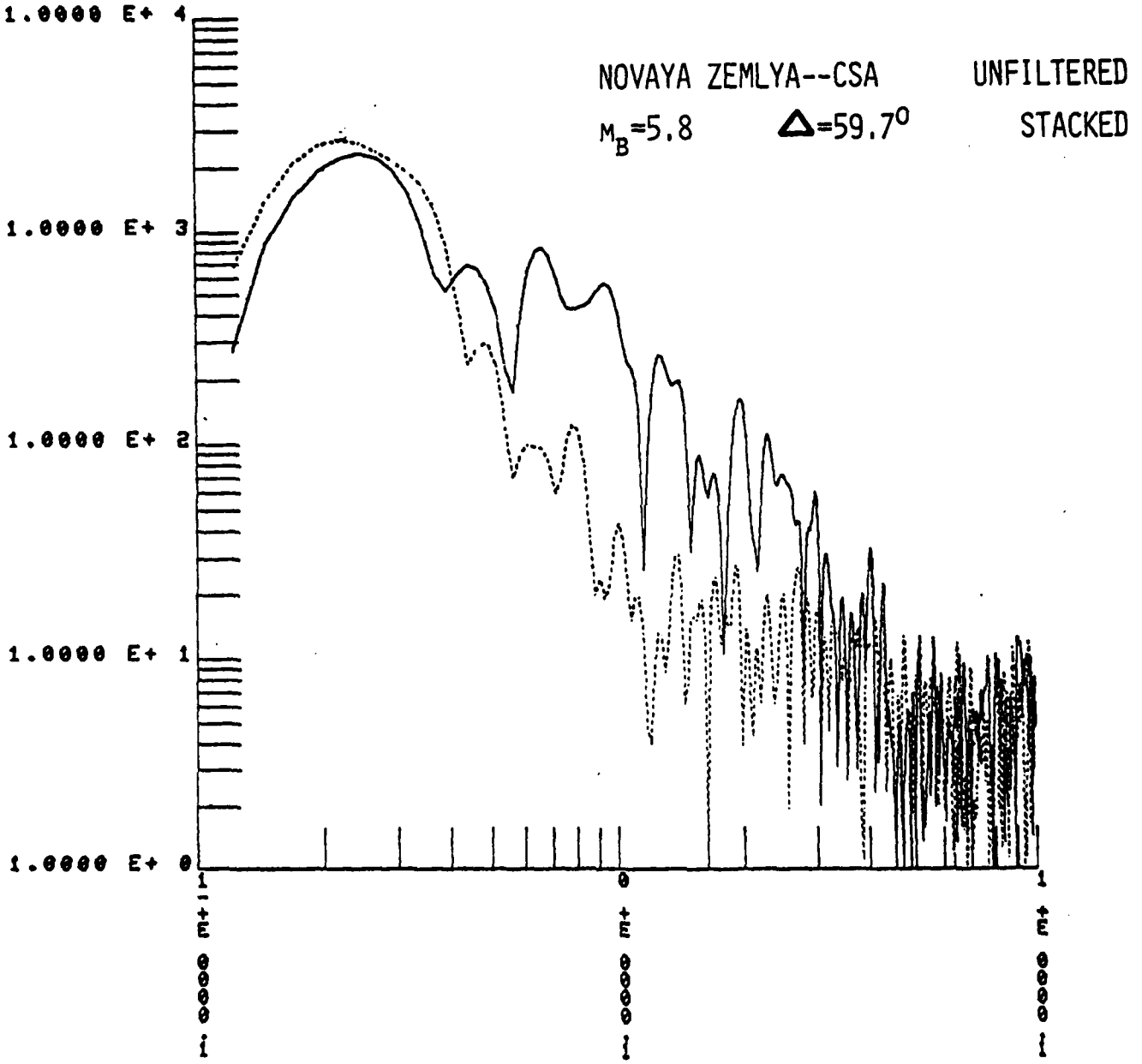

Figure5-8. Spectrum of P from Novaya Zemlya on stacked verticals, unfiltered; dashed spectrum is noise level before P.

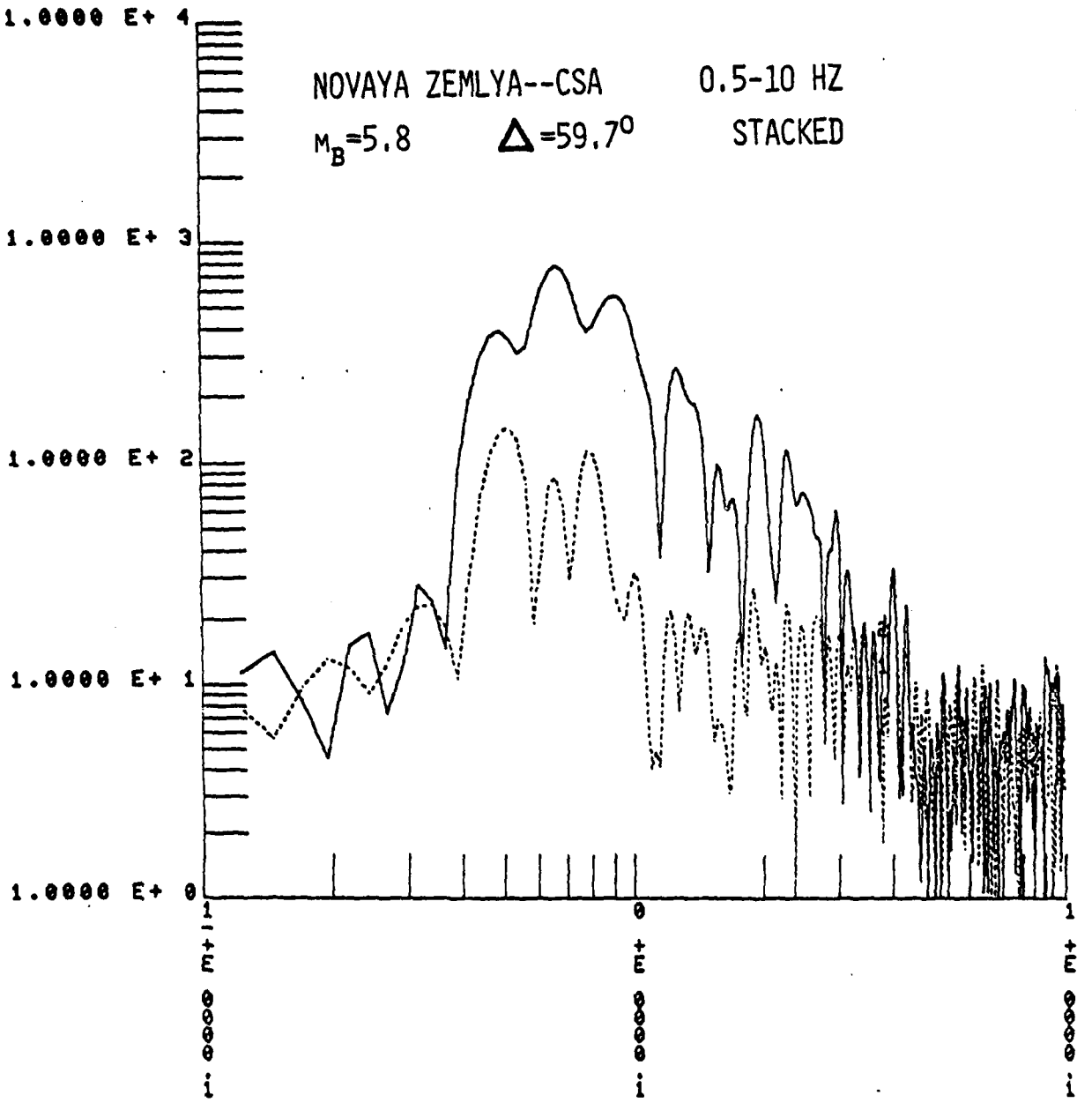

Figure 5-9. Spectrum of P from Novaya Zemlya on stacked verticals, 0.5-10 Hz band-pass; dashed spectrum is noise level before P.

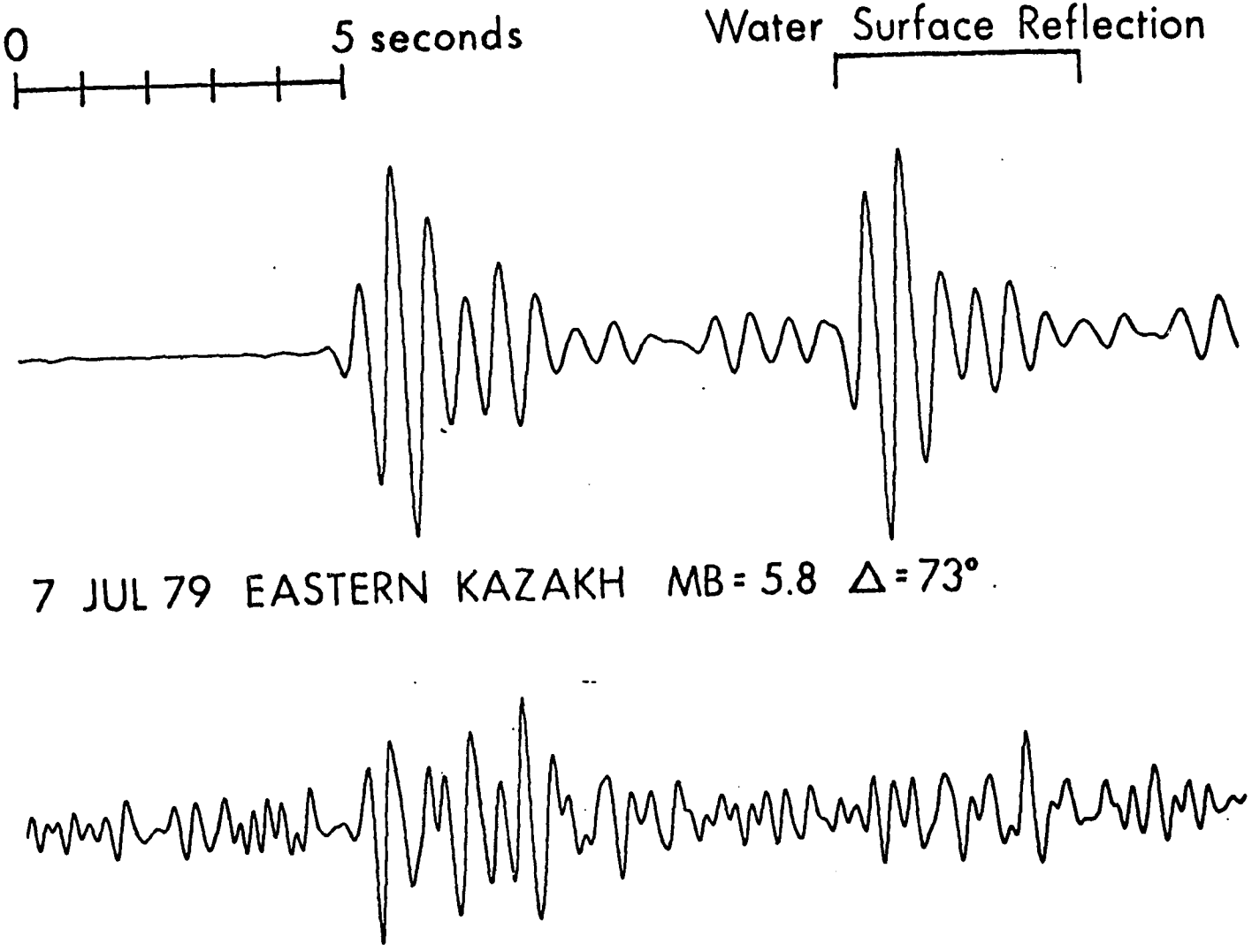

Figure 5-10 Examples of explosion P waves recorded on Wake Island Hydrophone Array, see text.

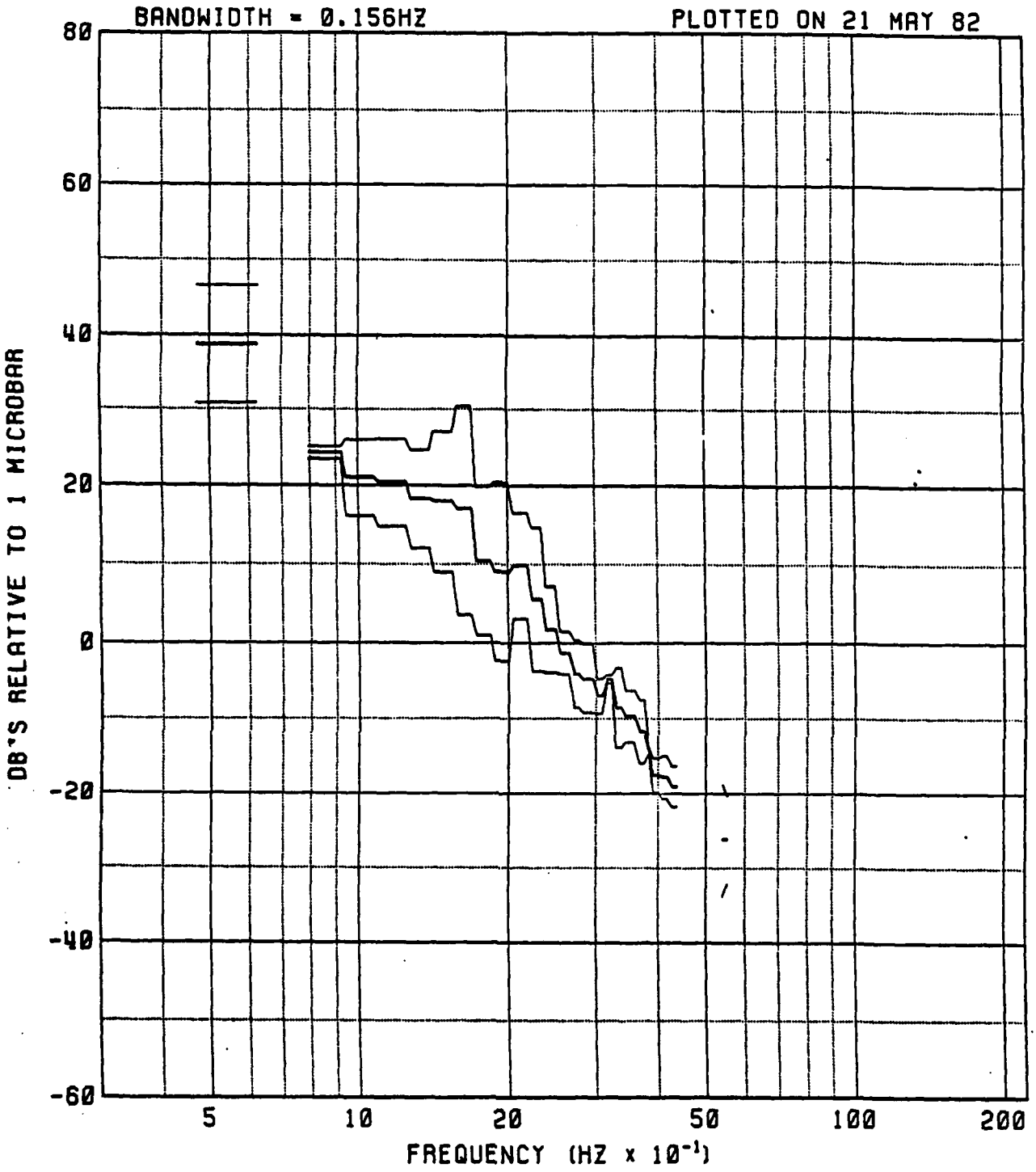

NOVAYA ZEMLYA DISTANCE = 77degrees $\overline{MB}$ = 5.7

2 Events, 4 Signals

Figure 5-11. Average spectrum and $\pm$ 1 σ of four individual signals from WHA for two Novaya Zemlya events;in blank areas (S+N)/N is less than 4 dB.

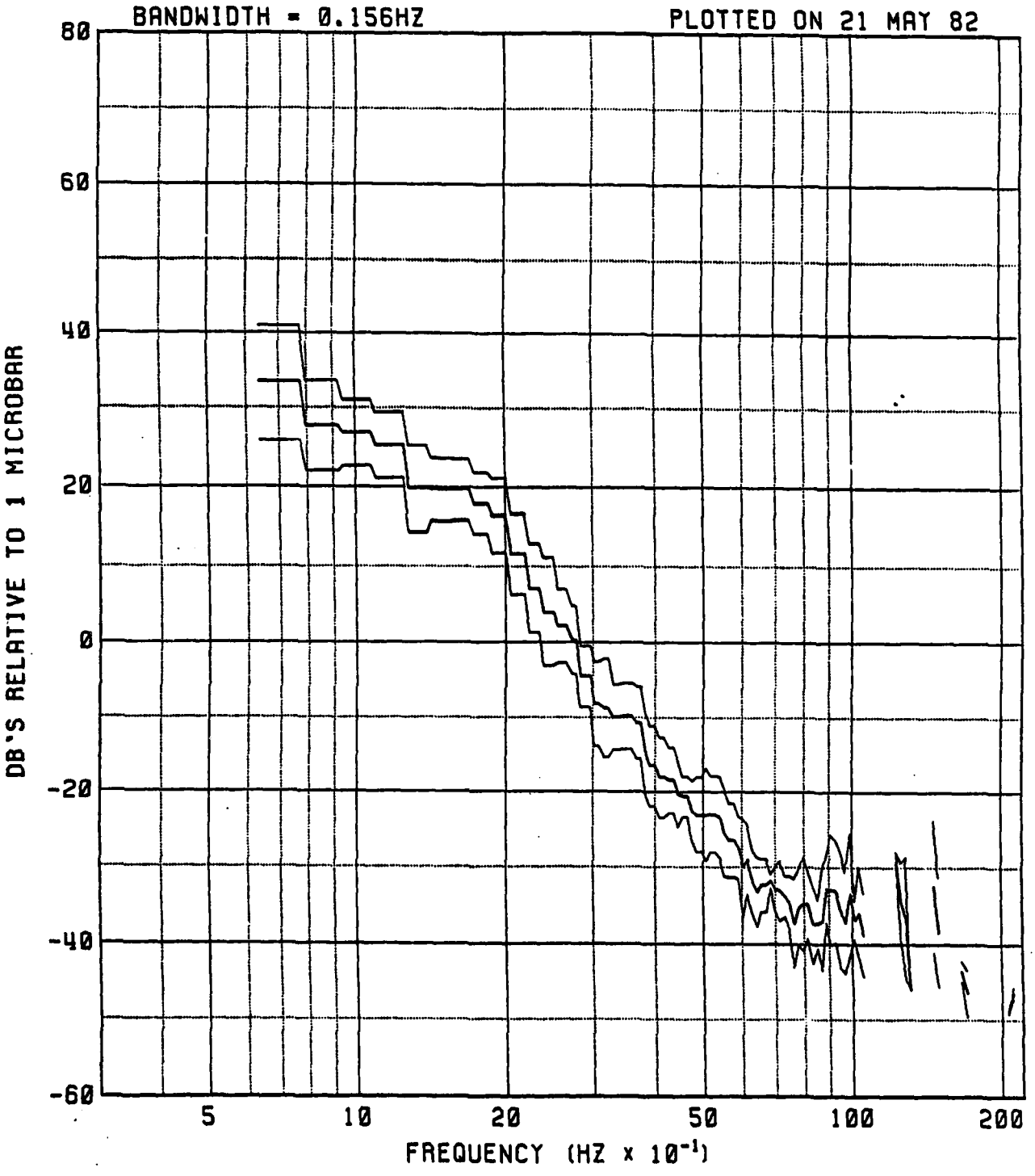

E. KAZAKH DISTANCE = 73degrees $\overline{MB}$ = 6.1

7 Events, 16 Signals

Figure 5-12. Average spectrum and $\pm$ 1 σ of 16 signals from WHA for seven East Kazakh events; in blank areas (S+N)/N is less than 4 dB.

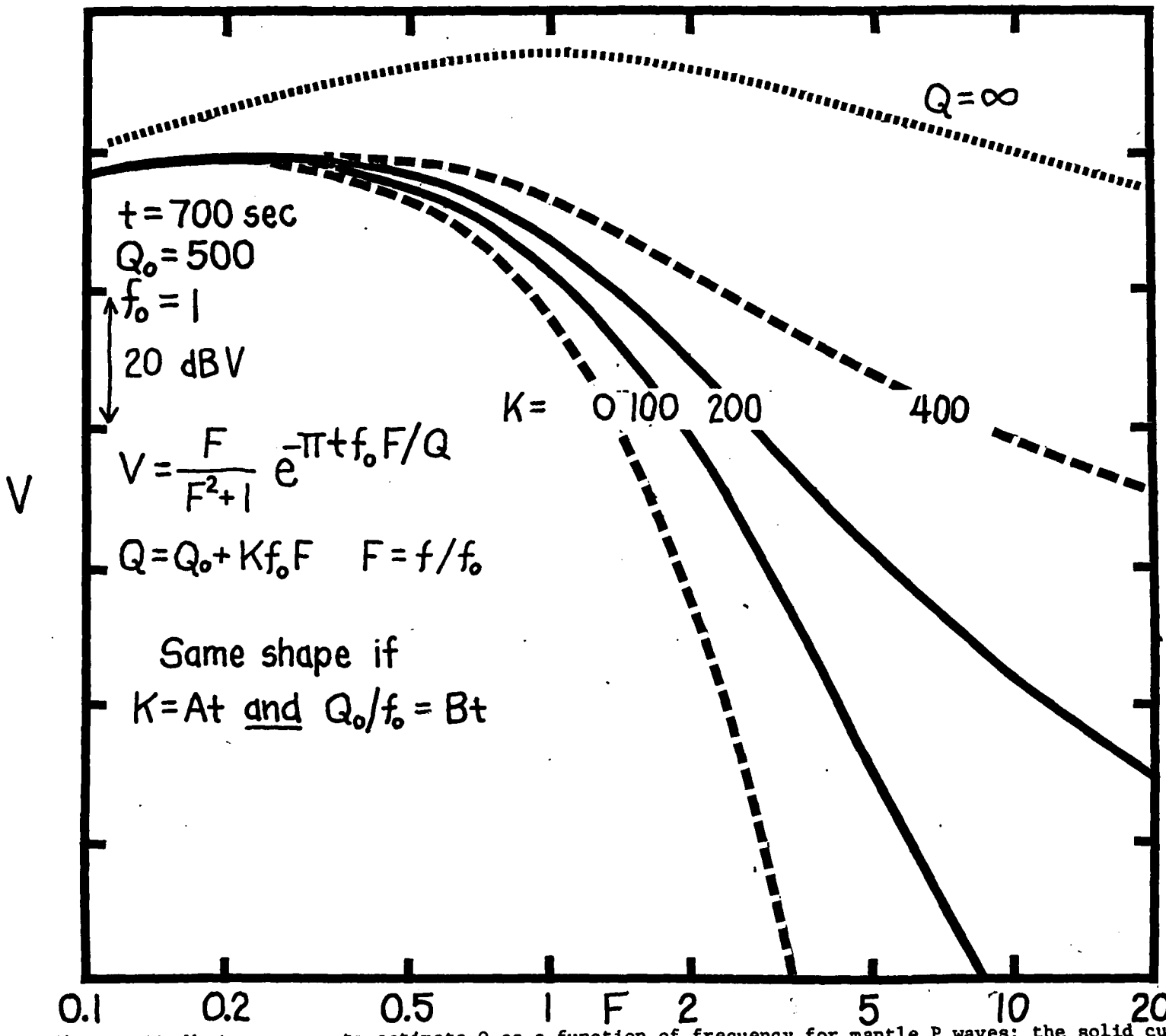

Figure 5-13. Master curves to estimate Q as a function of frequency for mantle P waves; the solid curves are those shown in Figure 5-14; see text for discussion.

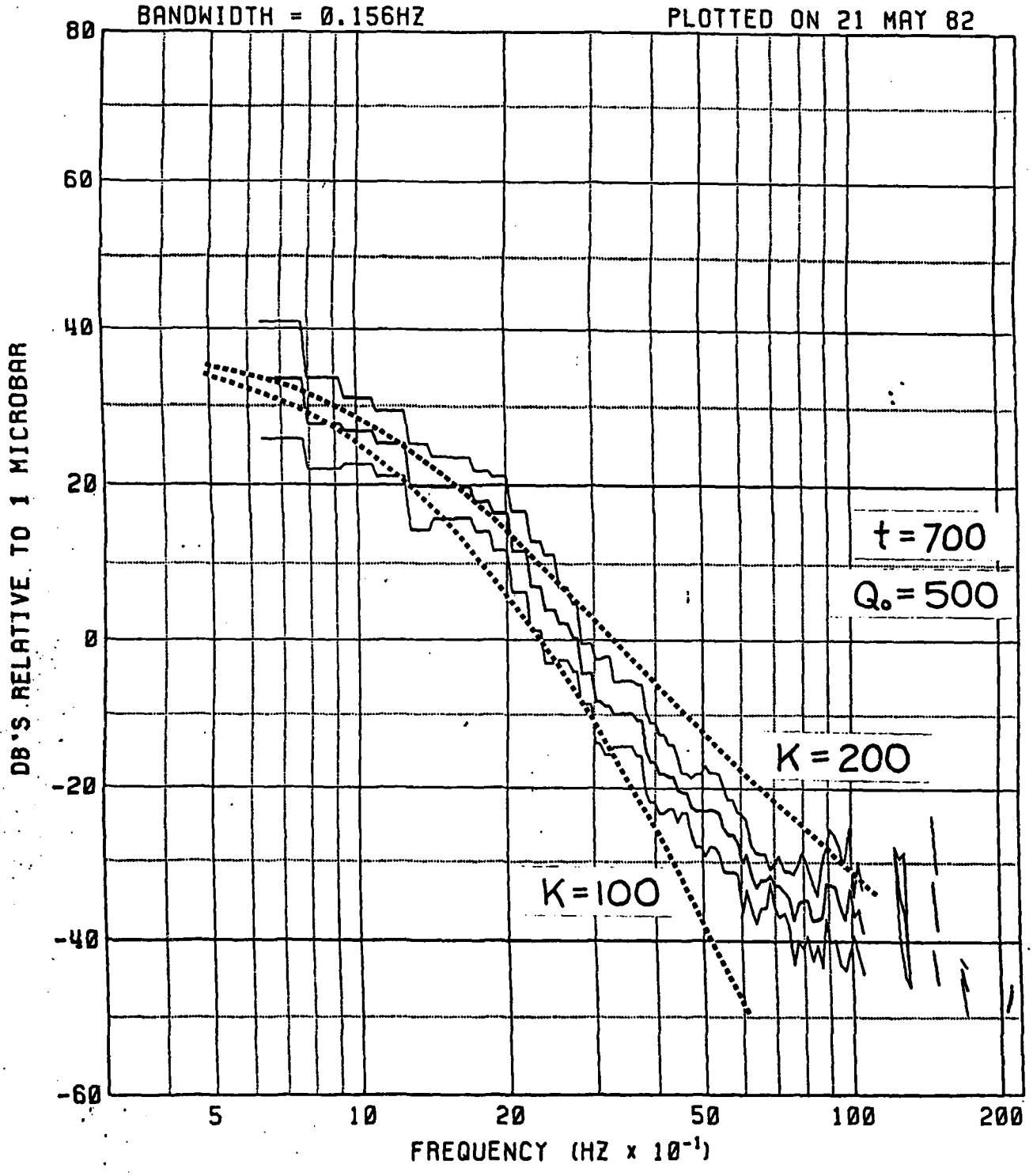

E. KAZAKH DISTANCE = 73degrees $\overline{MB}$ = 6.1

7 Events, 16 Signals

Figure 5-14. Match of EK-WHA spectrum to master curves for one Q_o and two values of K.

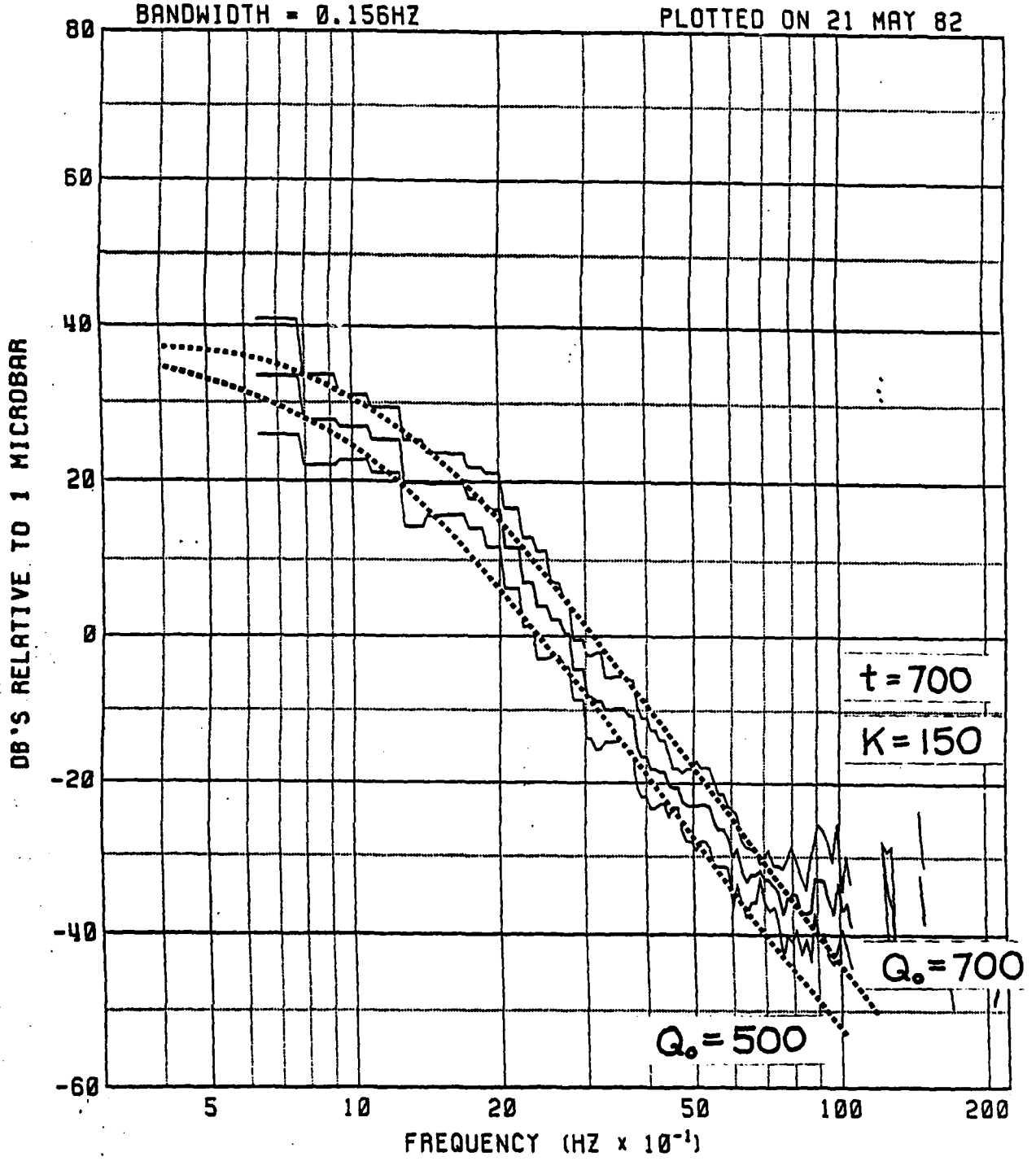

Figure 5-15. Match of EK-WHA spectrum to master curves for one K and two values of Q_o.

TABLE 5-1

$\bar{Q}(F)$ AND $T^*(F)$ FOR EXPLOSION P WAVES TO CSA AND WHA

PATH	DISTANCE	T (SEC)	M_B	$\bar{Q}/T^*$ ($T^*=T/\bar{Q}$) 1 Hz	5 Hz	10 Hz
NZ-CSA	60^0	611	5.8	1250/.49	1850/.33	2600/.24
NZ-WHA	77^0	716	5.8	1100/.65	1700/.42	2450/.29
EK-CSA	85^0	759	6.1	1100/.69	1700/.45	2450/.31
WS-WHA	77^0	716	4.5	1000 ± /.72 ±	1500 ± /.48 ±	2500 ± /.29 ±
EK-WHA	73^0	693	6.1	850/.82	1450/.48	2200/.32
NTS-WHA	68^0	663	5.8	650/1.02	1250/.53	2000/.33
NTS-CSA	33^0	399	5.6	250/1.60	600 ± /.67 ±	1000 ± /.40 ±

References

McCreery, C. S., D. A. Walker, and G. H. Sutton, 1983, Spectra of Nuclear Explosions, Earthquakes, and Noise from Wake Island Bottom Hydrophones, Geophys. Res. Let., (in press).

6. Q OF THE NORTHWEST PACIFIC LITHOSPHERE

Introduction

Using a unique data set of high-frequency, teleseismic Pn and Sn wavetrains recorded on the Wake Island Hydrophone Array (WHA; Figure 6-1) from circum-Pacific earthquakes. We have been able to estimate apparent Q as a function of frequency between about 1 and 10 to 15 Hz for the lithospheric waveguide.

The lithosphere of the northwest Pacific is an extremely efficient seismic waveguide, passing frequencies as high as 30 and 35 Hz to 2000 km (for Pn and Sn, respectively) and as high as 15 and 20 Hz to 3300 km (for Pn and Sn, respectively) (Walker et al., 1983). Although details of the generation and propagation of Pn/Sn are not well understood, it is generally agreed that they are guided waves propagating within the lithosphere. Recent theoretical work involving the generation of synthetic seismograms (Menke and Richards, 1980; Gettrust and Frazer, 1981; and Sutton and Harvey, 1981) is beginning to improve our understanding of these phases. However, work is still required in several areas. As an example, there still seems to be disagreement concerning the relative importance of scattering as opposed to some laterally uniform velocity-depth function in producing the drawn-out character of Pn and Sn. In addition, little theoretical work has been done on the effects of focal depth and sediment velocity structure near the receiver.

Our observational studies of Pn/Sn across the northwestern Pacific have shown that the apparent Q of the lithosphere is high, higher for Sn than for Pn, and that Q increases strongly with frequency above about 1 Hz (Walker, et al., 1978; McCreery and Sutton, 1981).

The WHA data have provided a unique opportunity to study the generation and propagation of Pn/Sn through mature ($>$ 100MY) oceanic lithosphere over pure oceanic paths. The data are recorded on analog magnetic tape with response to over 30 Hz, and a facility for efficient digitization is available at HIG. (The installation has recently been upgraded to a fully digital recording system, as described in Section 7.)

In understanding the chemical, physical, and dynamic conditions within the earth, detailed knowledge of the anelastic properties is perhaps of as great or greater importance than of the elastic properties. Anelasticity, for example, is likely to be a more sensitive indicator of phase change, high temperature, or the presence of interstitial fluids; it may be more directly related to deformation and failure mechanisms, and to electrical conductivity.

The attenuation of seismic waves provides a means for observing the anelastic properties of the earth's interior. Conversely, adequate knowledge of the attenuation of the seismic waves is required in order to use them with confidence to infer dynamic conditions at the earthquake source.

Q or Q^{-1} is a convenient measure of seismic wave attenuation (Q normally being defined by the expression: $A \propto \exp(-\pi t/2Q)$, or by $t^* = t/Q$ for work on teleseismic body waves). Q may be sub-classified as Q_α or Q_β for P or S waves, respectively. Q_β is generally expected to be smaller than Q_α since most loss mechanisms appear to be associated with the rigidity modulus. Attenuation as a function of depth within the earth, for frequencies lower than 1 Hz, has been investigated with considerable success for many years (e.g. Anderson and Hart, 1978). Regional variations of attenuation in the continental crust and upper mantle have also been investigated (e.g. Sutton et al., 1967; Cheng and Mitchell, 1981).

Recently, there has been an increase of interest in the frequency dependence of Q (e.g. Aki and Chouet, 1975; Aki, 1980a and b, 1981; Mitchell, 1981). Especially for frequencies above 1 Hz, scattering appears to make an important contribution to attenuation within the continental crust and upper mantle (Aki and Chouet, 1975; Aki, 1980a and b, 1981; Dainty, 1981; Dainty and Toksoz, 1981; Wu, 1982). Attenuation from scattering (Q_s) takes the same exponential form as that from internal dissipation (Q_i) and the two mechanisms can be difficult to differentiate, i.e., $\frac{1}{Q} = \frac{1}{Q_i} + \frac{1}{Q_s}$. Dainty, 1981, for lithospheric S waves in central Asia and Japan, obtained $Q_i = 2000 \pm 500$ and $Q_s = \omega/g_o v$, with v assumed to be 3.5 km/sec and $g_o = 0.005$ and $0.01\ km^{-1}$ for Asia and Japan, respectively, between about 1 and 30 Hz. Both scattering theory and relaxation theory of internal friction predict that Q will increase with frequency above a certain frequency; depending upon the size distribution for scattering and upon the highest relaxation frequency for internal friction. For the earth this seems to be the case, for one or the other or both mechanisms, above about 1 Hz.

The estimates of Q obtained for the western Pacific lithosphere from high-frequency teleseismic Pn and Sn, in agreement with the continental studies referenced above, show a strong increase with frequency. However, the values of Q are an order of magnitude larger (Walker et al., 1978; McCreery and Sutton, 1981).

Until now, our analyses for Q have been limited to essentially single station methods. Because of the distribution of the epicenters and the location of WHA, there is a correlation between distance and path location; there is also

some correlation between distance and magnitude of the events studied. These correlations can produce uncertainty and bias in the estimates of Q.

Data

During the nearly three years of operation of WHA, many Pn/Sn recordings have been obtained. Examples of Pn/Sn and their spectra illustrating their emergent and diffuse character and their high frequency content are shown in Figures 6-2 and 6-3. Results of some preliminary analyses for Q as a function of frequency are presented in the following section. As mentioned in the introduction, data are routinely digitized from analog magnetic tape recordings with good fidelity to above 30 Hz.

We have taken care in these studies to assure that the high frequencies observed are not the result of non-linear response to large signals.

Analytical Procedures and Results

An expression for the spectral amplitude of a seismic signal is

$$A(f) = M_o S(f) r^{-n} \exp(-\pi f p q r) \qquad (1)$$

where M_o represents the source amplitude

$S(f)$ represents the normalized source spectrum

f = frequency

r = distance

$q = Q^{-1}$ is the apparent anelastic attenuation coefficient and may include some contribution from scattering and/or tunneling

p represents the "group" slowness; travel time divided by distance; $pr = t$

n is the spreading parameter, e.g., ½ for cylindrical, 1 for spherical.

In general, for a given set of observational data, q and n could be somewhat correlated with f, r, and/or p; S(f) could be correlated with r and/or p; and M_o could be correlated with r. These relationships would be the result of: choosing events having acceptable signal levels at different distances, i.e. bigger earthquakes at greater distances; interdependence between M_o and S, e.g., changing source corner frequency with magnitude; some relationship between p and the portions of the waveguide through which the signal propagates, i.e. averaging properties of different depths within the waveguide at different group velocities; and/or lateral variations in the waveguide. Uncertainty about these relationships translate into uncertainty in empirical estimates of Q.

Using Equation 1, we can derive the relations for three independent procedures to obtain estimates of Q. First we take the logarithm of Equation 1 and then different derivatives:

$$\ell nA(f) = \ell n\, M_o + \ell nS - n\, \ell nr - \pi fpqr \qquad (1')$$

$$q_r = -\underline{\frac{1}{\pi fp}\left(\frac{\partial \ell nA}{\partial r} + \frac{n}{r}\right)} + \frac{1}{\pi fp}\left(\frac{\partial \ell nM_o}{\partial r} + \frac{\partial \ell nS}{\partial r}\right) - \frac{\partial q}{\partial \ell nr} - \frac{\ell nr}{\pi fp}\frac{\partial n}{\partial r} \qquad (2)$$

$$q_{fr} = -\underline{\frac{1}{\pi p}\frac{\partial^2 \ell nA}{\partial f \partial r}} - \frac{\partial q}{\partial \ell nf} - \frac{\partial q}{\partial \ell nr} - \frac{\partial^2 q}{\partial \ell nf\, \partial \ell nr} - \frac{1}{\pi pr}\frac{\partial n}{\partial f} - \frac{\ell nr}{\pi p}\frac{\partial^2 n}{\partial f \partial r} \qquad (3)$$

$$+ \frac{1}{\pi p}\frac{\partial^2 \ell nS}{\partial f \partial r}$$

$$q_{pr} = -\underline{\frac{1}{\pi f}\frac{\partial^2 \ell nA}{\partial p \partial r}} - \frac{\partial q}{\partial \ell np} - \frac{\partial q}{\partial \ell nr} - \frac{\partial^2 q}{\partial \ell np\, \partial \ell nr} - \frac{1}{\pi fr}\frac{\partial n}{\partial p} - \frac{\ell nr}{\pi f}\frac{\partial^2 n}{\partial p \partial r} \qquad (4)$$

$$+ \frac{1}{\pi f}\frac{\partial^2 \ell nS}{\partial p \partial r}$$

In Equations 2, 3, and 4, the underlined terms represent alternate ways to estimate Q and the remaining terms on the right hand side are possible sources of error. These equations can be expressed also in terms of derivatives with respect to t rather than r, since t = pr. Most empirical estimates of Q have used relationships equivalent to Equations 2 or 3.

Equation 2 can be used effectively for a given source recorded at different distances. Some station corrections may be required. If different sources are used, the amplitudes must be normalized to a common M_o and S. Uncertainty in the spreading term, n, can produce difficulties.

Equation 3 can be used effectively for different sources recorded at a single station since the source terms M_o and S have been nearly eliminated. However, this approach can be seriously in error if q varies with frequency.

For example, if Q is proportional to frequency, i.e. $q = c/f$, the slope of the spectrum will be constant with distance; the underlined term will be identically zero; and apparent Q will be infinite. Including the second term in the definition removes the error but makes the value of Q indeterminate. Nakamura and Koyama (1982) overcome this difficulty be obtaining a least square match between q_r (with an additional station correction term) and q_{fr} obtained by integration using the first two terms on the right hand side of Equation 3.

Figures 6-4 and 6-5 from McCreery and Sutton, 1981, summarize the results of our first attempt to determine Q as a function of frequency for Pn and Sn recorded at WHA. Previous estimates (Walker et al., 1978) were based on the assumption that Q is independent of frequency. We now believe that assumption was incorrect.

In Figure 6-4 on the left side, the estimates of Q for Pn and Sn are based on Equation 4. This procedure was adopted to avoid problems, when using Equations 2 and 3. In Equation 2, the problems are associated with uncertainties in the spreading law (n) and in the source strength of Pn and Sn as a function of magnitude. In Equation 3, the problems are associated with uncertainties in the variation of Q with frequency.

The method of Equation 4 seems appropriate since both Pn and Sn contain appreciable energy over a wide range of "group" velocities (great circle distance/travel time). The analytical procedure is as follows:

> For each individual earthquake the spectral amplitude averaged over a 1 Hz band is determined as a function of "group" slowness, p, (travel time/great circle distance) over a range of p appropriate for Pn or Sn. The averaged slope of this function is then considered as a function of distance, using all the earthquakes, and its slope is determined, providing the required second derivative.

Although the results of this procedure might appear to give reasonable results, we believe it to be seriously in error, as explained below. One (or more) of the possible error terms in Equation 4 seems to be of importance but at this time it (or they) is not identified. We should note, however, that the Q obtained for Sn using Equation 4 is essentially identical to that found for the Q of coda waves by Aki and Chouet, 1975: "from 50 to 200 at 1 Hz to about 1000 to 2000 at 20 Hz."

The results of an alternate analysis based on Equation 2 are shown on the right in Figure 6-4. Apparent Q increases with frequency at about the same rate as that obtained by the previous method but the absolute levels are considerably higher, reaching over 5000 and 10,000 for Pn and Sn, respectively, at 10 Hz.

The available data were comprised of a number of events of various magnitudes at different distances along the northwestern margin of the Pacific, recorded at essentially one location near Wake Island. For this reason, in using the method of Equation 2, it was necessary to normalize the spectral amplitudes for magnitude and for distance. That was accomplished as follows:

Modifying Equation 1'

$$\ell nA' = \ell nA + n\ell nr - \ell nK - m_b \ell n\alpha \quad = - \pi fpqr \qquad (1'')$$

Using the appropriate range of p for Pn and Sn, for each frequency range, f, coefficients ℓnK, $\ell n\alpha$, and q were determined by linear regression using the known variables A, r, and m_b; and using $n = \frac{1}{2}$ or 1, for cylindrical or spherical spreading, respectively. The slope of $\ell nA'$ versus r provides the estimate of Q.

In Figure 6-5, we show the results of removing the effect of attenuation (with no correction for spreading) for two earthquakes differing in epicentral distance by 10.5°. In addition to providing an estimate of the Pn and Sn source spectra, this procedure allows us to check which of the two methods produced more reasonable estimates of Q(f). The higher Q values obtained by the method of Equation 2 seem more reasonable. The resulting source spectra, for both Pn and Sn, at both distances, fall off at about 12 dB/oct in pressure, which is equivalent to a displacement amplitude spectrum of f^{-3}; the equivalent ground amplitude for both Pn and Sn at 1 Hz is about 1 μm for the m_b = 5.3 event and about 10 μm for the m_b = 6.2 event, close to the expected ratio; and the spectral chape seems reasonably independent of distance. On the other hand, using the lower Q values obtained by the method of Equation 4, the source spectra appear to result from strong overcorrection: the spectral fall-off is between f^{-1} and f^{-2}, in displacement, at the shorter distance and actually increases with frequency for higher frequencies at the longer distance; equivalent ground amplitudes at 1 Hz are 20 μm and 3mm for Pn and Sn, respectively, at the shorter distance and 2mm and 2m for Pn and Sn at the longer distance.

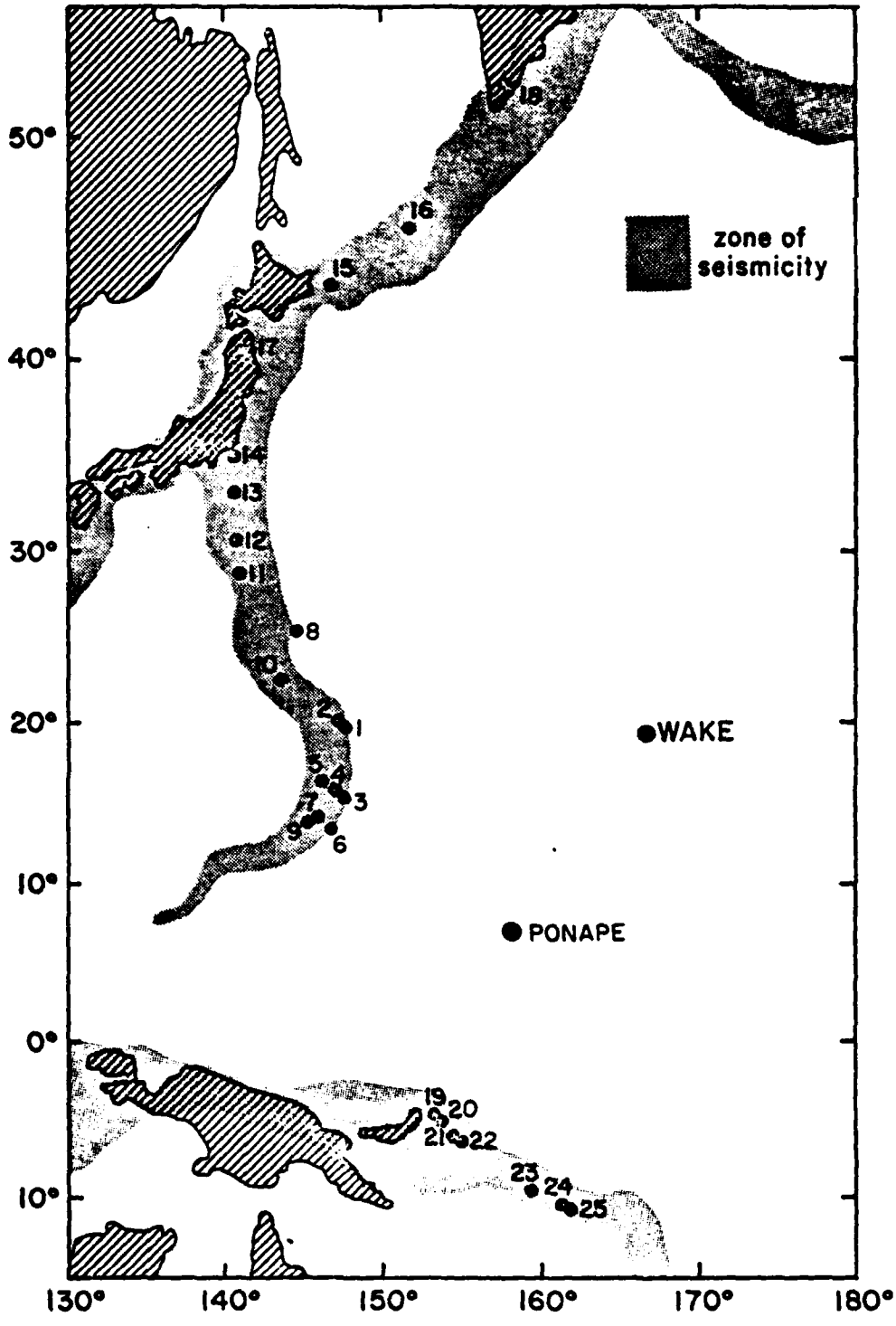

Figure 6-1. Locations of earthquakes used by Walker et al. (1983) in studies of Pn and Sn. All sources used in this work are north of Ponape.

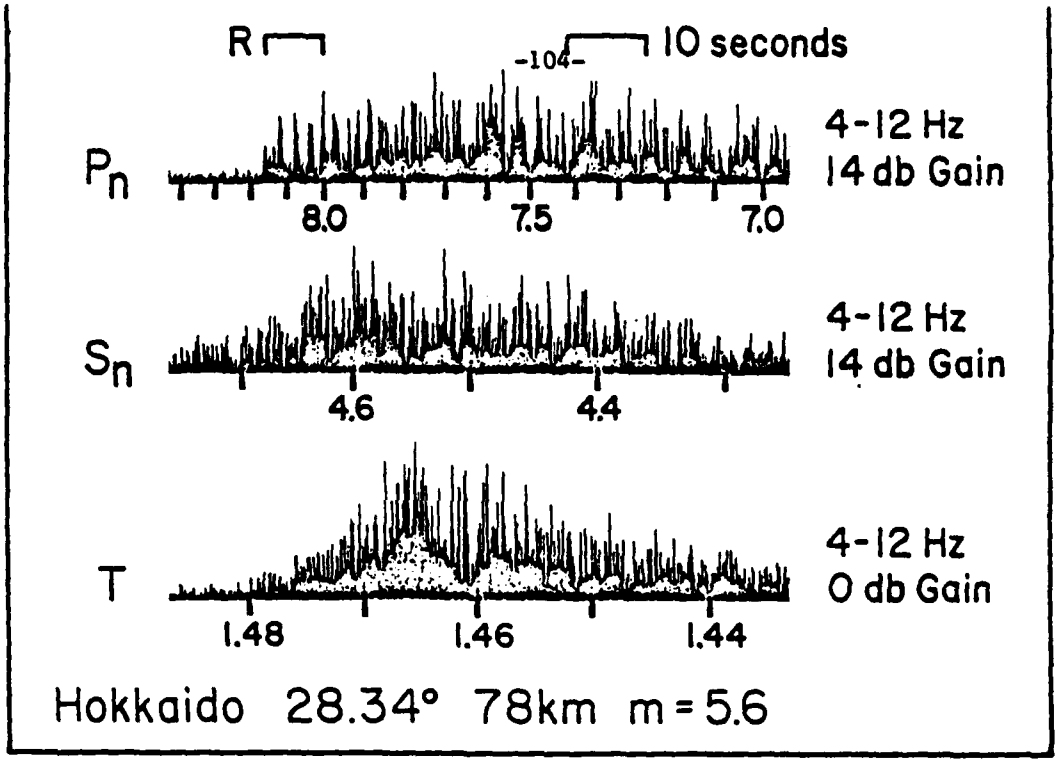

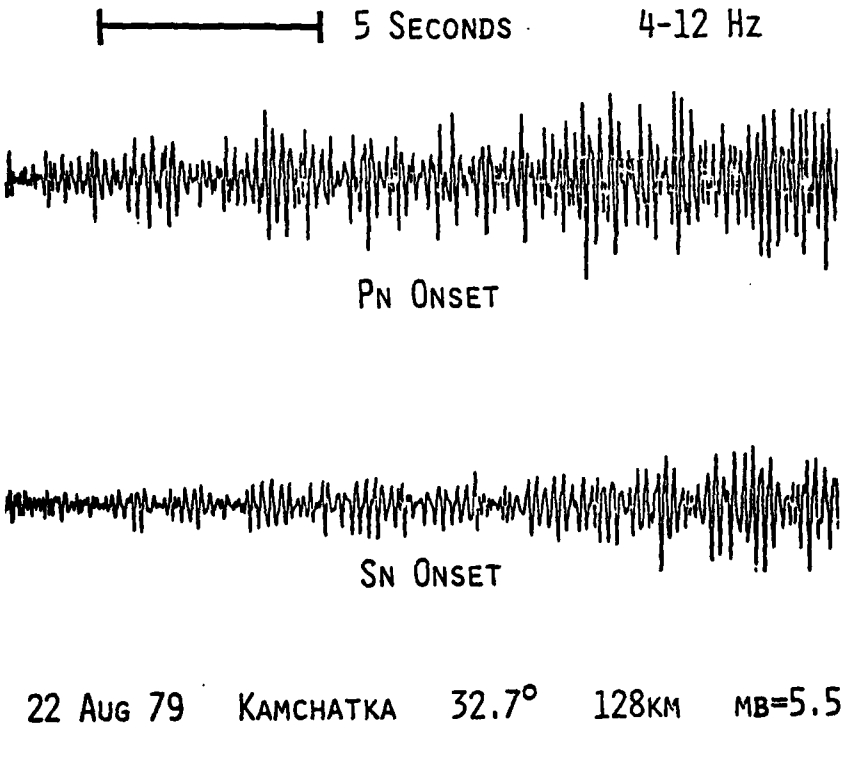

Figure 6-2. Seismograms from the Wake hydrophone array. Top: rectified record of an earthquake near Hokkaido. Pn, Sn and the T-phase all have the same time scale; numbers under the traces are great-circle velocity in km/sec. R is the vertical reflection time to the ocean surface. Bottom: beginnings of Pn and Sn for an earthquake at 32.7° distance. The predominant frequency is about 5 Hz.

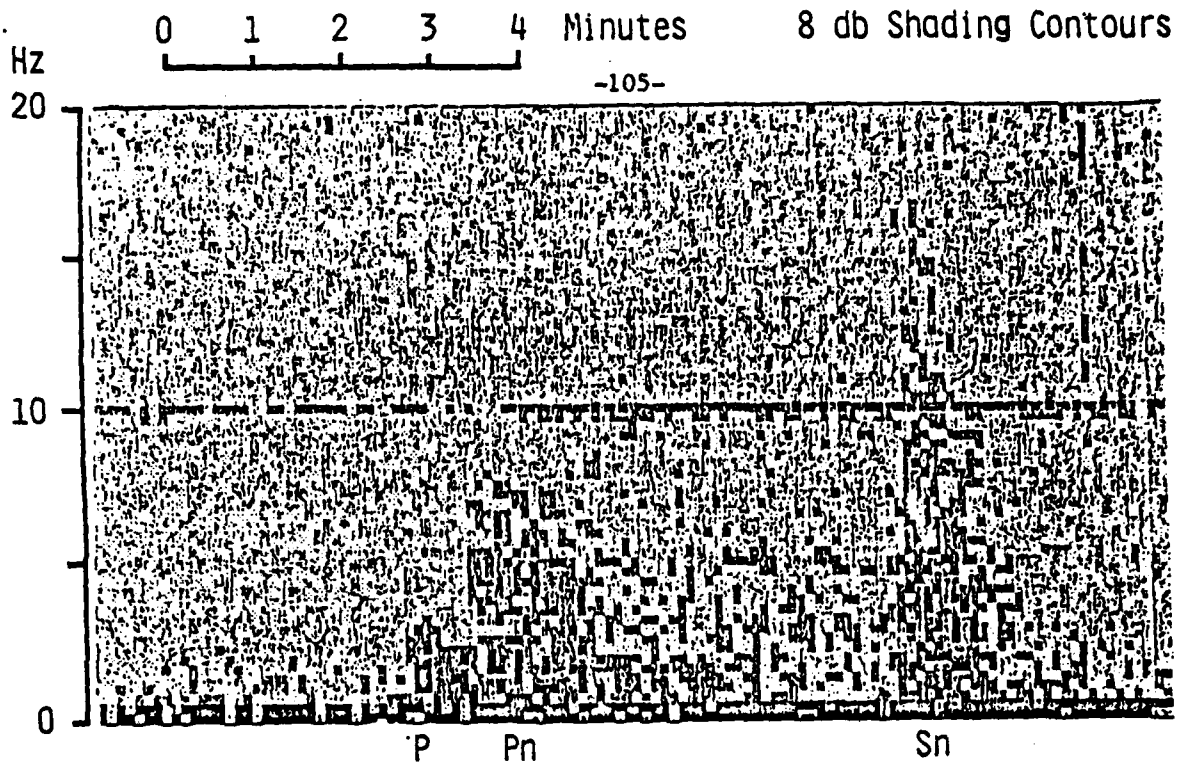

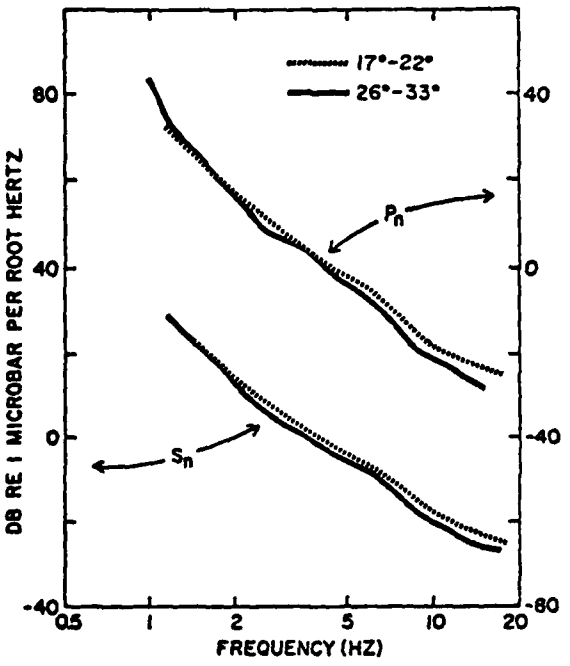

Figure 6-3. Top: spectrogram of P, Pn and Sn. Note that Sn is richer in high frequencies than Pn which, in turn, is richer in high frequencies than P; also note that both Pn and Sn are extended in time with Pn well above background until the arrival of Sn which tends to tail-off more rapidly. Bottom: averaged spectra for Pn and Sn in two distance ranges; from 10 and 6 earthquakes for the 17°-22° and 26°-33° spectra, respectively. Average magnitudes are m_b = 5.3 and 5.8. The very slight change in spectral fall-off with distance is the combined result of high Q and of increase in Q with increasing frequency.

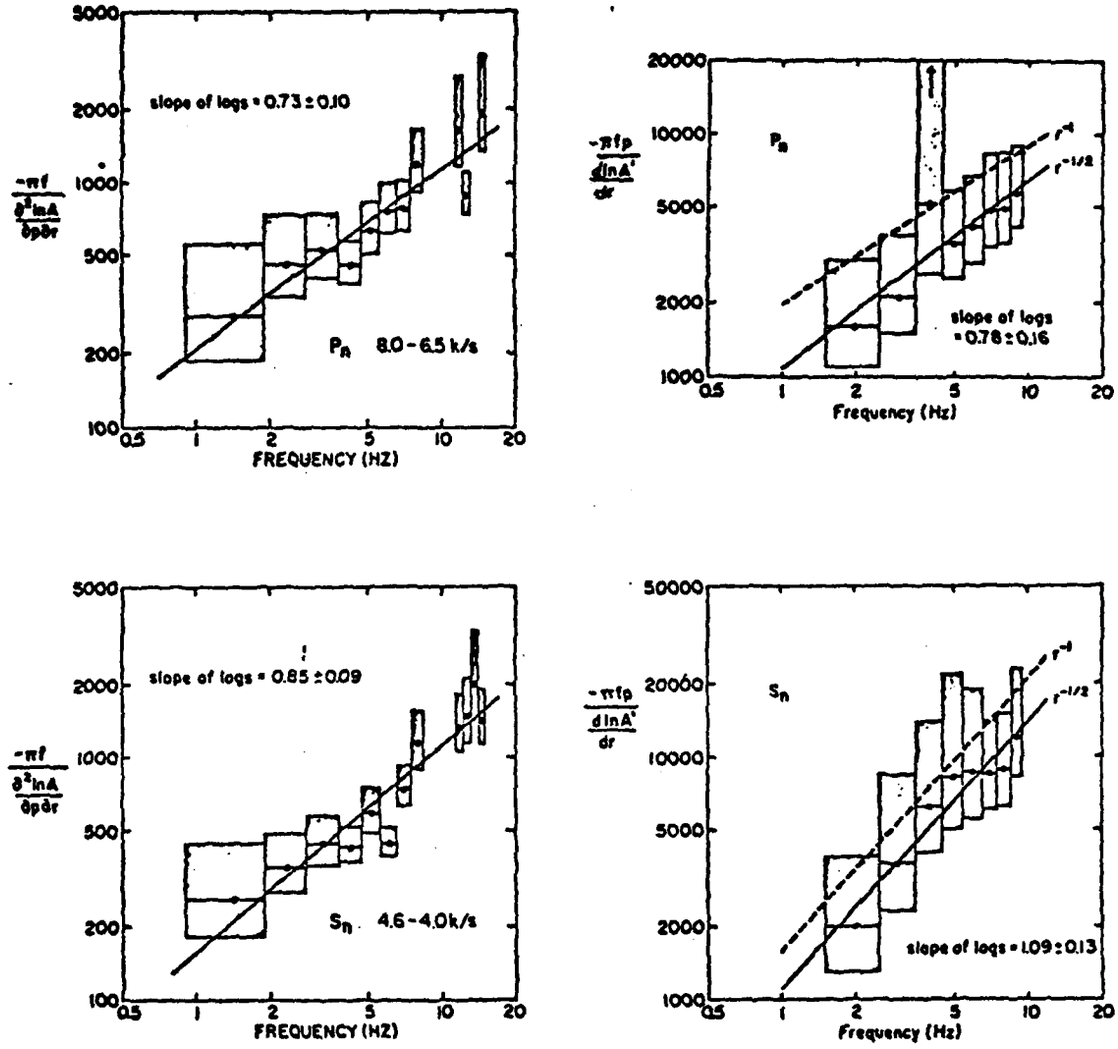

Figure 6-4. Apparent Q as a function of frequency for Pn and Sn obtained in two ways. *Left:* $Q = 1/q_{pr}$ as in Equation 4. Right: $Q = 1/q_r$ as in Equation 2, with an assumed spreading law and amplitudes normalized to a common distance and magnitude; the points and boxes are for cylindrical spreading, $r^{-1/2}$. On all plots the boxes indicate the 1 Hz interval over which spectral amplitudes are averaged (width) and plus and minus the standard error of the (reciprocal of) the point plotted (height). The solid lines are least square fits to the points shown. The dashed lines are the result of a similar analysis assuming spherical spreading, r^{-1}.

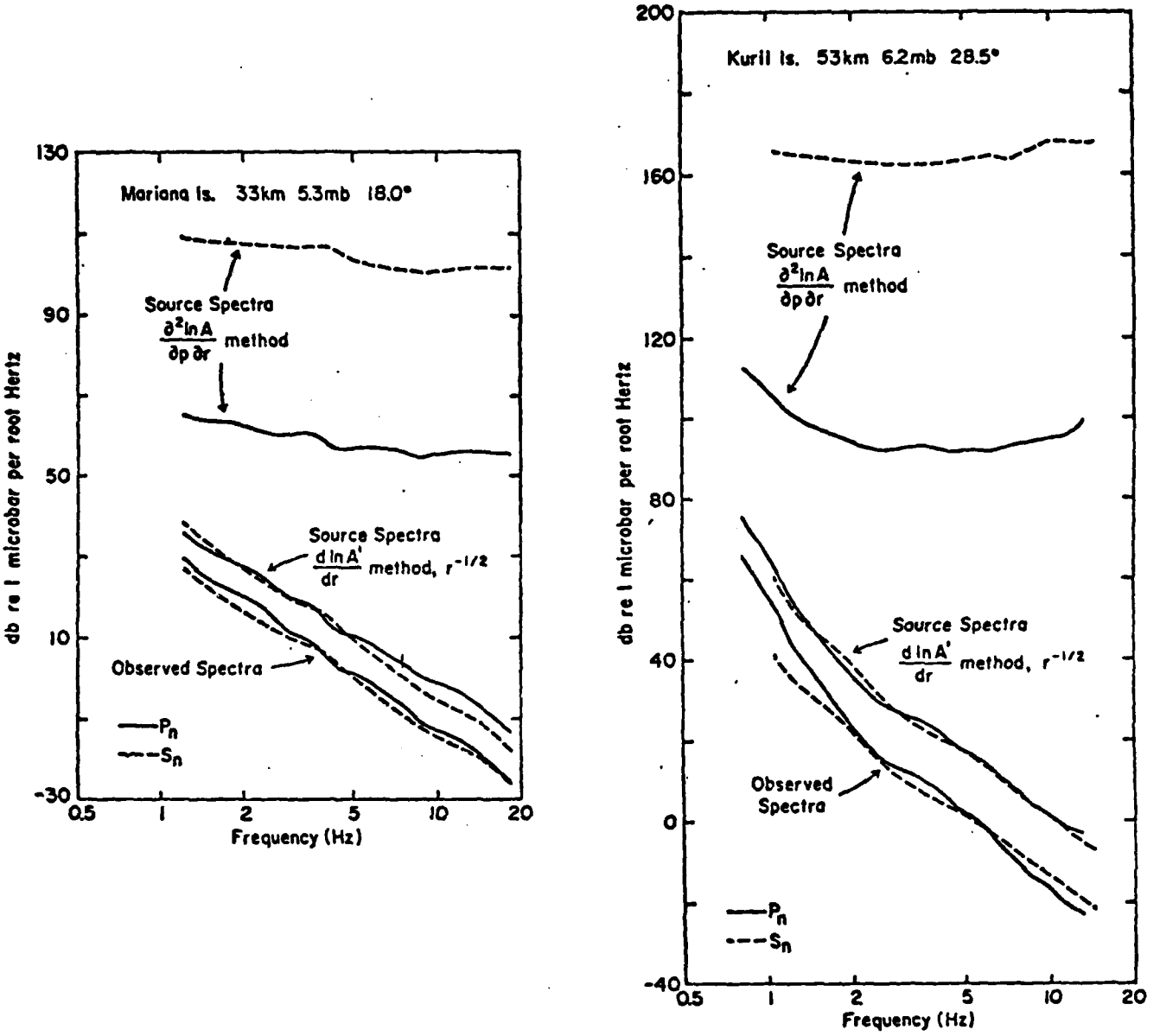

Figure 6-5. Pn and Sn apparent source spectra obtained by correcting observed spectra for attenuation using Q(f) obtained in two ways. Left: Mariana quake at 18.0°, m_b = 5.3. Right: Kurile quake at 28.5°, m_b = 6.2. Note that the d ln A'/dr method, which produced the higher values for Q, gives more reasonable results.

REFERENCES

Aki, K., 1980, Attenuation of shear-waves in the lithosphere for frequencies from 0.05 to 25 Hz. Phys. Earth Planet. Inter., 21, 50-60.

Aki, K., 1980, Scattering and attenuation of shear waves in the lithosphere, J. Geophys. Res., 85, B11, 6496-6504.

Aki, K., Source and scattering effects on the spectra of small local earthquakes, Bull. Seism. Soc. Am., 71, 6, 1687-1700.

Aki, K., and B. Chouet, 1975, Origin of coda waves: source, attenuation, and scattering effects, J. Geophys. Res., 80, 23, 3322-3342.

Anderson, D. L. and R. S., Hart, 1978, Attenuation models of the earth, Phys. Earth Planet. Interiors, 16, 289-306.

Cheng, C.-C., and B. J. Mitchell, 1981, Crustal Q structure in the United States from multi-mode surface waes, Bull. Seism. Soc. Am., 71, 1, 161-181.

Dainty, A. M., 1981, A scattering model to explain seismic Q observations in the lithosphere between 1 and 30 Hz, Geophys. Res. Lett., 8, 11, 1126-1128.

Dainty, A. M., and M. N. Toksoz, 1981, Seismic codas on the Earth and the moon: a comparison, Physics of the Earth and Plan. Interiors, 26, 250-260.

Gettrust, J. and L. N. Frazer, 1981, A computer model study of the propagation of the long-range Pn phase, Geophys. Res., Lett., 8, 749-752.

McCreery, C. S., and G. H. Sutton, 1981, Attenuation and source spectra of high-frequency teleseismic Pn and Sn in the northwestern Pacific, EOS, Trans. Am. Geophys. Un., 62, 17, 334, (abstract).

Menke, W., and P. Richards, 1980, Crust-mantle whispering gallery phases: a deterministic model of teleseismic Pn wave propagation, J. Geophys. Res., 85, 5416-5422.

Mitchell, B. J., 1981, Regional variation and frequency dependence of Q_β in the crust of the United States, Bull. Seism. Soc. Am., 71, 5, 1531-1538.

Nakamura, Y., and J. Koyama, 1982, Seismic Q of the lunar upper mantle, Jour. of Geophys. Res., 87, in press.

Sutton, G. H. and D. Harvey, 1981, Complete synthetic seismograms to 2 Hz and 1000 km for an oceanic lithosphere, EOS, Trans. Am. Geophys. Un., 62, p. 327 (abstract).

Sutton, G. H., W. Mitronovas, and P. W. Pomeroy, 1967, Short-period seismic energy radiation patterns from underground nuclear explosions and small-magnitude earthquakes, Bull. Seism. Soc. Am., 57, 2, 249-267.

Walker, D. A., C. S. McCreery, and G. H. Sutton, 1983, Spectral Characteristics of High-Frequency Pn, Sn Phases in the Western Pacific, J. Geophys. Res., (in press).

Walker, D. A., C. S. McCreery, G. H. Sutton, and F. K. Duennebier, 1978, Spectral analyses of high-frequency P_n and S_n phases observed at great distances in the western Pacific, Science, 199, 1333-1335.

Wu, R. S., 1982, Attenuation of short period seismic waves due to scattering, Geophy. Res. Lett., 9, 1, 9-12.

7. UPGRADE OF WHA FOR DIGITAL RECORDING

Introduction

The hydrophone array installed near Wake Island (WHA) was reactivated as a seismic station in June 1979 by the Hawaii Institute of Geophysics. WHA consists of six bottom phones, at 5.5 km depth, in an array 40 km across and an additional four pairs of phones, at larger spacing, suspended at SOFAR depth (Figure 7-1). The bottom array lies in a flat area on high Q lithosphere $>10^8$ years old. All of the deep and five of the SOFAR phones are operational. Until September 1982, data were generally recorded from only three phones on a slow speed analog cassette recorder. In early September, the station was upgraded by HIG in cooperation with RAI for digital recording of all eleven phones. Many circum-Pacific earthquakes and nuclear tests have been well recorded by WHA, its location being ideally suited for monitoring such events. Nearly pure oceanic paths between WHA and circum-Pacific sources facilitate studies of the ocean-lithosphere waveguide such as propagation and attenuation of high-frequency, teleseismic Pn and Sn as discussed in other sections of this report. For frequencies above 3 Hz, WHA is quieter than most quiet continental stations.

Description of Upgraded System

The newly installed digital recording system is shown in Figure 7-2. The system is quite flexible, e.g. the choice of hydrophones monitored and digitizing rates can be modified easily. A brief description of the system components follows:

> Signals from up to 12 hydrophones drive low-noise, isolation pre-amps (Analog Devices model 277) and pre-whitening anti-aliasing filters. The filters have maximum response between 8 and 20 Hz, fall at 12 dB/octave toward lower frequencies to 0.25 Hz, are flat down to 0.025 Hz and then continue to fall at 12 dB/octave toward lower frequencies. These filters are designed to take advantage of the low noise levels above 2 to 3 Hz at WHA. Two analog signals are used to produce visible monitor records. After filtering, the signals are multiplexed and digitized in a 16 bit A/D converter (Data Translation DT2784-SE/DT57161B) which has direct memory access to the CPU. The manually adjustable digitization rate is controlled by a 1kHz pulse from a satellite synchronized clock (Kinemetrics Realtime 468DC). The CPU is a DEC LSI 11/2 16-bit microprocessor with 64k bytes of

memory. It forms the data into blocks and links it to the four recording tape drives (Datum D451; 45ips, 1600 bpi, 14 inch reels) through the controller-formatter (Datum model 15221). A dual floppy disk drive (512kB each) is included for booting and programming tasks. Also included is a printer (DEC LA 38) for hard-copy operations logging.

Under nominal operation, eleven hydrophones are recorded, at 80 samples/sec (fn = 40 Hz), at 16 bits per sample, producing four tapes per day. At this time, no real-time event triggering mode is being implemented. Several months requirement of tape are available and data retrieval and selection are being conducted at HIG. Means of timely communication of epicenter information, needed for data selection for many small events, are being established through the Center for Seismic Studies in Arlington, Virginia and RAI in Stone Ridge, New York since RAI has a dedicated leased phone link to CSS. WHA data from events of interest will be transmitted to CSS for archiving and the use of others.

Examples of Seismic Data

In Figures 7-3 and 7-4 , signals recorded on hydrophone 74 of WHA soon after the installation of the upgraded system provide an example of the capabilities of the system. The record in Figure 7-3 and spectra in Figure 7-4 from a large earthquake south of Honshu, Japan show energy of interest with frequencies exceeding 20 Hz lasting more than 30 minutes; the maximum signal to noise and dynamic range of interest approach 50 dB. The spectrum of the background noise shows that the pre-whitening filter has flattened the noise above 5 Hz and reduced the rise at low frequencies to a moderate 15 to 18 dB.

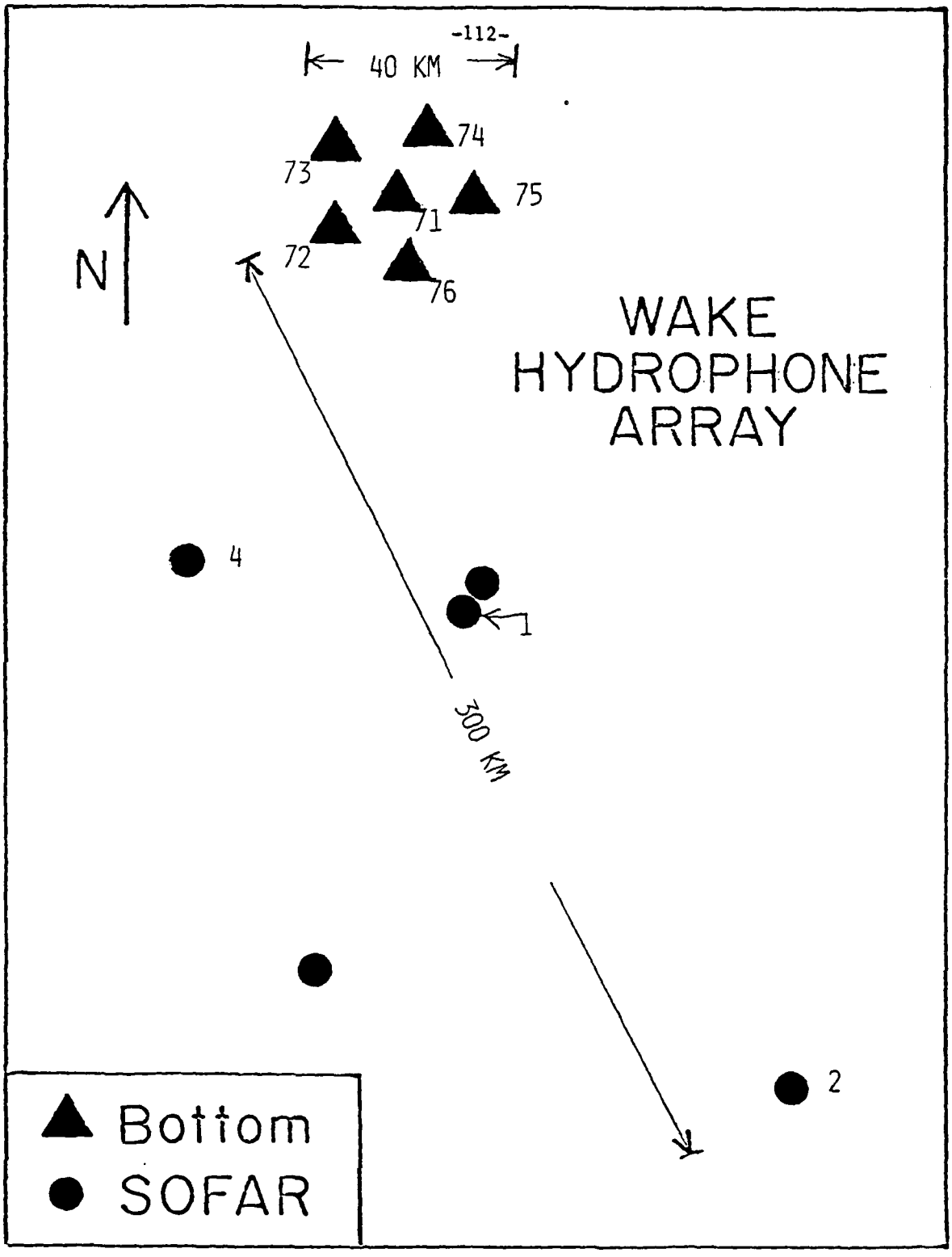

Figure 7-1. Locations of WHA hydrophones.

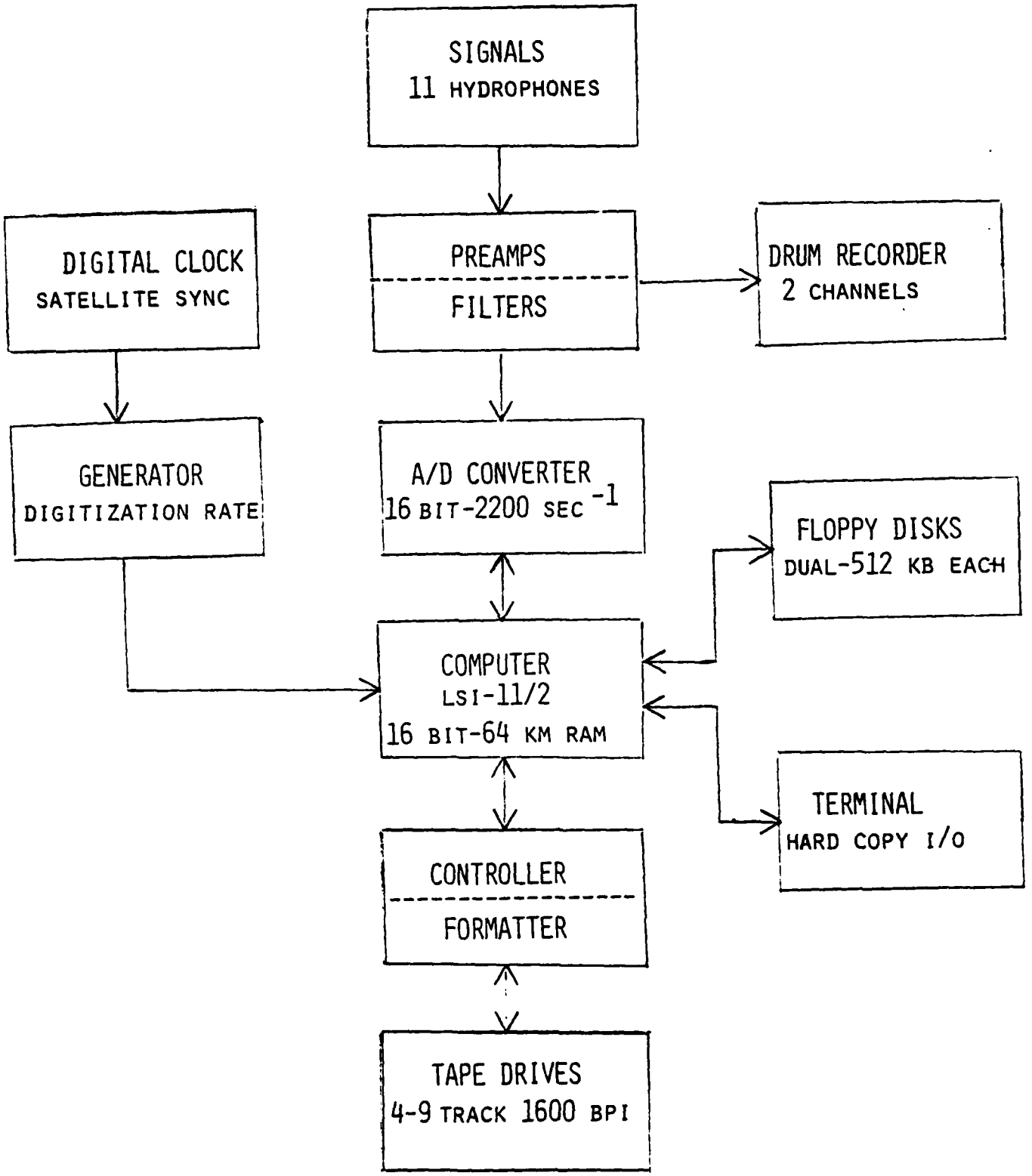

Figure 7-2. Diagram of WHA digital recording system.

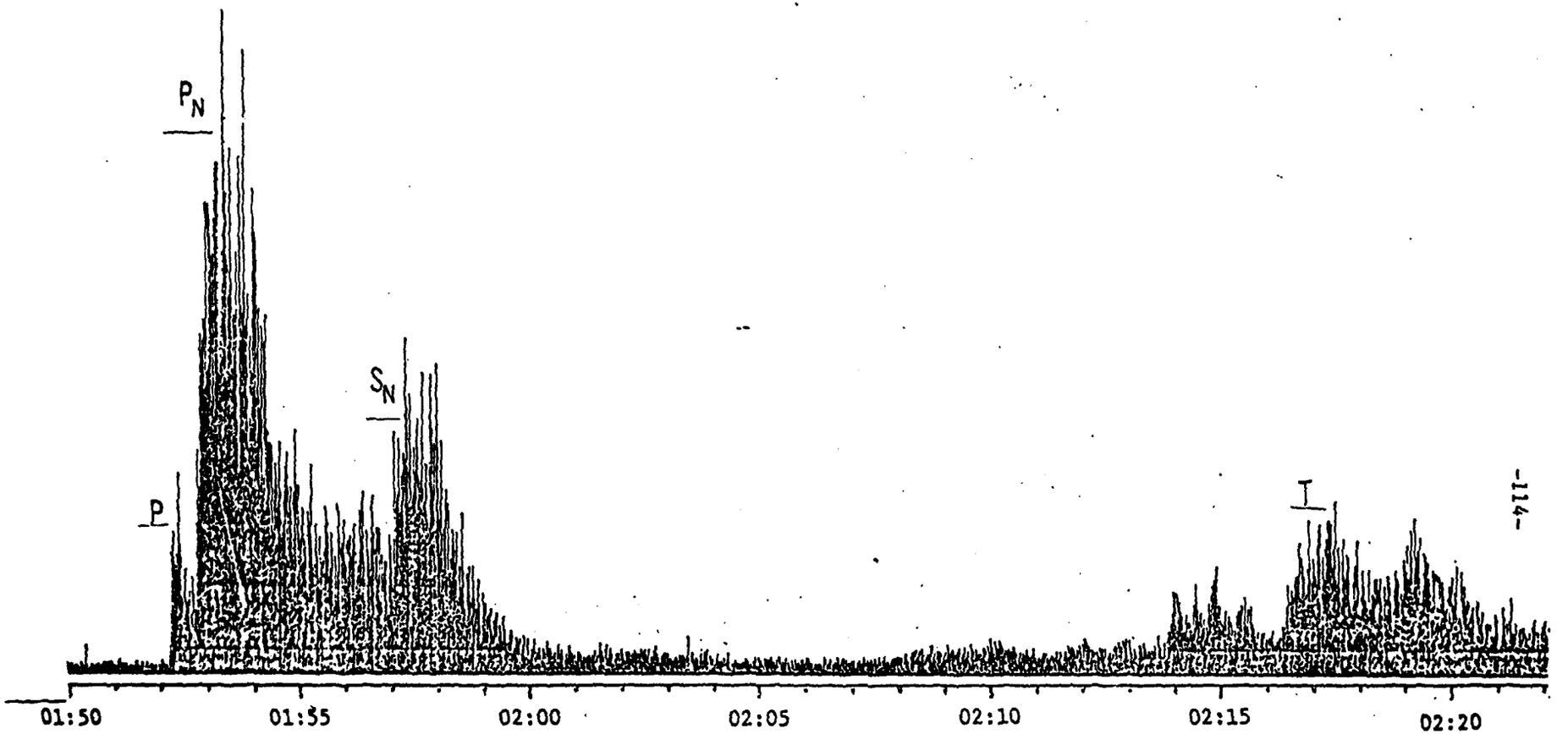

Figure 7-3 Rectified seismogram from hydrophone 74 (linear amplitude scale) of large earthquake recorded on WHA digital system; 7 September 1981; 01:47:02; 29.3N, 140.3E; 6.6 m_b; 167 km; South of Honshu; distance = 25.2°; times are in hours and minutes.

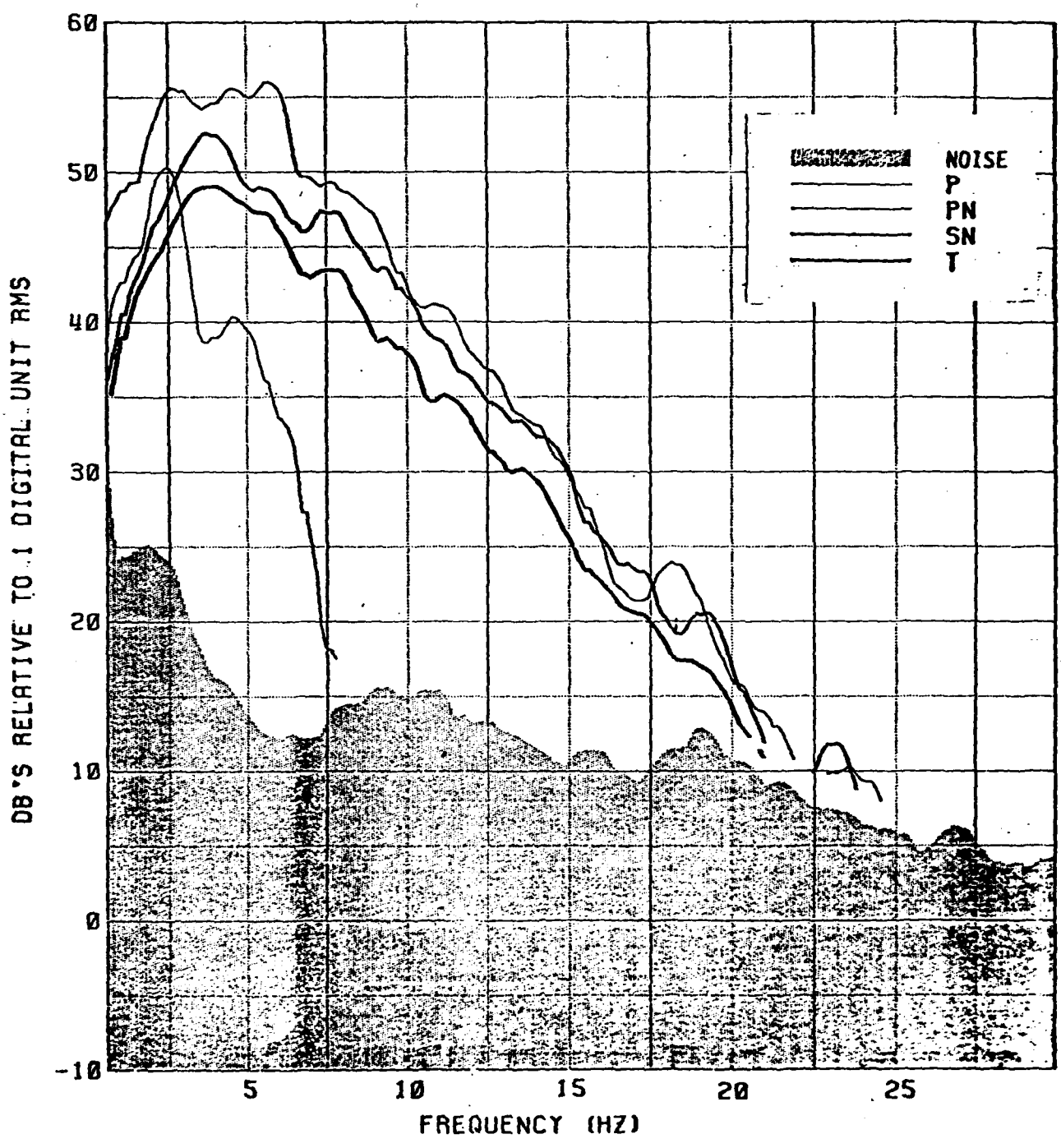

Figure 7-4 Spectra of P, Pn, Sn, and T from hydrophone 74 of WHA for the earthquake shown in Figure 7-3. Spectra are averaged over a 1 Hz window. Uncorrected for system response. Spectra were taken near maxima of signals. over 32, 64, 52, 196, and 96 sec for P, Pn, Sn, T, and noise samples, respectively. Maximum S/N is 30 to 40 dB between about 2.5 and 10 Hz.